Analysis of a Single-Degree-of-Freedom Roll Motion Model: Simulation, Sensitivity Study, and Comparison to Multi-Degree-of-Freedom Models

by

Erica Sahler

A PROJECT

submitted to

Oregon State University

In partial fulfillment of
the requirement for the
degree of

Master of Science

DISTRIBUTION STATEMENT A
Approved for public release;
Distribution Unlimited

Completed April 3, 1996

19960628 015

DTIC QUALITY INSPECTED 1

AN ABSTRACT OF THE PROJECT OF

Erica Sahler for the Degree of Master of Science in Civil Engineering
presented on April 3, 1996.
Title: Analysis of A Single Degree of Freedom Roll Motion Model: Simulation, Sensitivity Study, and Comparison to Multi-Degree-of-Freedom Models

Abstract approved: _____
Solomon C.S. Yim

This study models roll motion response of a barge subjected to beam sea conditions as a single-degree-of-freedom system. The measured wave, either regular or random, is input into a computer program which uses a fourth-order Runge-Kutta integration method to numerically predict roll motion response. The simulated results are compared to measured data to determine the best system damping parameters. Four different forms of the damping moment of the SDOF model are analyzed. In each form all coefficients are known except for the linear and nonlinear damping parameters. Each form uses a combination of relative motion "Morison" damping and/or linear structural damping. Predicted results of the four forms of the damping moment are examined to determine the most suitable model. A sensitivity study on the response to various system parameters is then conducted on the selected form. Each form of the model uses a thirteenth-order polynomial restoring moment. An analysis is also conducted to determine the effects of using lower order terms to represent the restoring moment. Finally, results of the SDOF model from this report are compared with a 3DOF and a 2DOF model subjected to the same wave environment to determine which model more accurately predicts roll response.

DISTRIBUTION STATEMENT A
Approved for public release
Distribution Unlimited

Analysis of a Single-Degree-of-Freedom Roll Motion Model: Simulation, Sensitivity Study, and Comparison to Multi-Degree-of-Freedom Models

by

Erica Sahler

A PROJECT

submitted to

Oregon State University

In partial fulfillment of
the requirement for the
degree of

Master of Science

Completed April 3, 1996

ACKNOWLEDGEMENTS

My studies at Oregon State would not have been successful without the patience, help and assistance I received from each of the members of my Graduate Committee. I will always be grateful to Dr. Solomon C.S. Yim for giving me the opportunity to work for him on this project. He challenged me with high standards and a demanding project which I will look back on with a great deal of pride and sense of accomplishment. I would also like to thank Dr. Charles K. Sollitt and Professor Harold D. Pritchett for their input and guidance throughout my studies.

In addition I would like to thank Mr. Warren A. Bartel for his endless patience and willingness to provide advice and assistance. I have a great deal of admiration for Warren's work ethic and dedication. Warren was a major contributor to the NFESC Report "Nonlinear Roll Motion and Capsizing of Barges in Random Seas, Part I; Modelling and System Identification" (Yim et al. 1995). This report provided a great deal of background information for my project and was the foundation for my research.

Partial support from the Naval Facilities Engineering Service Center Contract N47408-94-C-7426 and the Office of Naval Research Grant N00014-92-J-1221 are gratefully acknowledged. Thanks to the OSU Computer Science Department for use of the Meiko CS-2 supercomputer. This computer support is made possible by National Science Foundation Grant CDA-9216172.

My studies at OSU were funded by the U.S. Navy's Fully Funded Graduate Education Program. I gratefully acknowledge their contribution and am thankful I was given the opportunity to pursue a graduate degree.

And finally I would like to thank my family and friends who gave me encouragement throughout my studies. Without their love and support successful completion of my graduate study would not have been possible.

TABLE OF CONTENTS

1.0 Introduction 1

1.1 Objective 1
1.2 Literature Review 2
1.3 Scope 3

2.0 System Description 4

2.1 Assumptions 5
2.2 Equation of Motion 5
2.3 Description of Wave Field 6
2.4 Inertia and Added Inertia Coefficients 7
2.5 Damping Moment 8
2.6 Roll Restoring Moment 8
2.7 Various Forms of Equation of Motion 9

3.0 Model Tests and Identification of Damping Parameters 12

3.1 Model Test Procedure 13
3.2 Description of Analytical Prediction Procedure 14
3.3 Form 1: Relative Motion Damping Moment 18

3.3.1 Regular Wave, H= 6.6 Ft, T= 5 Sec (SB26) 19
3.3.2 Regular Wave, H=6 Ft, T= 6 Sec (SB27) 19
3.3.3 Regular Wave, H= 7.2 Ft, T= 8 Sec (SB29) 19
3.3.4 Regular Wave, H= 5.7 Ft, T= 10 Sec (SB30) 23
3.3.5 Bretschneider Spectrum, Hs= 6 Ft, Tp= 8 Sec (SB25) 26
3.3.6 White Noise Spectrum, Hs= 6 Ft (SB33) 31

3.4 Form 2: Relative Motion Neglected in Damping Moment 31

3.4.1 Regular Wave, H= 6.6 Ft, T= 5 Sec (SB26) 36
3.4.2 Regular Wave, H= 6 Ft, T= 6 Sec (SB27) 38
3.4.3 Regular Wave, H= 7.2 Ft, T= 8 Sec (SB29) 38
3.4.4 Regular Wave, H= 5.7 Ft, T= 10 Sec (SB30) 41
3.4.5 Bretschneider Spectrum, Hs= 6 Ft, Tp= 8 Sec (SB25) 41
3.4.6 White Noise Excitation, Hs= 6 Ft (SB33) 47

3.5 Alternative Forms Considered 47

Table of Contents (cont'd)

4.0 Sensitivity Study 57

4.1 Variation of Damping Parameters of Form 2, Equation 2.8 57

4.1.1 Regular Wave, H= 6.6 Ft, T= 5 Sec (SB26) 57
4.1.2 Regular Wave, H= 6 Ft, T= 6 Sec (SB27) 58
4.1.3 Regular Wave, H= 7.2 Ft, T= 8 Sec (SB29) 64
4.1.4 Regular Wave, H= 5.7 Ft, T= 10 Sec (SB30) 67
4.1.5 Random Wave Tests 70

4.2 Variation of Nonlinear Restoring Moment 72

4.2.1 Cubic Fit to Restoring Moment Curve 72
4.2.2 5th, 9th, and 13th Order Restoring Moment Curves 75

5.0 Comparison of Single, 2- and 3-Degree-of-Freedom Models 80

6.0 Concluding Remarks 87

6.1 Conclusions 87
6.2 Recommendations for Future Studies 89

References 90

LIST OF FIGURES

Figure		page
2.1	13th Order Roll Restoring Moment Curve	10
3.1	Comparison of Measured and Filtered Wave, Measured and Predicted Roll, Regular Wave, H=6.6 Ft, T= 5 Sec (SB26)	15
3.2	Comparison of Spectral Densities, Measured and Filtered Wave (SB26)	16
3.3	Comparison of Measured and Filtered Wave, Measured and Predicted Roll, 17 Regular Wave, H= 6.6 Ft, T= 5 Sec (SB26)	17
3.4	Comparison of Measured and Filtered Wave, Measured and Predicted Roll, Regular Wave, H=6.6 Ft, T= 5 Sec (SB26, eqn 2.2)	20
3.5	Comparison of Measured and Filtered Wave, Measured and Predicted Roll, Regular Wave, H= 6 Ft, T = 6 Sec (SB27, eqn 2.2)	21
3.6	Comparison of Measured and Filtered Wave, Measured and Predicted Roll, Regular Wave, H= 7.2 Ft, T= 8 Sec (SB29, eqn 2.2)	22
3.7	Comparison of Measured and Filtered Wave, Measured and Predicted Roll, Regular Wave, H= 5.7 Ft, T=10 Sec (SB30, eqn 2.2)	24
3.8	Comparison of Spectral Densities, Measured and Predicted Roll H= 5.7 Ft, T= 10 Sec (SB30, eqn 2.2)	25
3.9	1024 Sec Time Series of Predicted Roll H= 5.7 Ft, T= 10 Sec (SB30, eqn 2.2)	25
3.10	Comparison of Measured and Filtered Wave, Measured and Predicted Roll, Bretschneider Spectrum, H= 6 Ft, Tp= 8 Sec (SB25, eqn 2.2)	27
3.11	Comparison of Spectral Densities, Measured and Filtered Wave, Bretschneider Spectrum, Hs= 6 Ft, Tp= 8 Sec (SB25, eqn 2.2)	28
3.12	Comparison of Spectral Densities, Measured and Predicted Roll, Bretschneider Spectrum, Hs= 6 Ft, Tp= 8 Sec (SB25, eqn 2.2)	29

List of Figures (cont'd)

Figure		page
3.13	Histograms of Measured and Predicted Roll, Bretschneider Spectrum (SB25, eqn 2.2)	30
3.14	Comparison of Measured and Filtered Wave, Measured and Predicted Roll, White Noise Spectrum, Hs= 6 Ft (SB33, eqn 2.2)	32
3.15	Comparison of Spectral Densities, Measured and Filtered Wave White Noise Spectrum, Hs= 6 Ft (SB33, eqn 2.2)	33
3.16	Comparison of Spectral Densities, Measured and Predicted Roll White Noise Spectrum, Hs= 6 Ft (SB33, eqn 2.2),	34
3.17	Histograms of Measured and Predicted Roll, White Noise Spectrum (SB33, eqn 2.2)	35
3.18	Comparison of Measured and Filtered Wave, Measured and Predicted Roll, Regular Wave, H= 6.6 Ft, T= 5 Sec (SB26, eqn 2.8)	37
3.19	Comparison of Measured and Filtered Wave, Measured and Predicted Roll, Regular Wave, H= 6 Ft, T= 6 Sec (SB27, eqn 2.8)	39
3.20	Comparison of Measured and Filtered Wave, Measured and Predicted Roll, Regular Wave, H= 7.2 Ft, T= 8 Sec (SB29, eqn 2.8)	40
3.21	Comparison of Measured and Filtered Wave, Measured and Predicted Roll, Regular Wave, H= 5.7 Ft, T= 10 Sec (SB30, eqn 2.8)	42
3.22	Comparison of Spectral Densities, Measured and Predicted Roll, H= 5.7 Ft, T= 10 Sec (SB30, eqn 2.8)	43
3.23	Comparison of Measured and Predicted Wave and Roll, Bretschneider Spectrum, Hs= 6 Ft, Tp= 8 Sec (SB25, eqn 2.8)	44
3.24	Comparison of Spectral Densities, Measured and Predicted Roll, Bretschneider Spectrum, Hs= 6 Ft, Tp= 8 Sec (SB25, eqn 2.8)	45
3.25	Histograms of Measured and Predicted Roll, Bretschneider Spectrum (SB25, eqn 2.8)	46
3.26	Comparison of Measured and Filtered Wave, Measured and Predicted Roll, White Noise Spectrum, Hs= 6 Ft (SB33, Eqn 2.8)	48

List of Figures (cont'd)

Figure		page
3.27	Comparison of Spectral Densities, Measured and Predicted Roll, White Noise Spectrum, Hs= 6 Ft (SB33, eqn 2.8)	49
3.28	Histograms of Measured and Predicted Roll, White Noise Spectrum (SB33, eqn 2.8)	50
3.29	Comparison of Roll Responses Using Four Different Forms (SB26)	51
3.30	Comparison of Roll Responses Using Four Different Forms (SB27)	53
3.31	Comparison of Roll Responses Using Four Different Forms (SB29)	54
3.32	Comparison of Roll Responses Using Four Different Forms (SB30)	55
4.1	Variation of Linear Damping Parameter, Constant Nonlinear Damping Parameter, ξ_N =0.07, H= 6.6 Ft, T=5 Sec (SB26, eqn 2.8)	59
4.2	Variation of Nonlinear Damping Parameter, Constant Linear Damping Parameter, ξ_L = 0.09, H= 6.6 Ft, T=5 Sec (SB26, eqn 2.8)	60
4.3	Variation of Linear Damping Parameter, Constant Nonlinear Damping Parameter, ξ_N = 0.07, H= 6.0 Ft, T=6 Sec (SB27, eqn 2.8)	62
4.4	Variation of Nonlinear Damping Parameter, Constant Linear Damping Parameter, ξ_L = 0.10, H= 6.0 Ft, T= 6 Sec (SB27, eqn 2.8)	63
4.5	Variation of Linear Damping Parameter, Constant Nonlinear Damping Parameter, ξ_N = 0.40, H= 7.2 Ft, T=8 Sec (SB29, eqn 2.8)	65
4.6	Variation of Nonlinear Damping Parameter, Constant Linear Damping Parameter, ξ_L = 0.33, H= 7.2 Ft, T= 8 Sec (SB29, eqn 2.8)	66
4.7	Variation of Linear Damping Parameter, Constant Nonlinear Damping Parameter, ξ_N = 0.07, H= 5.7 Ft, T=10 Sec (SB30, eqn 2.8)	68
4.8	Variation of Linear Damping Parameter, Constant Nonlinear Damping Parameter, ξ_N = 0.07, H= 5.7 Ft, T=10 Sec (SB30, eqn 2.8)	69
4.9	Variation of Nonlinear Damping Parameter, Constant Linear Damping Parameter, ξ_L = 0.03, H= 5.7 Ft, T= 10 Sec (SB30, eqn 2.8)	71

List of Figures (cont'd)

Figure		page
4.10	Comparison of Numerical and Analytical Restoring Moment Curves, Cubic Fit	73
4.11	Comparison of Measured and Predicted Roll, Cubic Restoring Moment, H= 7.2 Ft, T= 8 Sec (SB29)	74
4.12	Comparison of Spectral Densities, Measured and Simulated Roll, Cubic Restoring Moment, H= 7.2 Ft, T= 8 Sec (SB29)	74
4.13	Comparison of Numerical and Analytical Restoring Moment Curves, 5th Order Restoring Moment	76
4.14	Comparison of Measured and Predicted Roll, 5th Order Restoring Moment H= 7.2 Ft, T= 8 Sec (SB29)	77
4.15	Comparison of Spectral Densities, Measured and Predicted Roll, 5th Order Restoring Moment, H= 7.2 Ft, T= 8 Sec (SB29)	77
4.16	9th Order Fit to Restoring Moment Curve	78
4.17	13th Order Fit to Restoring Moment Curve	78
4.18	Comparison of Measured and Predicted Roll, 9th Order Restoring Moment, H=7.2 Ft, T= 8 Sec (SB29)	79
4.19	Comparison of Measured and Predicted Roll Using 13th Order Restoring Moment, H= 7.2 Ft, T= 8 Sec (SB29)	79
5.1	Comparison of 3DOF, 2DOF and SDOF Models, H= 6 Ft T= 5 Sec (SB26)	81
5.2	Comparison of 3DOF, 2DOF and SDOF Models, H= 7.2 Ft T= 8 Sec (SB29)	83
5.3	Comparison of 3DOF and SDOF Models, H= 5.7 Ft, T= 10 Sec (SB30)	84
5.4	Comparison of 2DOF and SDOF Models, H=5.7 Ft, T= 10 Sec (SB30)	85
5.5	Comparison of 3DOF, 2DOF and SDOF Models, Bretschneider Spectrum (SB25)	86

LIST OF TABLES

Table		Page
3.1	Linear and Nonlinear Damping Parameters for Form 1, Equation 2.2	18
3.2	Linear and Nonlinear Damping Parameters for Form 2, Equation 2.8	36
3.3	Linear and Nonlinear Damping Parameters for Form 3, Equation 2.9	56
3.4	Linear and Nonlinear Damping Parameters for Form 4, Equation 2.10	56
4.1	Variation in Damping Parameters and Resulting Standard Deviations (SB26)	57
4.2	Variation in Damping Parameters and Resulting Standard Deviations (SB27)	61
4.3	Variation in Damping Parameters and Resulting Standard Deviations (SB29)	64
4.4	Variation in Damping Parameters and Resulting Standard Deviations (SB30)	67
4.5	Variation in Damping Parameters and Resulting Standard Deviations (SB25)	70
4.6	Variation in Damping Parameters and Resulting Standard Deviations (SB33)	72
5.1	Damping Parameters for SDOF, 2DOF and 3DOF Models	80
6.1	Summary of Damping Parameters for Form 2, Equation 2.8	88

1.0 Introduction

For decades the U.S. Navy has used large steel barges as a vital part of their Military Preposition Force (MPF) offload process. The MPF is a fleet of cargo ships prepositioned at strategic locations ready for deployment when called upon. For any extended military action, the MPF is the main source of equipment transport. Many of the locations to which the U S military may be called into action do not have deep water facilities that can accommodate these vessels. As a result, the equipment is offloaded several miles off shore and transported to the beach or permanent/temporary pier via barges or "causeways" as the Navy has designated them.

The causeways currently being used by the Navy measure 21 foot (ft) wide, 90 ft long and have a 5 ft draft. The shape is very close to a rectangular steel box. Due to it's shallow draft and particular geometry, the causeways quite often have water on the deck even in relatively low sea states. Hence their stability is sensitive to wave action. To improve the reliability of their operation, a new generation of causeways, in which the dimensions increase to 25 ft wide, 120 ft long and a draft of 8 ft is currently under conceptual design and is the focus of this analysis.

1.1 Objective

A series of experiments have been conducted to provide data to calibrate the prediction capabilities of several time, frequency and probability domain computer programs developed by the Naval Facilities Engineering Service Center (NFESC), Amphibious Division. Of particular interest to the NFESC engineers is a study of capsizing when the causeways are subjected to high sea states for relatively long

durations. Simple low degree-of-freedom dynamic models of the barge motions have been developed for stochastic analytical and numerical studies to estimate the probability of capsize. The motivation behind this study is to identify suitable system damping parameters for the single-degree-of-freedom (SDOF) model.

1.2 Literature Review

The motion of free-floating vessels in open seas often contain complicated nonlinear behaviors due to large displacement and hydrodynamic effects. In particular, the stability of roll motion of barges with high centers of gravity is of great practical importance. Existing stability criteria are expressed in terms of minimum values of certain key features of the righting arm. For certain classes of vessels, static stability standards based on statistical and other analyses of intact static condition are sufficient for design purpose, and can give a qualitative understanding of the stability behavior for the naval architect (Soliman and Thompson 1991). Although this curve is found to be an important vessel characteristic in assuring safety (Falzarano et al. 1992), other vessel properties are also significant. These include hydrodynamic and viscous roll damping, as affected by the wave exciting force.

Because the cargo is carried above deck on a causeway, the center of gravity of the entire system is considerably higher in proportion to that of a conventional ship which carries most of its cargo below deck. The dynamics of a high center-of-gravity barge rolling in seaways can become difficult to model and predict because of the highly nonlinear characteristics encountered. Accidental capsize of log barges (which

have very similar geometry and loading conditions as those considered in this study) under average to calm sea condition has been well documented (McAllister 1995).

1.3 Scope

The scope of this study is to model the barge response when subjected to beam sea conditions as a SDOF system for roll motion. The measured wave, either regular or random, is input into a computer program which uses a fourth-order Runge-Kutta integration method to numerically predict roll motion response. The simulated results are compared to measured data to determine the best system damping parameters. Four different forms of the damping moment of the SDOF model are analyzed. In each form all coefficients are known except for the linear and nonlinear damping parameters. Each form uses a combination of relative motion "Morison" damping and/or linear structural damping. Predicted results of the four forms of the damping moment are examined to determine the most suitable model. A sensitivity study on the response to various system parameters is then conducted on the selected form. Each form of the model uses a thirteenth-order polynomial restoring moment. An analysis is also conducted to determine the effects of using lower order terms to represent the restoring moment. Finally, results of the SDOF model from this report are compared with a 3DOF and a 2DOF model subjected to the same wave environment to determine which model more accurately predicts roll response.

2.0 System Description

The system considered in this analysis is that of a free floating barge subjected to regular and random waves in open seaways. In general, a six degree-of-freedom (6DOF) model is required to fully specify the motions of the barge. Subjecting a barge to beam seas would be considered the most critical scenario for barge capsize. This simplifies the equations of motion because under ideal beam conditions, the response motions for a barge may be described by a three degree-of-freedom (3DOF) model with heave, sway and roll represented by

$$
\begin{aligned}
&m\ddot{y} + m_{a_{22}}\cos(\frac{\partial\eta}{\partial y})(\ddot{y}-\dot{v}) + m_{a_{33}}\sin(|\frac{\partial\eta}{\partial y}|)(\ddot{y}-\dot{v}) + C_{22_L}(\dot{y}-v) \\
&\quad + C_{22_N}(\dot{y}-v)|\dot{y}-v| - m\dot{\phi}\dot{z} - m(z_g\cos\phi)\ddot{\phi} \\
&\quad + R_{33}(\phi,z,\eta,\frac{\partial\eta}{\partial y})\sin(\frac{\partial\eta}{\partial y}) + K_{moor}y = 0 \\
&m\ddot{z} + m_{a_{33}}\cos(\frac{\partial\eta}{\partial y})(\ddot{z}-\dot{w}) + m_{a_{22}}\sin(|\frac{\partial\eta}{\partial y}|)(\ddot{z}-\dot{w}) + C_{33_L}(\dot{z}-w) \\
&\quad + C_{33_N}(\dot{z}-w)|\dot{z}-w| + m\dot{\phi}\dot{y} - m(z_g\cos\phi)\dot{\phi}^2 + mg \\
&\quad + R_{33}(z,\phi,\eta,\frac{\partial\eta}{\partial y})\cos(\frac{\partial\eta}{\partial y}) = 0 \\
&I_{44}\ddot{\phi} + I_{a_{44}}(\ddot{\phi}-\frac{\partial\ddot{\eta}}{\partial y}) + C_{44_L}(\dot{\phi}-\frac{\partial\dot{\eta}}{\partial y}) + C_{44_N}(\dot{\phi}-\frac{\partial\dot{\eta}}{\partial y})|\dot{\phi}-\frac{\partial\dot{\eta}}{\partial y}| \\
&\quad + m(z_g\cos\phi)\dot{\phi}\dot{z} - m(z_g\cos\phi)\ddot{y} + R_{44}(\phi,z,\eta,\frac{\partial\eta}{\partial y})\cos(\frac{\partial\eta}{\partial y}) \\
&\quad - mgz_g\sin\phi = 0
\end{aligned}
\tag{2.1}
$$

(see Bartel 1996 for derivation and definitions). Although this model is significantly simpler than a large number of time domain large body analysis models based on potential theory, it is evident that these equations are still relatively involved and computationally intensive to solve numerically compared to that of a SDOF model.

The 3DOF model based on these equations is currently being analyzed under a separate study (Bartel 1996).

2.1 Assumptions

There are several assumptions made in the development and application of the model equations for this analysis. The first is that the nominal wave length is significantly greater than the beam of the barge. As a result, the wave surface can be assumed linear across the beam. Secondly, wave forces and moments act at the center of gravity in lieu of integrating pressure over the surface. Finally, it is assumed that roll response can be uncoupled from heave and sway, therefore the focus will be only on the pure roll motion of the barge modeled by a SDOF system.

2.2 Equation of Motion

Uncoupled roll motion subjected to beam sea conditions, assuming long wave excitation and deep water conditions, is modeled by the equation

$$I_{44}\ddot{\phi} + I_{A44}(\ddot{\phi} - \partial\ddot{\eta}/\partial y) + C_{44L}(\dot{\phi} - \partial\dot{\eta}/\partial y) + C_{44N}(\dot{\phi} - \partial\dot{\eta}/\partial y)\,|\,\dot{\phi} - \partial\dot{\eta}/\partial y\,| + R_{44}(\phi,\eta,\partial\eta/\partial y) = 0 \qquad (2.2)$$

where I_{44} is the rotational inertia (in air) of the vessel about the roll axis, I_{A44} the hydrodynamic added inertia, $\ddot{\phi}$ the roll acceleration, $\partial\ddot{\eta}/\partial y$ the wave slope acceleration, C_{44L} the linear damping coefficient, $\dot{\phi}$ the roll velocity, $\partial\dot{\eta}/\partial y$ the wave slope velocity, C_{44N} the nonlinear damping coefficient, and $R_{44}(\phi,\eta,\partial\eta/\partial y)$ the nonlinear restoring moment.

2.3 Description of Wave Field

Based on linear wave theory, the velocity potential and related wave profile, time derivatives and partial spatial derivatives are as follows:

$$
\begin{aligned}
\Phi &= A\frac{g}{\omega}\frac{\cosh k(h+z)}{\cosh(kh)}\sin(ky - \omega t) \\
\eta &= \frac{1}{g}\frac{\partial \Phi}{\partial t}\Big|_{z=0} = A\cos(ky - \omega t) \\
\dot{\eta} &= \frac{\partial \eta}{\partial t} = \omega A\sin(ky - \omega t) \\
\ddot{\eta} &= \frac{\partial \dot{\eta}}{\partial t} = -\omega^2 A\cos(ky-\omega t) \\
\eta' &= \frac{\partial \eta}{\partial y} = -kA\sin(ky - \omega t) \\
\dot{\eta}' &= \frac{\partial \dot{\eta}}{\partial y} = \omega kA\cos(ky - \omega t) \\
\ddot{\eta}' &= \frac{\partial \ddot{\eta}}{\partial y} = \omega^2 kA\sin(ky - \omega t)
\end{aligned}
\tag{2.3}
$$

If deep water wave conditions are applied and water particle characteristics are considered at the surface, the wave number, k, can be represented by

$$k=\frac{\omega^2}{g} \tag{2.4}$$

and the resulting wave field characteristics reduce to

$$
\begin{aligned}
\eta &= A\cos(ky - \omega t) \\
\dot{\eta} &= \omega A\sin(ky - \omega t) \\
\ddot{\eta} &= -\omega^2\eta \\
\eta' &= -\frac{\omega}{g}\dot{\eta} \\
\dot{\eta}' &= \frac{\omega^3}{g}\eta \\
\ddot{\eta}' &= \frac{\omega^3}{g}\dot{\eta}
\end{aligned}
\tag{2.5}
$$

2.4 Inertia and Added Inertia Coefficients

For a given barge, the rotational inertia, I_{44}, can be analytically computed. The hydrodynamic added inertia, I_{A44}, depends on the frequency of the barge roll motion. The value of the added inertia under the range of frequencies of the roll motion response observed in this study is relatively constant. Therefore, a constant added inertia coefficient is adopted for convenience of analysis. The first two terms of equation 2.2 represent the inertial moment of the barge in air, $I_{44}\ddot{\phi}$, and the relative motion added inertia moment, $I_{A44}(\ddot{\phi}\text{-}\partial\ddot{\eta}/\partial y)$, respectively. The term $(\ddot{\phi}\text{-}\partial\ddot{\eta}/\partial y)$ is the relative motion between the roll acceleration of the barge and the wave slope acceleration resulting from wave excitation. For this analysis, the value of I_{44} = 2.161046e6 slug-ft^2 (Paulling 1995). With this information and knowing the natural period of the barge is approximately 5 seconds, the added inertia is calculated to be I_{A44} = 1.3725e6 slug-ft^2.

2.5 Damping Moment

In equation 2.2, the damping moment resulting from radiation of waves from the barge (corresponding to linear energy dissipation in potential theory) is represented by the linear term, $C_{44L}(\dot{\phi}-\partial\dot{\eta}/\partial y)$. The effects of damping resulting from flow separation and turbulence are represented by the nonlinear Morison term, $C_{44N}(\dot{\phi} - \partial\dot{\eta}/\partial y)\,|\,\dot{\phi} - \partial\dot{\eta}/\partial y\,|$. C_{44L} and C_{44N} are the linear and nonlinear damping coefficients expressed in the following convenient form:

$$C_{44L}=\frac{2 * \omega_n * \xi_L}{I_T} \qquad C_{44N}=\frac{2 * \omega_n * \xi_N}{I_T} \tag{2.6}$$

where ω_n is the "natural frequency" of the barge (determined by small amplitude free vibration tests) and is equal to approximately 5 seconds (Yim et al. 1995). ξ_N and ξ_L are the damping parameters associated with the linear and nonlinear damping terms (to be determined by system identification and/or numerical iteration). The terms have been normalized by the sum of the inertia and added inertia terms, $I_T = I_{44} + I_{A44}$. The term $(\dot{\phi} - \partial\dot{\eta}/\partial y)$ is the relative motion between the roll velocity of the barge and the wave slope velocity resulting from wave excitation.

2.6 Roll Restoring Moment

The restoring moment term, $R_{44}(\phi,\eta,\partial\eta/\partial y)$, represents the moment created from buoyancy and gravity forces acting on the barge under static conditions. The restoring moment is a thirteenth-order (13th-order) polynomial made up of coefficients of the righting moment curve multiplied by the corresponding power of

the relative motion between the roll displacement and the wave slope as shown in the following equation:

$$R_{44}(\phi,y,\partial\eta/\partial y) = \frac{B_{13,5}(\phi-\partial\eta/\partial y)^1}{I_T} + \frac{B_{11,5}(\phi-\partial\eta/\partial y)^3}{I_T} + \frac{B_{9,5}(\phi-\partial\eta/\partial y)^5}{I_T} + \frac{B_{7,5}(\phi-\partial\eta/\partial y)^7}{I_T} + \frac{B_{5,5}(\phi-\partial\eta/\partial y)^9}{I_T} + \frac{B_{3,5}(\phi-\partial\eta/\partial y)^{11}}{I_T} + \frac{B_{1,5}(\phi-\partial\eta/\partial y)^{13}}{I_T} \quad (2.7)$$

The coefficients $B_{1,5}$, $B_{3,5}$, etc. are established by fitting a thirteenth-order polynomial to the righting-moment curve shown in Figure 2.1 (Yim et al. 1995). The term is normalized by the total inertia, I_T. Although a lower-order polynomial can be used with sufficient accuracy for small angle motions, the additional time and effort associated with using a thirteenth-order polynomial is minimal, and in the case of large angle motions, the higher order terms are essential.

2.7 Various Forms of Roll Equation of Motion

Several combinations of the terms representing the damping moment in the equation of motion are examined here. In addition to equation 2.2 which uses relative motions in both the linear and nonlinear damping terms, models which approximately account for and neglect different physical effects will be analyzed. One combination assumes the magnitude of the wave-slope velocity is negligible compared to the roll velocity (e.g. near roll resonance). As a result only the roll velocity component will be considered in the linear and nonlinear damping terms. This is modeled by equation 2.8:

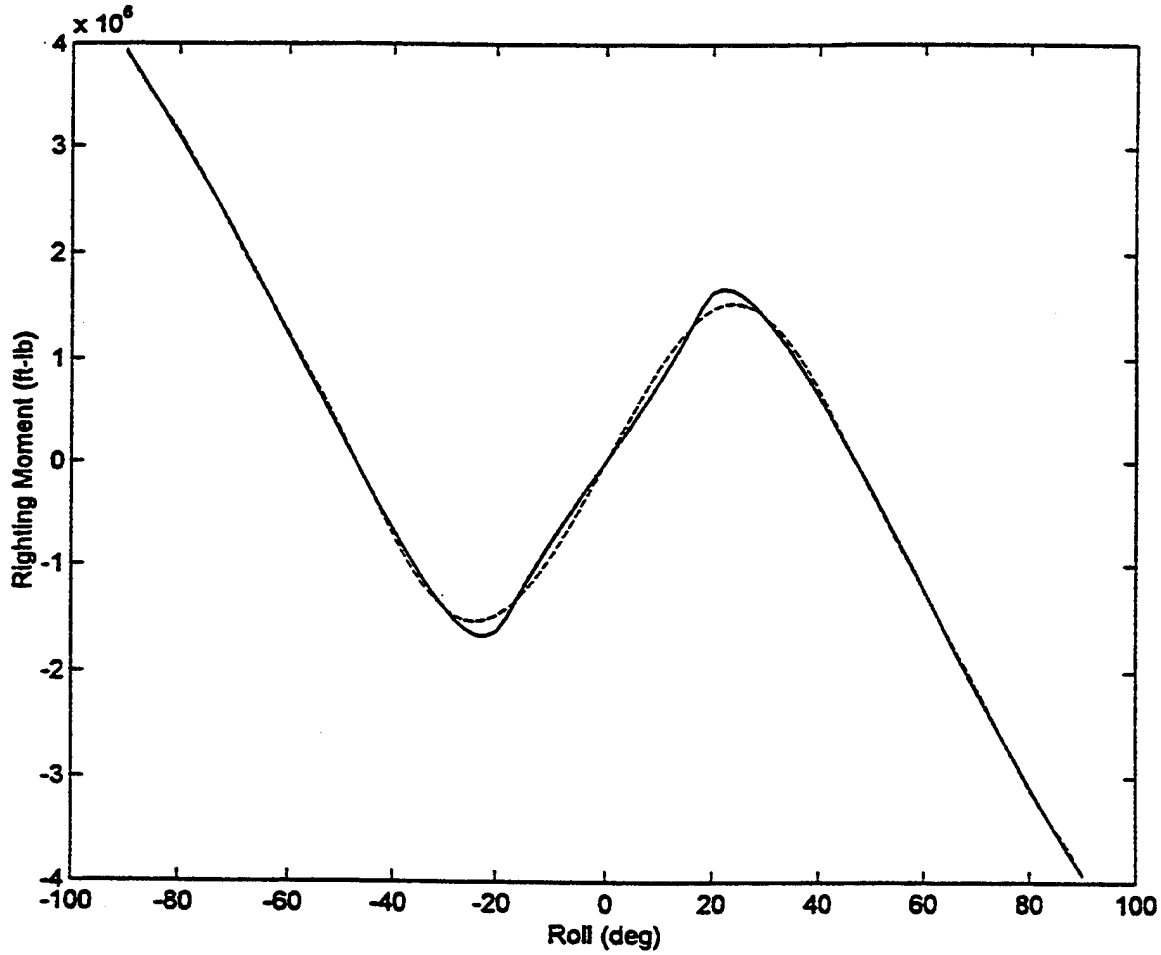

Figure 2.1 13th Order Roll Restoring Moment Curve. - numerical (Paulling 1995) -- polynomial fit (Yim et al. 1995). $B_{13,5}$ = 5.6051e6, $B_{11,5}$ =-1.1657e6, $B_{9,5}$= 1.7258e6, $B_{7,5}$= 9.6915e6, $B_{5,5}$= -9.3298e6, $B_{3,5}$= 3.3999e6, $B_{1,5}$= -4.4569e6.

$$I_{44}\ddot{\phi} + I_{A44}(\ddot{\phi} - \partial\ddot{\eta}/\partial y) + C_{44L}\dot{\phi} + C_{44N}\dot{\phi}\,|\,\dot{\phi}\,| + R_{44}(\phi,\eta,\partial\eta/\partial y) = 0 \tag{2.8}$$

Equation 2.9 below assumes that the linear damping coefficient is dominated by the barge characteristics (damping induced by the presence of mooring lines in the experiments which is not modeled explicitly in this study). The relative motion between the barge and wave slope velocity is accounted for only in the nonlinear damping term.

$$I_{44}\ddot{\phi} + I_{A44}(\ddot{\phi} - \partial\ddot{\eta}/\partial y) + C_{44L}\dot{\phi} + C_{44N}(\dot{\phi} - \partial\dot{\eta}/\partial y)\,|\,\dot{\phi} - \partial\dot{\eta}/\partial y\,| + R_{44}(\phi,\eta,\partial\eta/\partial y) = 0 \tag{2.9}$$

The final form of the model to be analyzed is equation 2.10:

$$I_{44}\ddot{\phi} + I_{A44}(\ddot{\phi} - \partial\ddot{\eta}/\partial y) + C_{44N}(\dot{\phi} - \partial\dot{\eta}/\partial y)\,|\,\dot{\phi} - \partial\dot{\eta}/\partial y\,| + R_{44}(\phi,\eta,\partial\eta/\partial y) = 0 \tag{2.10}$$

This model assumes that damping effects are strictly nonlinear and relative motion between the wave slope velocity and barge roll velocity significantly influences the roll response.

3.0 Model Tests and Identification of Damping Parameters

The four different forms of the model for roll motions are analyzed to determine which form best predicts roll response when the barge is subjected to beam sea conditions. In each case, the prototype measured wave is sampled at 2 Hertz (Hz). The data is then filtered so that frequencies above 0.25 Hz are disregarded because they do not contribute to the response motion. Wave profile and water particle velocity as well as wave slope, wave slope velocity and wave slope acceleration are then numerically computed. Regular wave cases analyzed are that of the 5, 6, 8, and 10 sec waves with a desired 6 ft wave height. In addition, two random cases are modeled; a Bretschneider spectrum of 6 ft significant wave height and 8 sec dominant wave period, and a white noise spectrum of 6 ft significant wave height and wave periods ranging from 4 to 20 secs.

In each of the forms, all terms are known except for the linear and nonlinear damping parameters, ξ_L and ξ_N used in the damping coefficients, C_{44L} and C_{44N}. An initial estimate for the damping parameters is obtained through system identification procedures. By comparing the standard deviation of predicted roll response to measured roll response, an iterative approach is then used to identify the most appropriate damping parameters for the model. The inertia coefficients and the nonlinear restoring moment coefficients, constant for all the wave cases, are determined through experimental measurements or computer analysis. The other coefficients are determined through the measured data for each particular wave excitation test.

3.1 Model Test Procedure

Regular and random wave model tests have been conducted on a single barge to simulate response in open seas. The facility used to conduct the tests was a 48 ft wide, 250 ft long basin which was capable of generating long crested waves up to 3 ft in height. A 1/16 scale model of the 120 ft long, 25 ft wide and 8 ft deep full scale barge was used. For this analysis, only results of the barge subjected to beam sea conditions are examined. Although the objective of the tests is to simulate motions of the barge in open seas, mooring lines were attached to the model to prevent it from drifting down the basin. The length, weight and sag of the mooring lines are designed to ensure the natural period of the mooring system would be much larger than the wave excitation period.

The particular wave conditions generated for this report were 4 regular wave and 2 random wave tests. Regular waves of approximately 6 ft wave height (full scale) were conducted for wave periods of 5, 6, 8 and 10 secs. The random wave tests were for a Bretschneider spectrum of 6 ft significant wave height with and 8 sec dominant wave period, and for a band limited "white noise" test of 6 ft significant wave height with wave periods ranging from 4 to 20 secs. Model tests were run until steady state had been reached before data collection began. Only 1024 secs (17 minutes) of data was collected for each run in order to avoid significant energy accumulation from wave reflection, re-reflection and other "tank noise" which might build up over time and could corrupt the wave excitation.

3.2 Description of Analytical Prediction Procedure

Test SB26, the 6 ft, 5 sec regular wave, will be used as an example of the procedure followed to establish damping coefficients and simulated roll response. The entire time series of the measured wave input is examined to confirm the desired wave height and period was consistent with the target spectrum. Figure 3.1a shows the 1024 sec time series used in this analysis. The measured data is then subjected to a low pass filter with cutoff frequency of 0.25 Hz after digital sampling. The filtered wave is then displayed as shown in Figure 3.1b, this is the wave data input into the simulation program. To ensure the input wave for simulation is correct, the spectral densities of the measured and filtered wave are compared as shown in Figure 3.2. The damping parameters for the linear and nonlinear damping coefficients are input into the model equation and the simulation is executed. The results of the measured roll response, Figure 3.1c, are then compared to those of the simulated roll response, Figure 3.1d. A small section of the time series is compared as well, as shown in Figure 3.3. The standard deviation of the measured and simulated data is then compared to ensure the most accurate match of roll response. In the random wave tests, the above procedure is performed and an additional comparison of the spectral and probability densities of roll response are made to ensure the most accurate match of roll response.

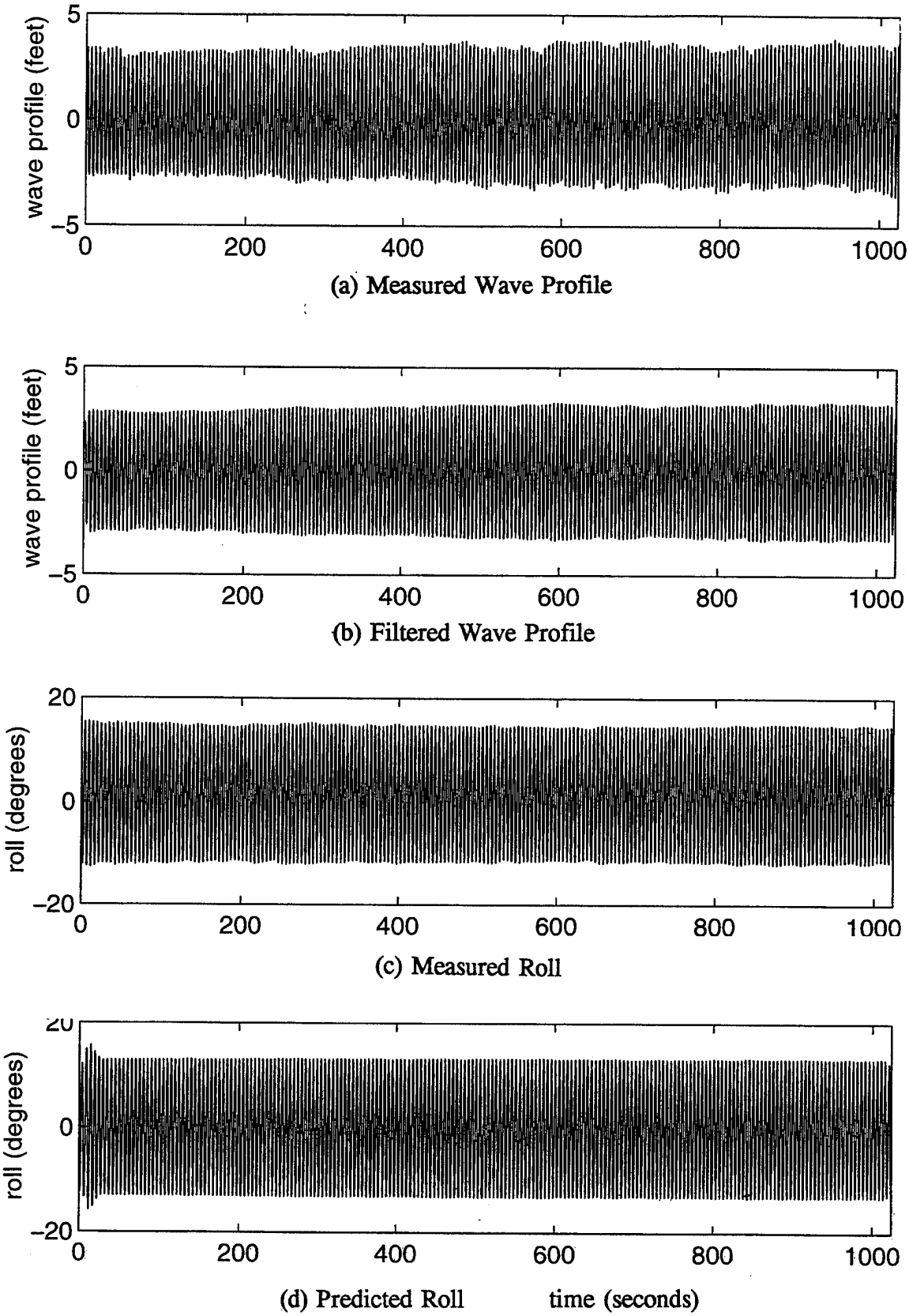

Figure 3.1 Comparison of Measured and Filtered Wave, Measured and Predicted Roll, Regular Wave H= 6.6 Ft, T= 5 Sec (SB26)

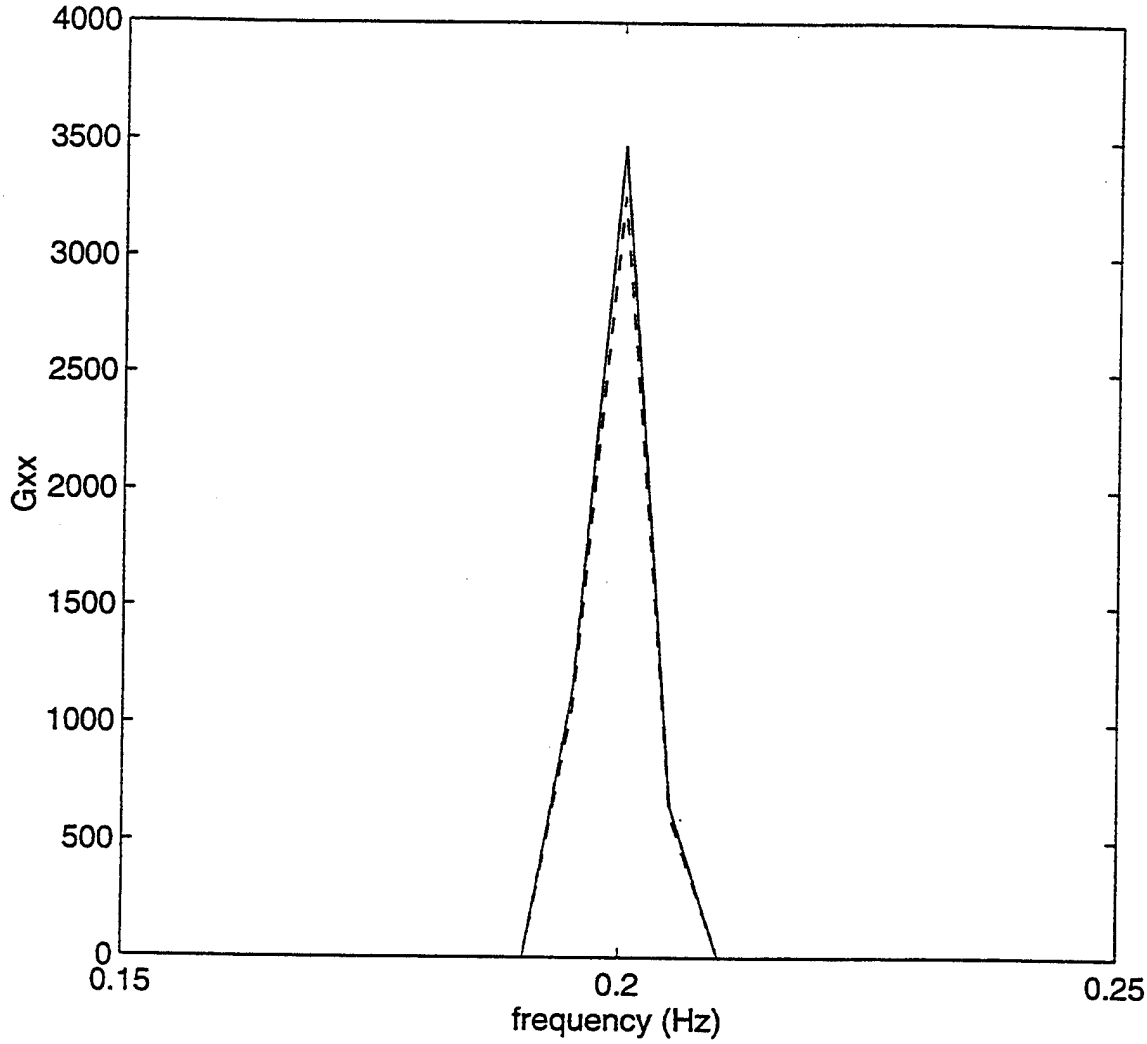

Figure 3.2 Comparison of Spectral Densities (Ft^2/Hz), Measured and Filtered Wave (SB26), - measured, -- predicted

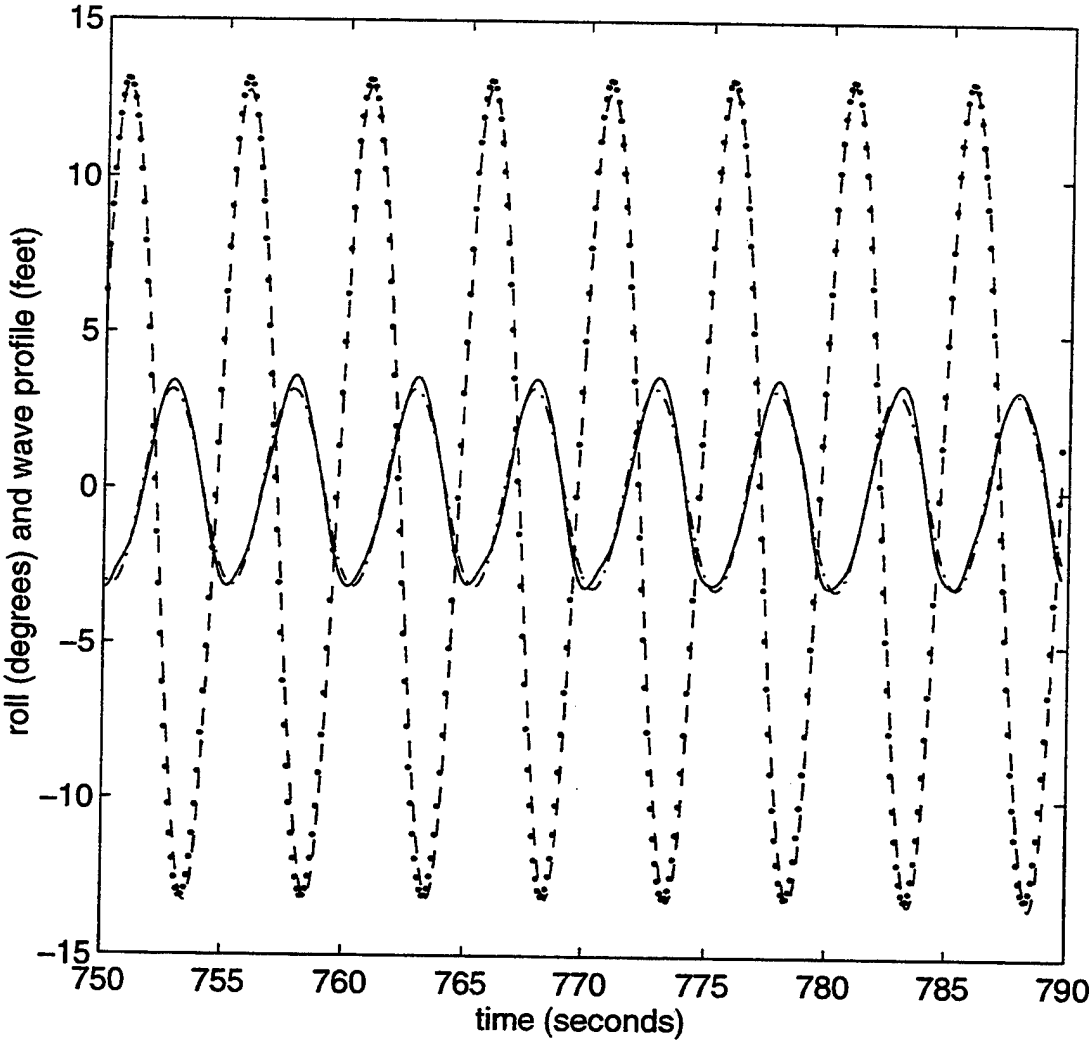

Figure 3.3 Comparison of Measured and Predicted Wave and Roll, Regular Wave, H= 6.6 Ft, T= 5 Secs (SB26)
- measured wave, -. predicted wave, -- measured roll, .. predicted roll.

3.3 Form 1: Relative Motion Damping Moment

The first model to be analyzed is that of equation 2.2:

$$I_{44}\ddot{\phi} + I_{A44}(\ddot{\phi} - \partial\ddot{\eta}/\partial y) + C_{44L}(\dot{\phi} - \partial\dot{\eta}/\partial y) + C_{44N}(\dot{\phi} - \partial\dot{\eta}/\partial y)\,|\,\dot{\phi} - \partial\dot{\eta}/\partial y\,| + R_{44}(\phi,\eta,\partial\eta/\partial y) = 0 \qquad (2.2)$$

Recall this form assumes both the linear (radiation damping) and nonlinear (Morison type local flow separation) have significant influence on the roll motion response. The resulting linear and nonlinear damping coefficients for this model are listed in Table 3.1:

Wave Test	Linear Damping Parameter	Nonlinear Damping Parameter
H=6.6 ft, T=5 sec (SB26)	0.19	0.19
H=6 ft, T=6 sec (SB27)	0.11	0.11
H=7.2 ft, T=8 sec (SB29)	0.80	0.20
H=5.7 ft, T=10 sec (SB30)	0.03	0.07
Bretschneider Spectrum (SB25)	0.04	0.04
White noise Spectrum (SB33)	0.08	0.06

Table 3.1 Linear and Nonlinear Damping Parameters for Form 1, Equation 2.2.

3.3.1 Regular Wave, H= 6 Ft, T= 5 Sec (SB26)

Figure 3.4 represents the roll response of the model barge subjected to a 6.6 ft wave with a 5 sec period. The maximum roll response is approximately 13 degrees. The model indicates a linear damping parameter of 0.19 and a nonlinear damping parameter of 0.19. The amplitude of the measured and predicted response is nearly identical. However, the predicted roll response is out of phase by approximately 1 sec (1/5 period) with the measured data.

3.3.2 Regular Wave, H= 6 Ft, T= 6 Sec (SB27)

Figure 3.5 represents the results of the model barge subjected to a 6 ft regular wave with a 6 sec wave period. The maximum roll response is 11.5 degrees. The model indicates both the linear and nonlinear damping parameters are 0.11. Figure 3.5 shows that amplitude of the predicted roll response matches the measured data well. As in the 5 sec wave case, the predicted roll response is approximately 1 sec (1/6 period) out of phase with the measured data.

3.3.3 Regular Wave, H= 7.2 Ft, T= 8 Sec (SB29)

Figure 3.6 represents the results of the model barge subjected to a 7.2 ft regular wave with an 8 sec wave period. The damping parameters established for this wave test are 0.80 for linear damping and 0.20 for nonlinear damping. Note that the linear damping parameter is significantly higher than the two previous test cases. The maximum roll response of the measured data is 4.1 degrees and is well matched by

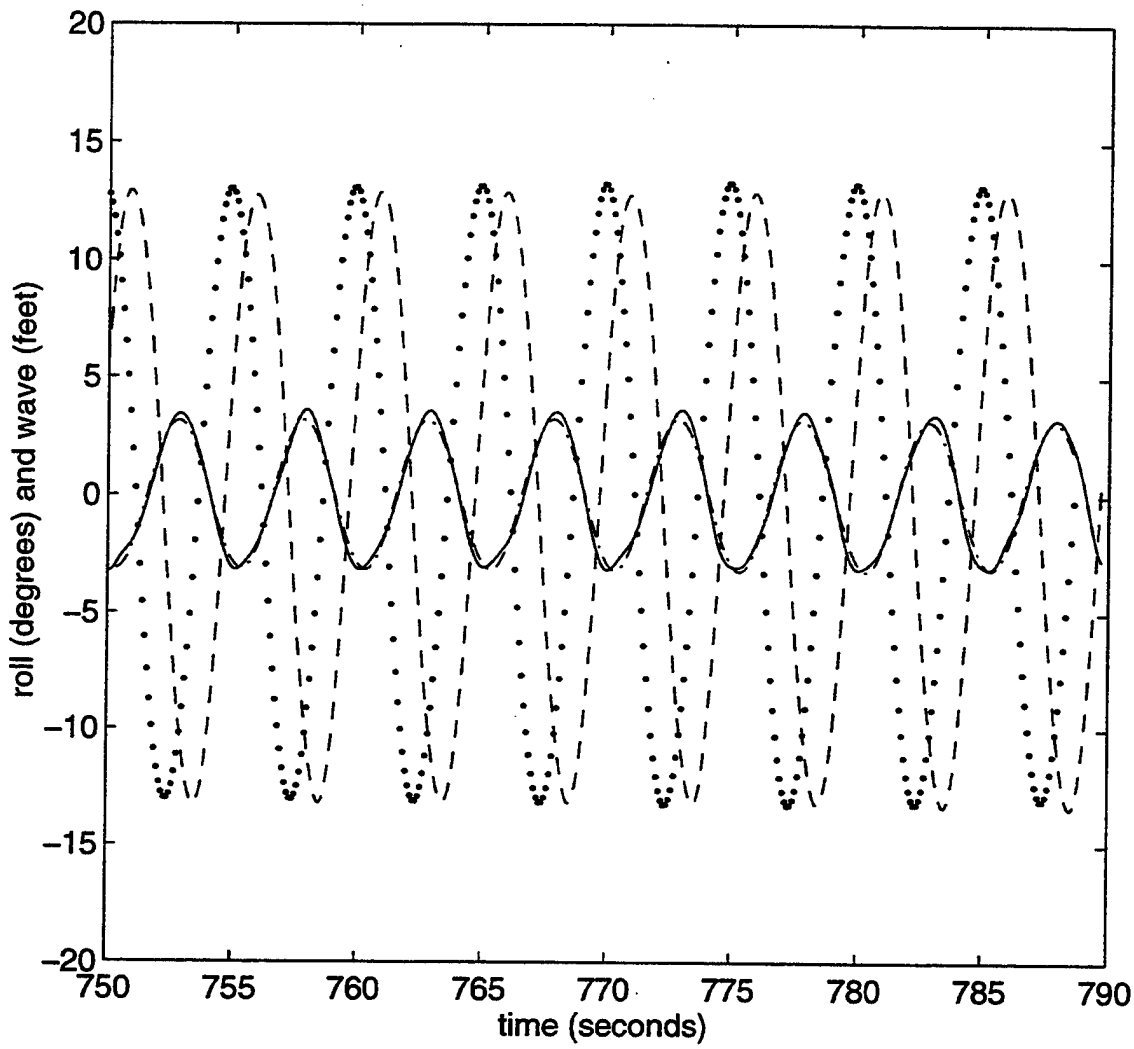

Figure 3.4 Comparison of Measured and Filtered Wave, Measured and Predicted Roll, Regular Wave, H= 6.6 Ft, T= 5 Sec (SB26, eqn 2.2)
- measured wave, -. predicted wave, -- measured roll, .. predicted roll.

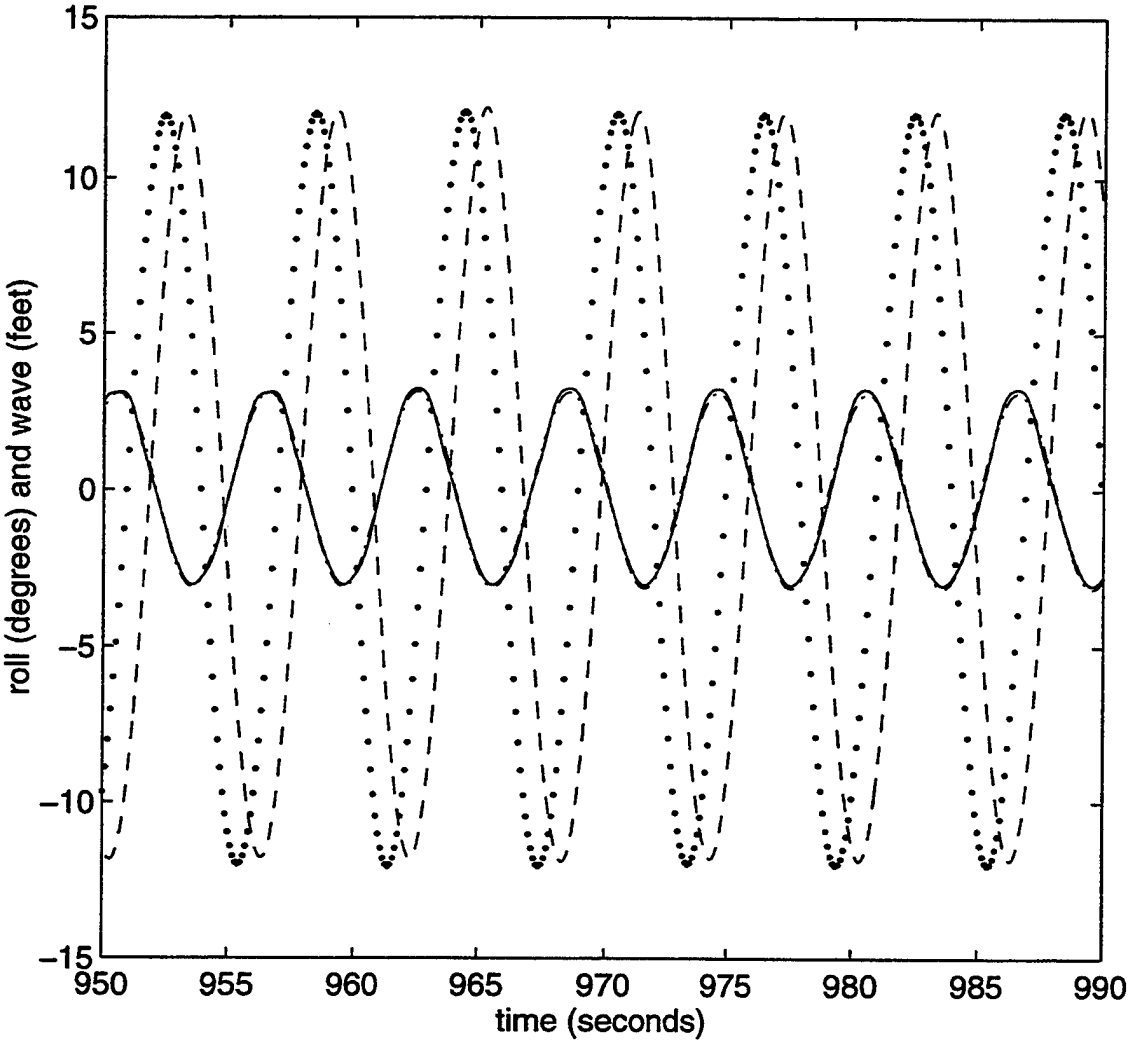

Figure 3.5 Comparison of Measured and Filtered Wave, Measured and Predicted Roll, Regular Wave, H= 6 Ft, T= 6 Sec (SB27, eqn 2.2)
- measured wave, -. predicted wave, -- measured roll, .. predicted roll.

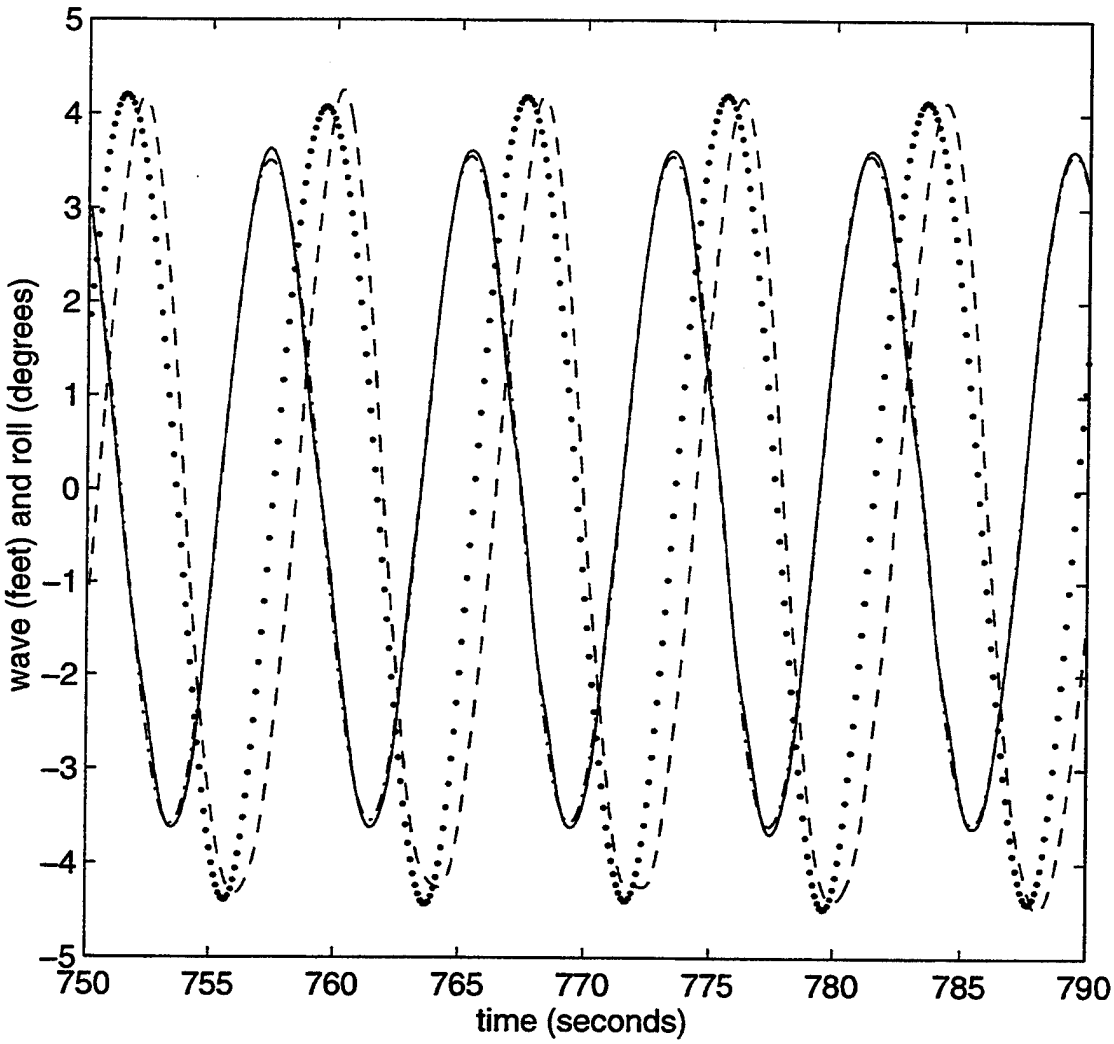

Figure 3.6 Comparison of Measured and Filtered Wave, Measured and Predicted Roll, Regular Wave H= 7.2 Ft, T= 8 Sec (SB29, eqn 2.2)
- measured wave, -. predicted wave, -- measured roll, .. predicted roll.

the predicted response of the model. This form of the model is not able to consistently match the phase of the response. The predicted data appears to be approximately 1 sec (1/8 period) out of phase (at the peak) with the measured data.

3.3.4 Regular Wave, H= 5.7 Ft, T= 10 Sec (SB30)

Test SB30, in which the excitation is a 5.7 ft wave with a 10 sec period, proves to be the most difficult response to match by any form of the model. Because the natural period of the barge is approximately 5 secs, which is a multiple of the wave excitation period, the response contains a superharmonic.

Figure 3.7 represents the best comparison of standard deviation and superharmonic response which could be obtained with the given form of the model equation (equation 2.2). If the damping parameter is increased, the superharmonic characteristics are eliminated. If the damping parameter is decreased, the simulated response amplitude is much greater than the measured response amplitude. The damping parameters used in this figure are 0.03 for the linear coefficient and 0.07 for the nonlinear coefficient. The standard deviation for the measured response is calculated to be 1.84. The standard deviation of the simulated response is 1.90. Figure 3.8 shows a good comparison of the measured and simulated spectral densities for roll response.

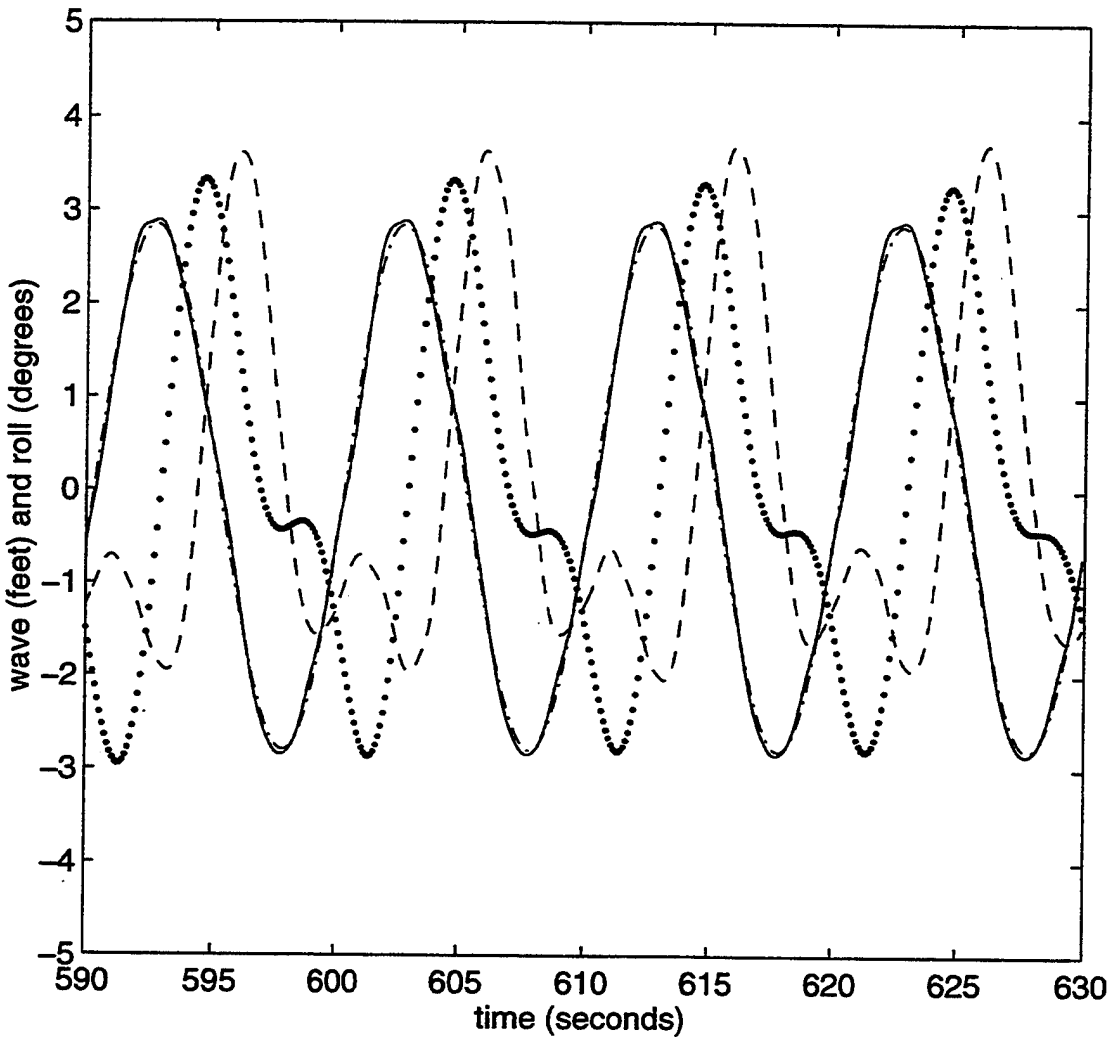

Figure 3.7 Comparison of Measured and Predicted Wave, Measured and Predicted Roll, Regular Wave, H= 5.7 Ft, T= 10 Sec (SB30, eqn 2.2)
- measured wave, -. predicted wave, -- measured roll, .. predicted roll.

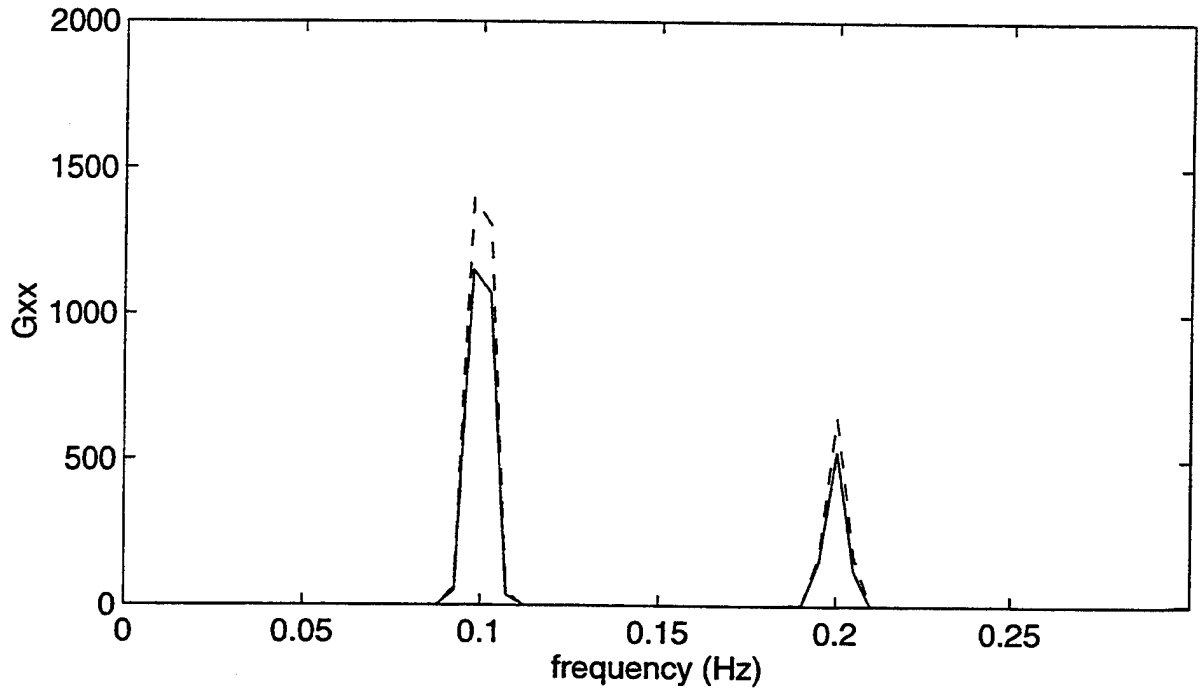

Figure 3.8 Comparison of Spectral Densities (Deg^2/Hz), Measured and Predicted Roll, H= 5.7 Ft, T= 10 Sec (SB30, eqn 2.2), - measured, -- predicted

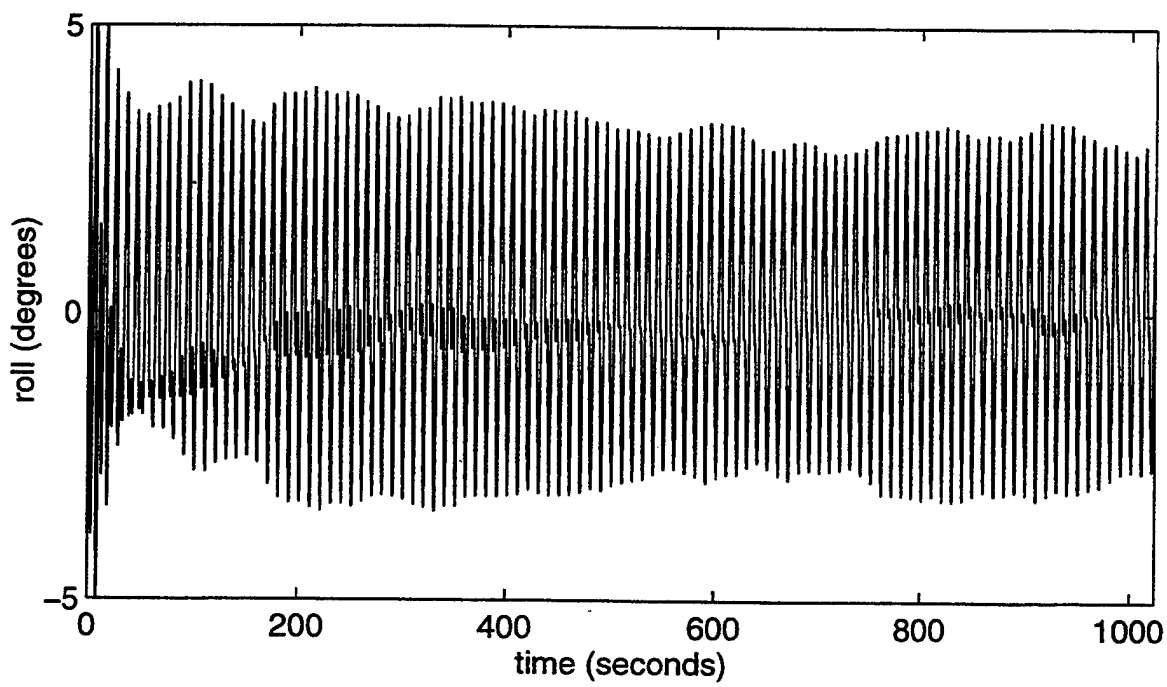

Figure 3.9 1024 Sec Time Series of Predicted Roll, H= 5.7 Ft, T= 10 Sec (SB30, eqn 2.2)

Figure 3.9 provides a representation of predicted roll response for the entire 1024 sec time series. It is evident that the superharmonic does not occur in all locations with the same amplitude. A parametric study presented in a later section of this report will provide a better understanding of the effects of varying the linear and nonlinear damping parameters.

3.3.5 Bretschneider Spectrum, Hs= 6 Ft, Tp= 8 Sec (SB25)

Figure 3.10a - 3.10d represent the measured and filtered wave input and the resulting measured roll response and predicted roll response (to filtered wave excitation) for a Bretschneider wave spectrum. As shown in Figure 3.11, the spectral densities of the measured and filtered wave excitation input are compared to ensure the proper input is being used for prediction. The damping parameters used for prediction are equal to 0.04 for both the linear and the nonlinear terms. A visual comparison of Figures 3.10c and 3.10d indicates the model provides an accurate prediction. The standard deviation for the predicted roll response is 3.95 which compared favorably to the standard deviation of 3.95 for the measured data. Figure 3.12 indicates the spectral densities are a very close match. The final comparison made between measured and simulated data is a histogram of roll response. Figures 3.13a and b confirm that the model provides an accurate representation of roll response motion.

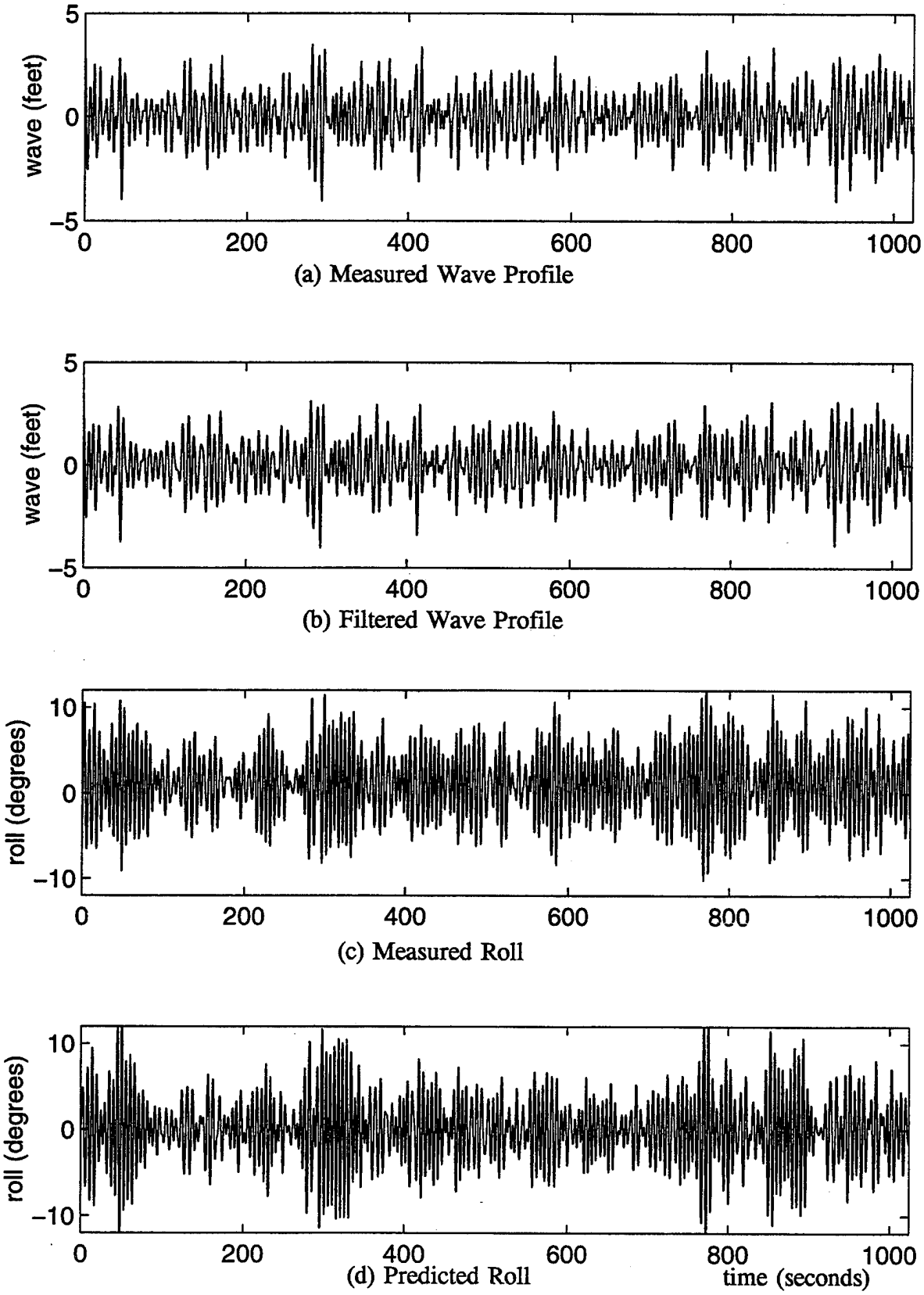

Figure 3.10 Comparison of Measured and Filtered Wave, Measured and Predicted Roll, Bretschneider Spectrum, Hs= 6 Ft, Tp= 8 Sec (SB25, eqn 2.2)

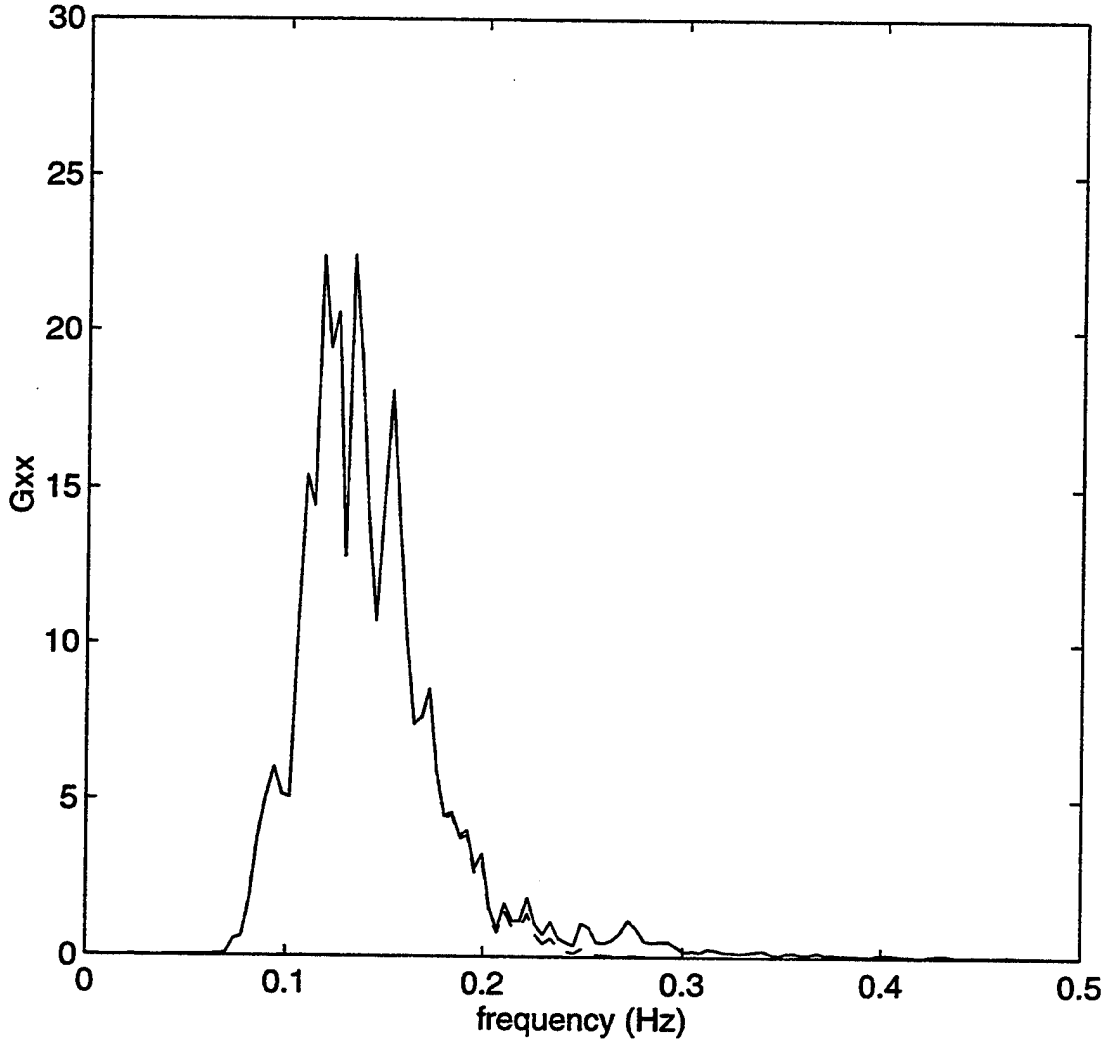

Figure 3.11 Comparison of Spectral Densities (Ft^2/Hz), Measured and Filtered Wave, Bretschneider Spectrum Hs= 6 Ft, Tp= 8 Sec (SB25, eqn 2.2)
- measured, -- predicted

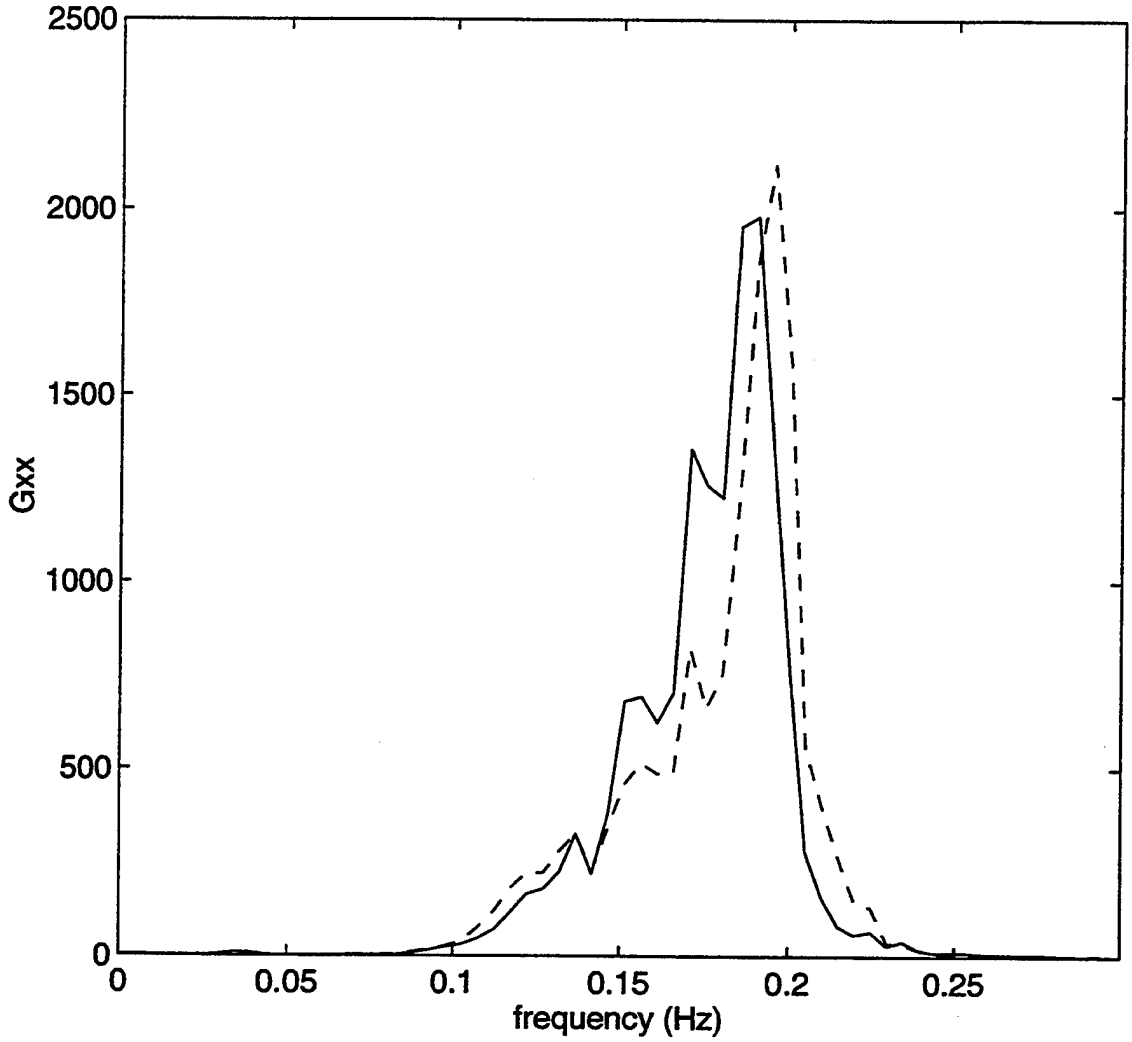

Figure 3.12 Comparison of Spectral Densities, Measured and Predicted Roll (Deg^2/Hz), Bretschneider Spectrum , Hs= 6 Ft, Tp= 8 Sec (SB25, eqn 2.2)
- measured, -- predicted

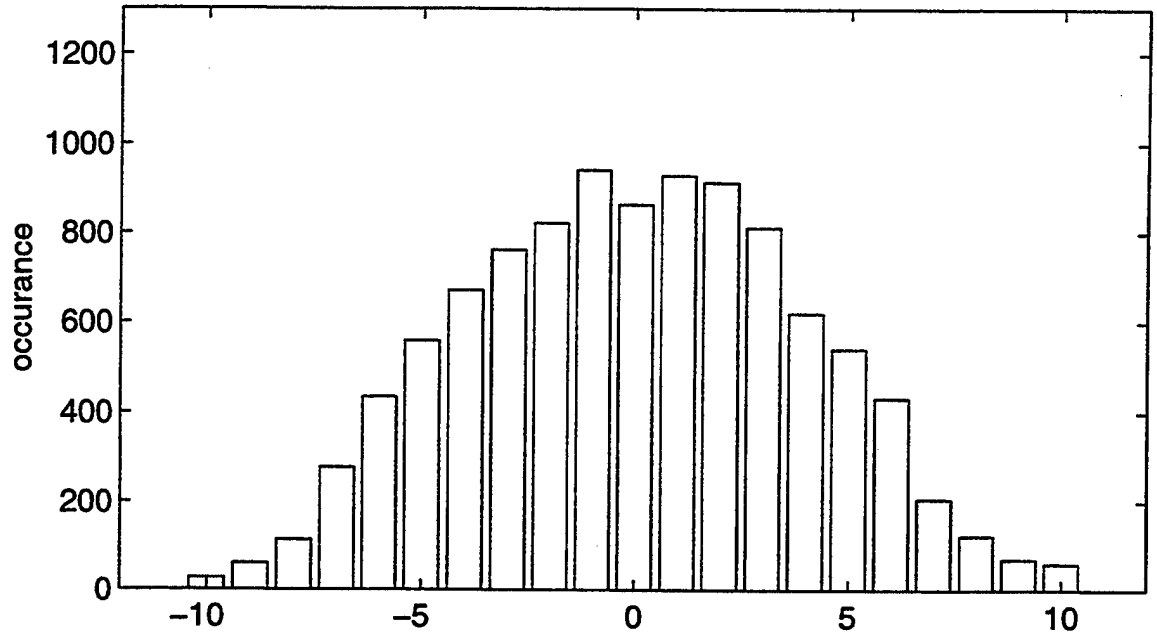

(a) Measured Roll Amplitude (degrees)

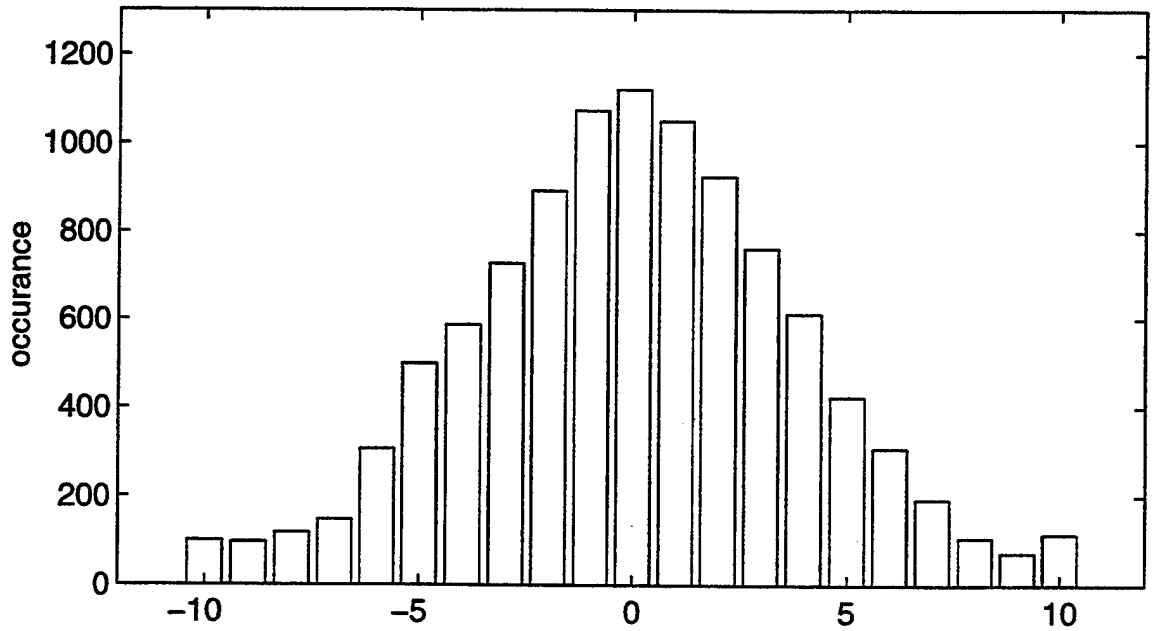

(b) Predicted Roll Amplitude (degrees)

Figure 3.13 Histograms of Measured and Predicted Roll, Bretschneider Spectrum (SB25, eqn 2.2)

3.3.6 White Noise Excitation, Hs= 6 Ft (SB33)

Figures 3.14a through 3.14d represent the measured and predicted wave input and measured and predicted roll response for a white noise excitation with wave periods of 4 to 20 secs and a 6 ft significant wave height. A comparison of the spectral densities, Figure 3.15, confirms that the simulated wave input matches the measured wave excitation. The linear and nonlinear damping parameters used in the model are 0.08 and 0.06 respectively. A visual comparison of Figures 3.14c and 3.14d indicate the model provides a good simulation of roll response. The standard deviation of predicted roll response, 5.30, compared well with the measured roll response which is 5.29. A comparison of spectral densities, Figures 3.16, and histograms, Figures 3.17a and 3.17b, confirm that measured and predicted roll response compare quite well. Note that the there is a significant increase in probability mass at the extreme values. This behavior is typical of nonlinear systems with a softening stiffness (which is the case for barge roll motion).

3.4 Form 2: Relative Motion Neglected in Damping Moment

The second form of damping representation to be examined is the following

$$I_{44}\ddot{\phi} + I_{A44}(\ddot{\phi} - \frac{\partial \ddot{\eta}}{\partial y}) + C_{44L}\dot{\phi} + C_{44N}\dot{\phi}\,|\,\dot{\phi}\,| + R_{44}(\phi, \eta, \frac{\partial \eta}{\partial y}) = 0 \qquad (2.8)$$

In this form, the relative motion between the wave slope velocity and the barge roll velocity is neglected. As a result, only the barge roll velocity contributes to the equation. The following results will show this model displays an equal ability to

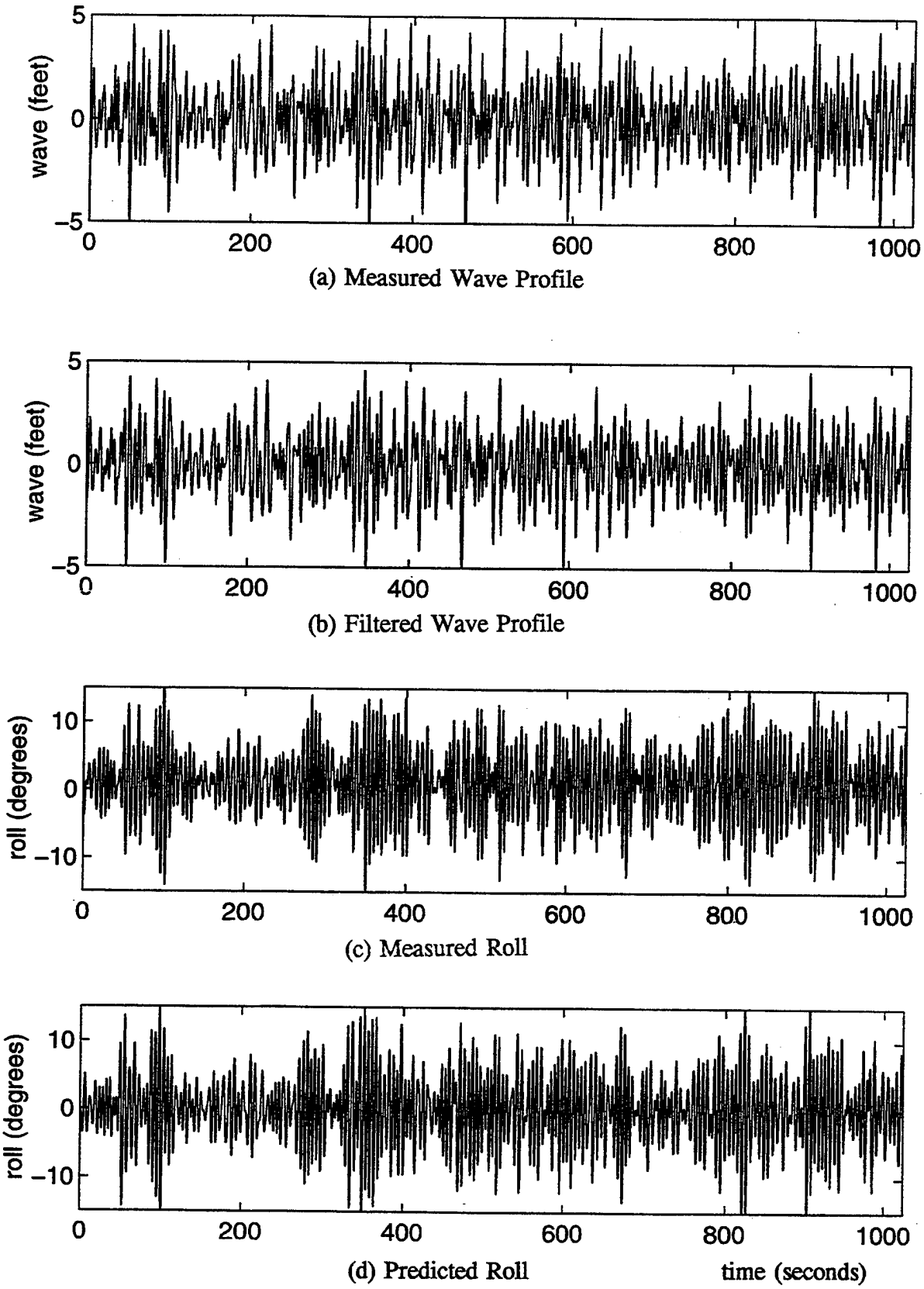

Figure 3.14 Comparison of Measured and Filtered Wave, Measured and Predicted Roll, White Noise Spectrum, Hs= 6 Ft (SB33, eqn 2.2)

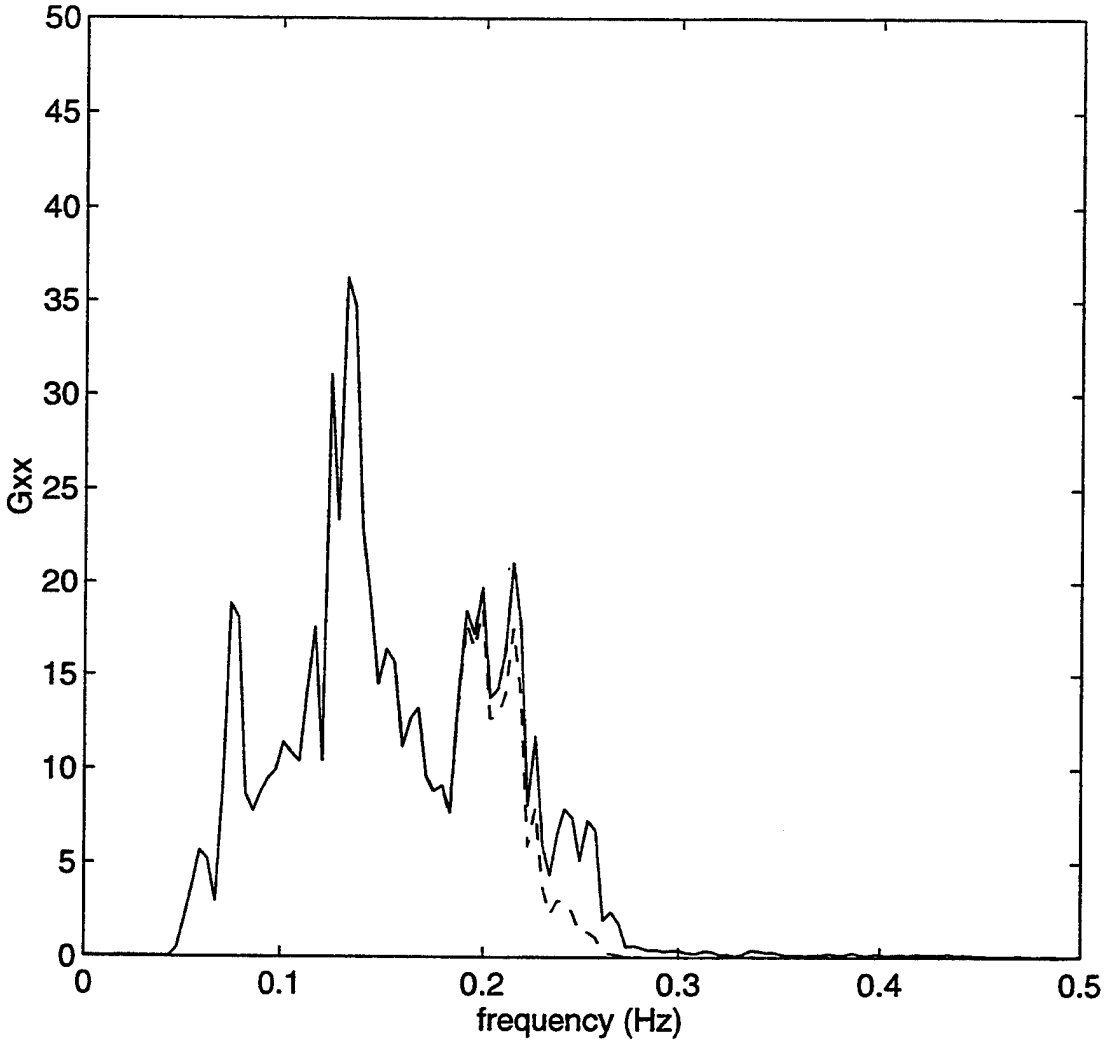

Figure 3.15 Comparison of Spectral Densities (Ft^2/Hz), Measured and Filtered Wave, White Noise Spectrum, Hs= 6 Ft (SB33, eqn 2.2), - measured, -- predicted

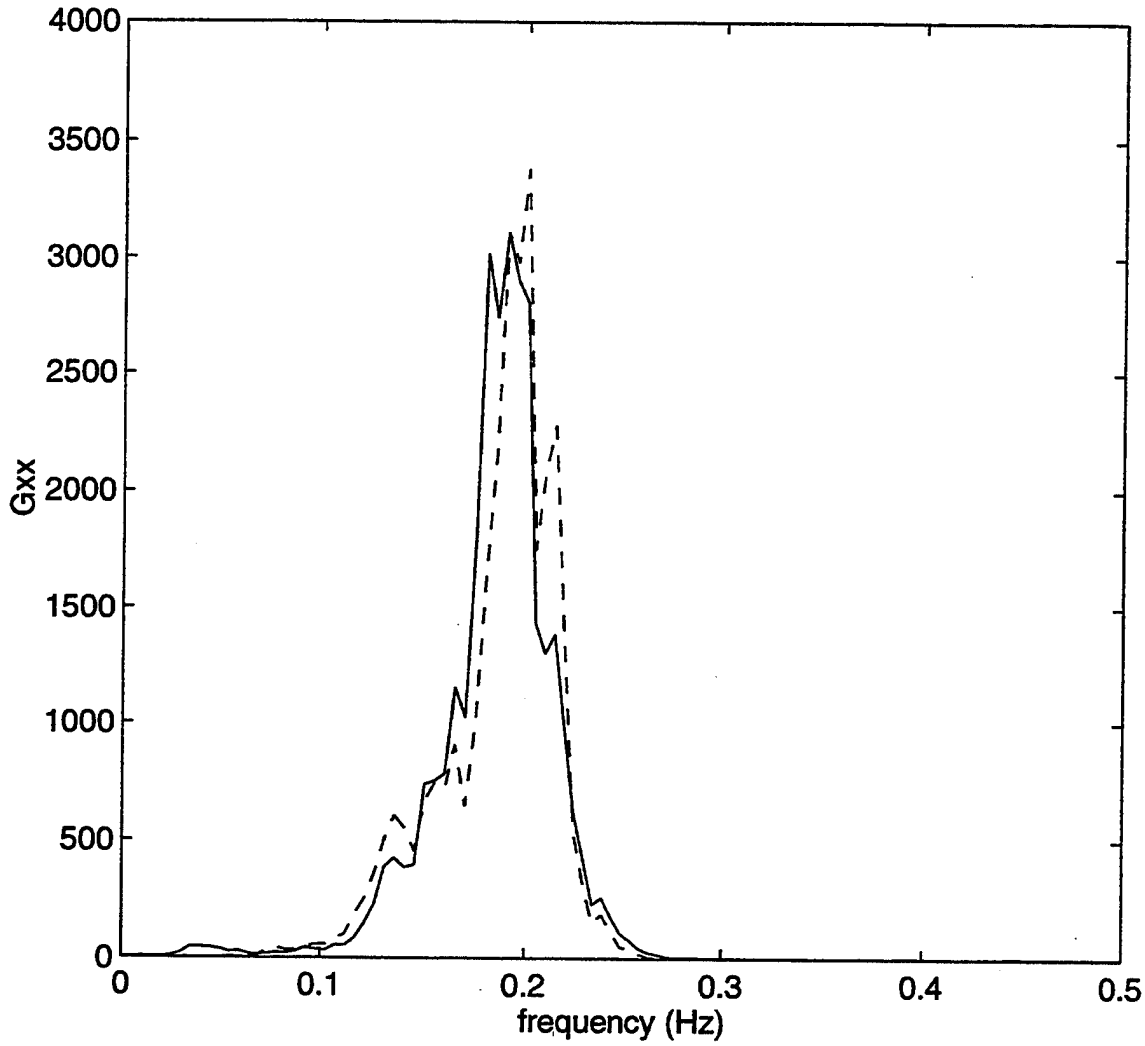

Figure 3.16 Comparison of Spectral Densities (Deg^2/Hz), Measured and Predicted Roll, White Noise Spectrum, Hs= 6 Ft (SB33, eqn 2.2), - measured, -- predicted

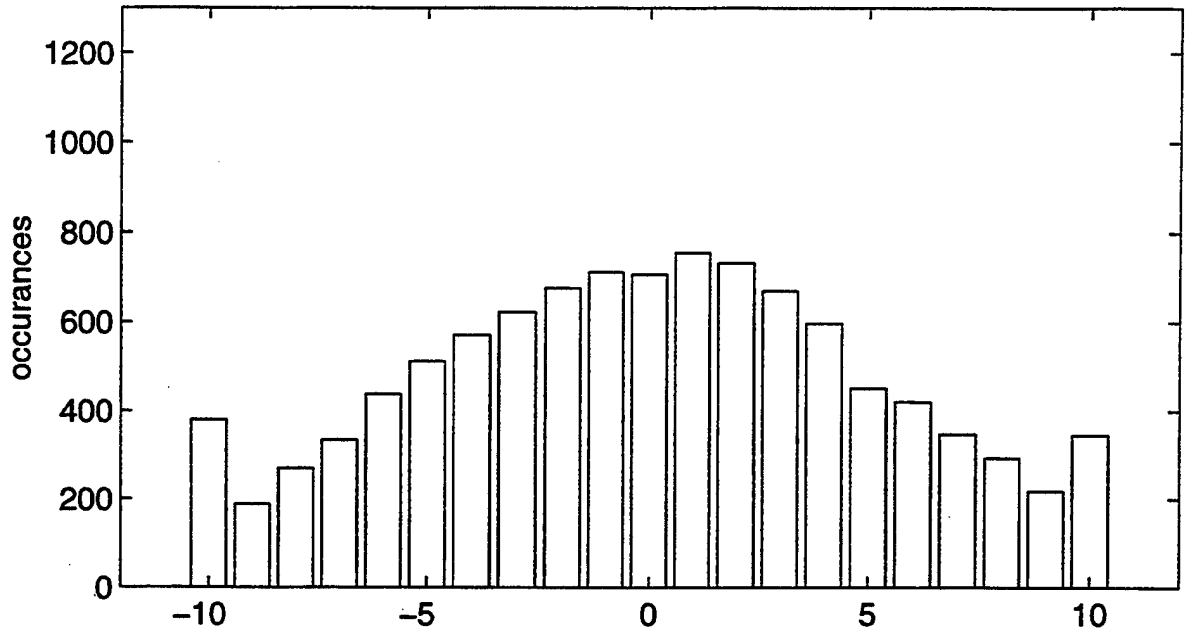

(a) Measured Roll Amplitude (degrees)

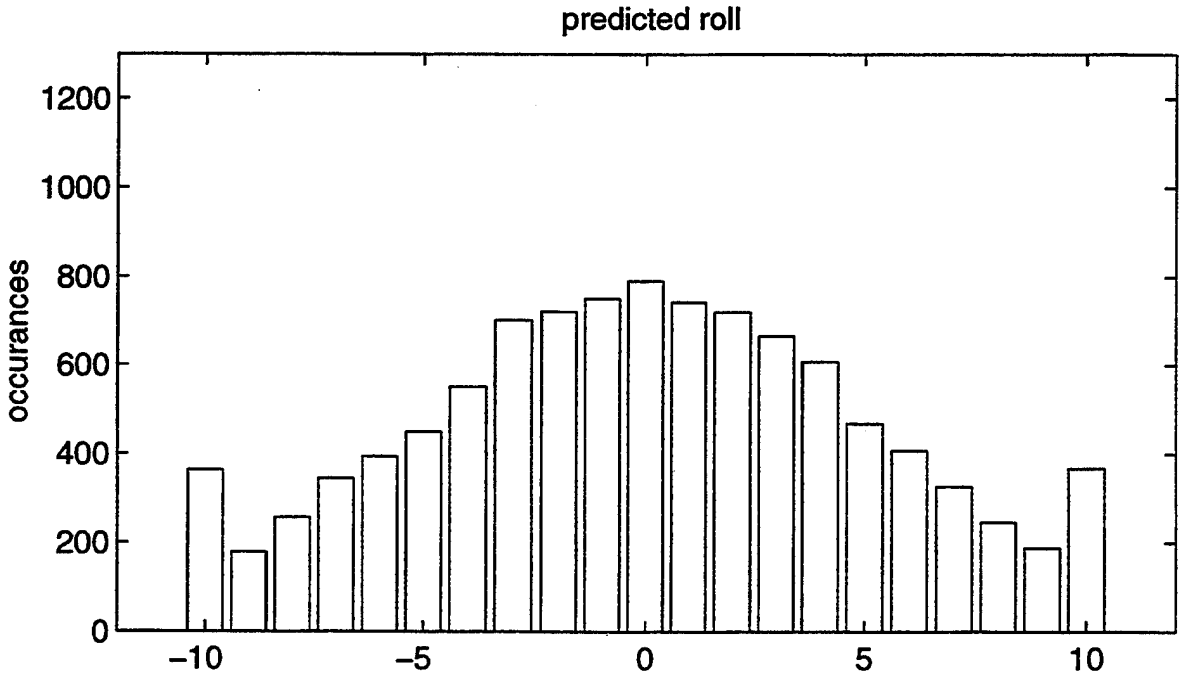

(b) Predicted Roll Amplitude (degrees)

Figure 3.17 Histograms of Measured and Predicted Roll, White Noise Spectrum (SB33, eqn 2.2)

predict response amplitude and a marked improvement in matching the phase of the measured roll response. Table 3.2 lists the resulting damping parameters for this model.

Test Case	Linear Damping Parameter	Nonlinear Damping Parameter
H=6.6 ft, T=5 sec (SB26)	0.09	0.07
H=6 ft, T=6 sec (SB27)	0.10	0.07
H=7.2 ft, T=8 sec (SB29)	0.33	0.40
H=5.7 ft, T=10 sec (SB30)	0.03	0.07
Bretschneider Spectrum (SB25)	0.04	0.04
White Noise Spectrum (SB33)	0.07	0.08

Table 3.2 Linear and Nonlinear Damping Parameters for Form 2, Equation 2.8

3.4.1 Regular Wave, H= 6.6 Ft, T= 5 Sec (SB26)

Figure 3.18 displays the results of the model barge subjected to a 6.6 ft wave with a 5 sec period considering only barge roll velocity. The damping parameters used to achieve these results are 0.09 for the linear term and 0.07 for the nonlinear term. The predicted amplitude closely matches the measured data. In addition, the predicted roll response motion is nearly identical in phase to that of the measured data.

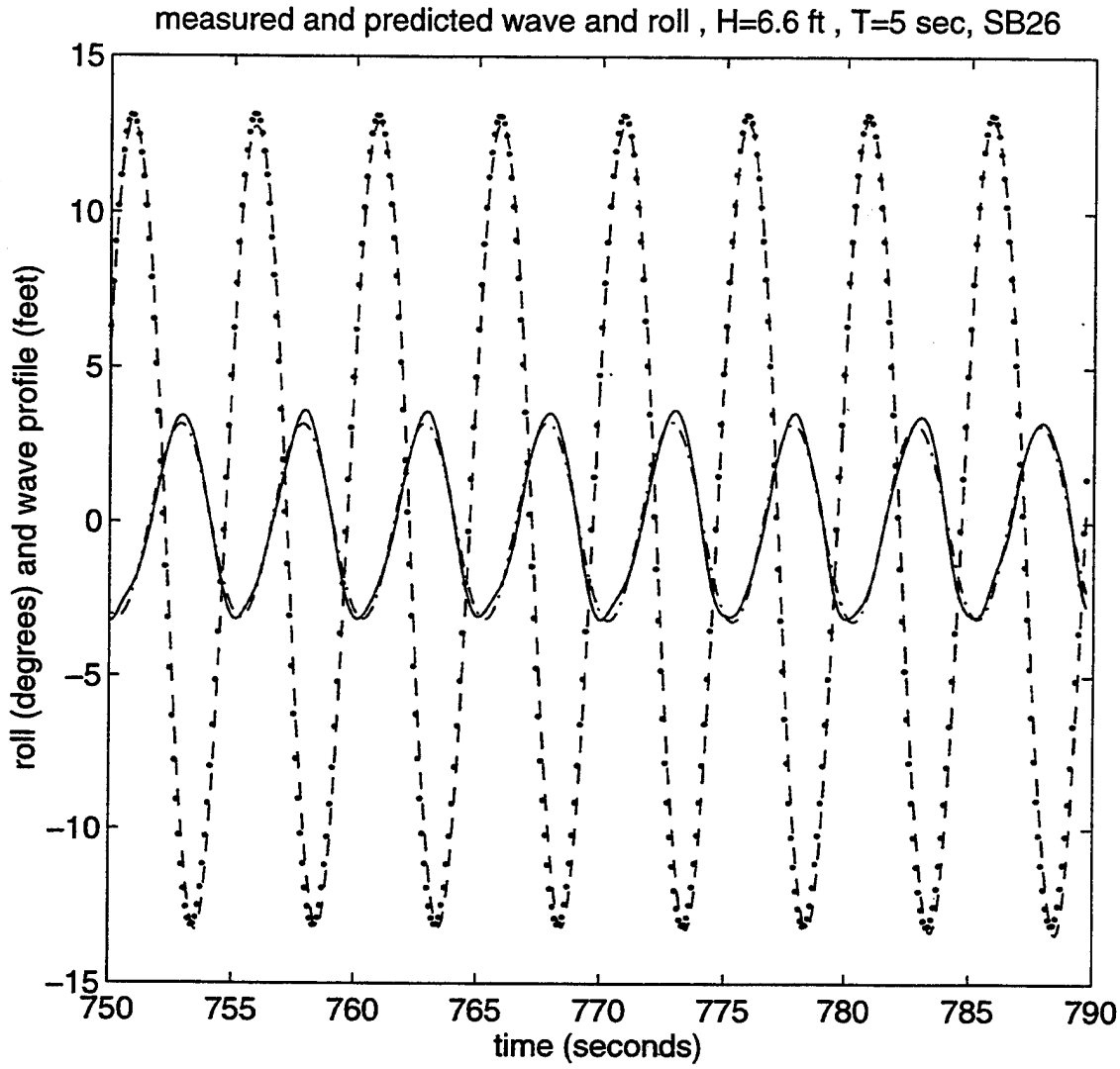

Figure 3.18 Comparison of Measured and Filtered Wave, Measured and Predicted Roll, Regular Wave, H= 6.6 Ft, T= 5 Sec (SB26, eqn 2.8)
- measured wave, -. predicted wave, -- measured roll, .. predicted roll.

3.4.2 Regular Wave, H= 6 Ft, T= 6 Sec (SB27)

Figure 3.19 represents the barge response when subjected to a 6 ft, 6 sec wave considering only barge roll velocity in the damping term. The damping parameters used to achieve these results are 0.10 for the linear term and 0.07 for the nonlinear term. The response amplitude adequately matches the measured response of 11.5 degrees. However, the predicted roll response is approximately 0.5 sec (1/12 period) out of phase with the measured data. Although not an exact match, this is an improvement over the phase difference of approximately 1 sec (1/6 period) produced in the relative motion damping form.

3.4.3 Regular Wave, H= 7.2 Ft, H= 8 Sec (SB29)

Figure 3.20 represents the barge response when subjected to a 7.2 ft, 8 sec period wave considering only the barge roll velocity in the damping term for predicted response. The damping parameters used to match the measured roll response of 4.1 degrees are 0.33 for the linear coefficient and 0.40 for the nonlinear coefficient. As with the relative motion damping case, these coefficients are significantly higher than the previous test cases. Further study should be conducted to evaluate this phenomenon. This form of the model is an improvement over the relative motion damping form because it more adequately matches the measured behavior, particularly in the phase (at the peaks).

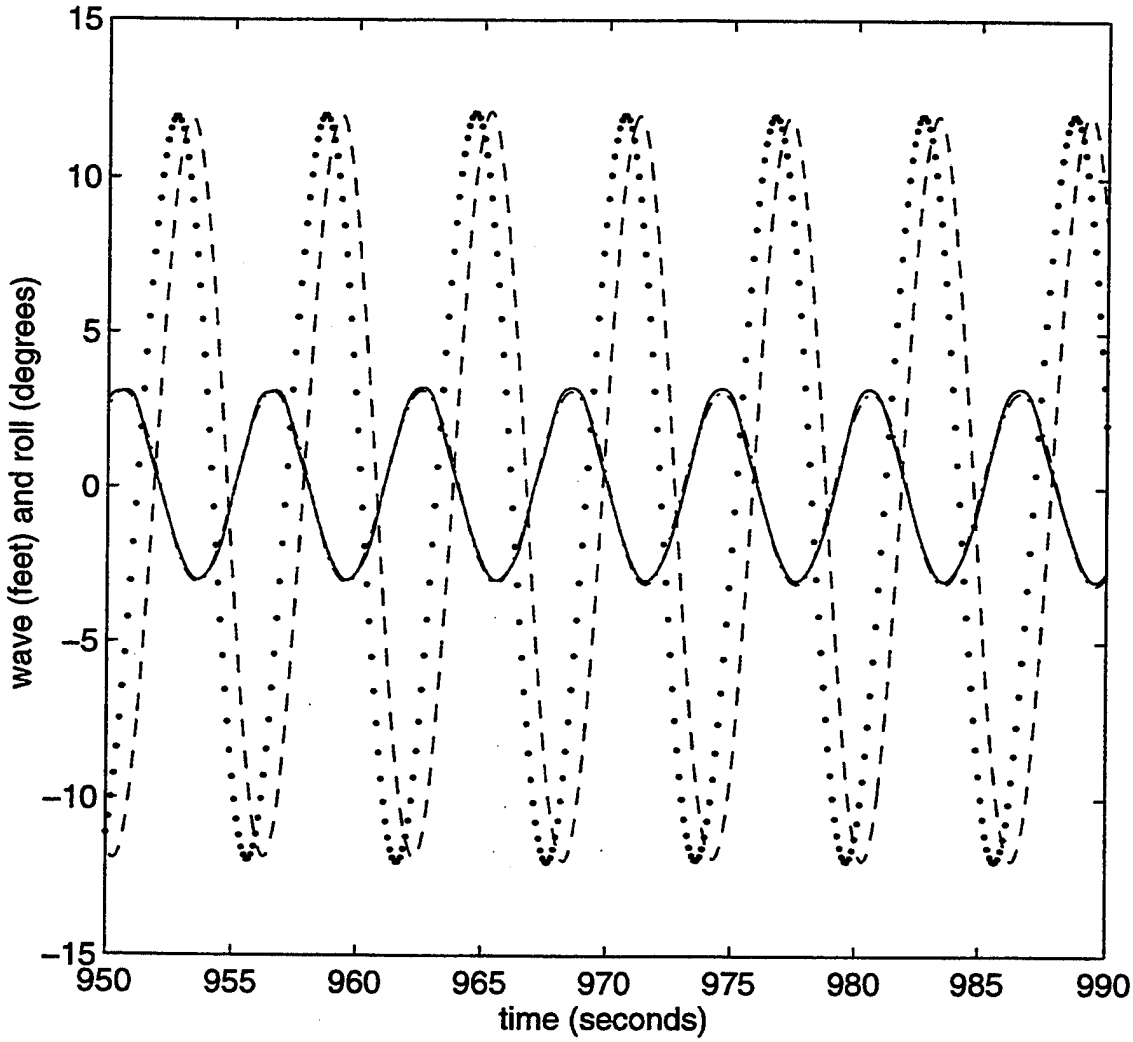

Figure 3.19 Comparison of Measured and Filtered Wave, Measured and Predicted Roll, Regular Wave, H= 6 Ft, T= 6 Sec (SB27, eqn 2.8)
- measured wave, -. predicted wave, -- measured roll, .. predicted roll.

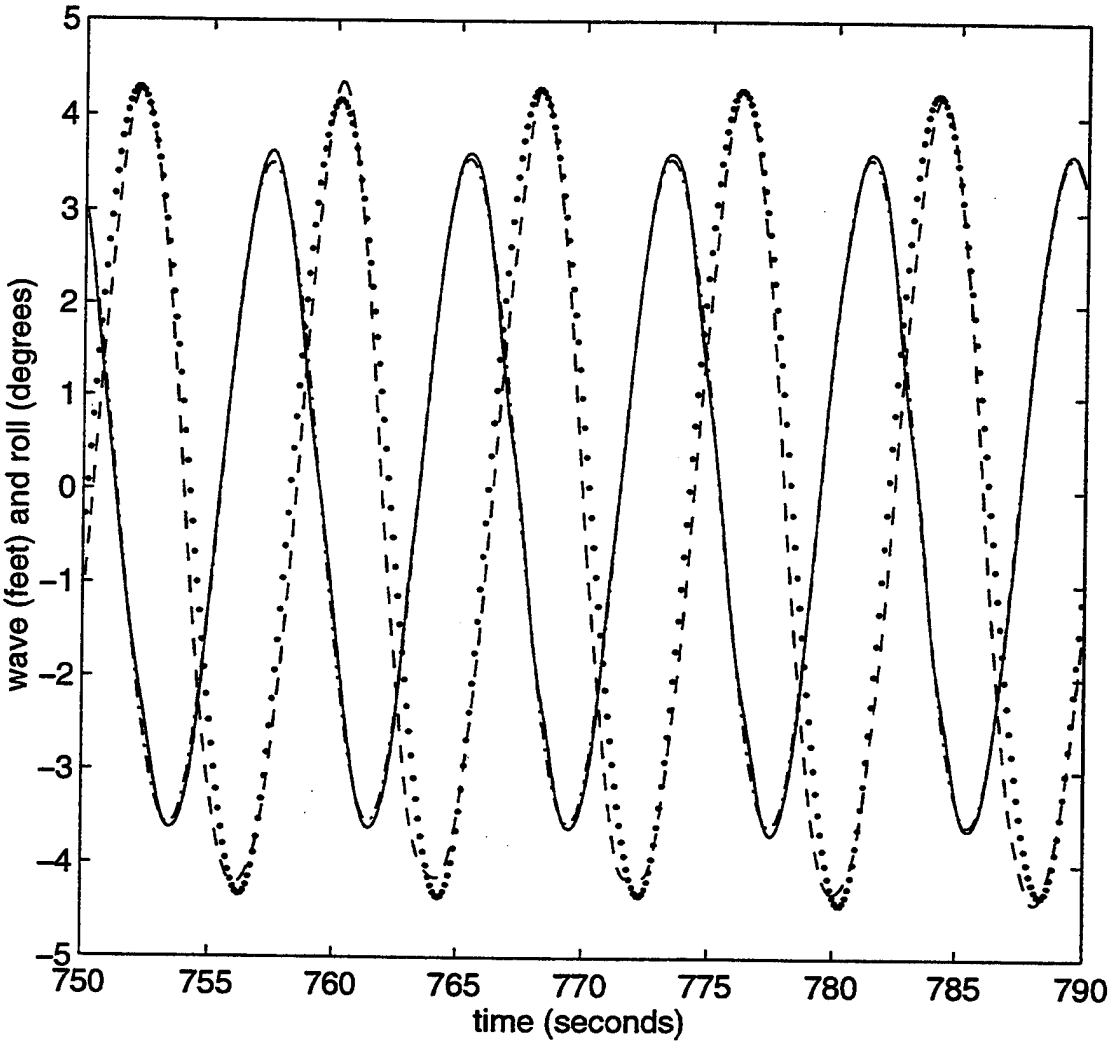

Figure 3.20 Comparison of Measured and Filtered Wave, Measured and Predicted Roll, Regular Wave, H= 7.2 Ft, T= 8 Sec (SB29, eqn 2.8)
- measured wave, -. predicted wave, -- measured roll, .. predicted roll.

3.4.4 Regular Wave, H= 5.7 Ft, T= 10 Sec (SB30)

Figure 3.21 represents the roll response of the barge subjected to 5.7 ft regular waves with a 10 sec period, considering only barge roll velocity in the damping term of the predicted response. As with the relative motion case, it is difficult to match response amplitude with the superharmonic effect. A damping parameter of 0.03 for the linear damping term and 0.07 for the nonlinear term provides the closest match to the measured roll response of 2 degrees. The standard deviation of the measured data is 1.84 compared with 1.87 for the simulated roll response. This is a small improvement over the prediction using relative motion damping which resulted in a standard deviation of 1.88. Figure 3.22 shows that the spectral densities of the measured and simulated roll response compare favorably for this form of the model.

3.4.5 Bretschneider Spectrum, Hs= 6 Ft, Tp= 8 Sec (SB25)

Figures 3.23a - 3.23d display the measured and simulated wave excitation and measured and predicted roll response. The damping parameters used in the model are 0.04 for both the linear and nonlinear damping terms. Figures 3.23c and 3.23d indicate a good visual comparison between the measured and simulated responses. The standard deviation of 3.96 for measured data compared well to a predicted standard deviation of 3.96. The energy under measured and simulated spectral density curves are a close match although there is a slight shift in peak frequencies, as shown in Figure 3.24. A final comparison of probability densities, Figures 3.25a and 3.25b, confirm that this form of the model provides a good simulation for the random wave environment.

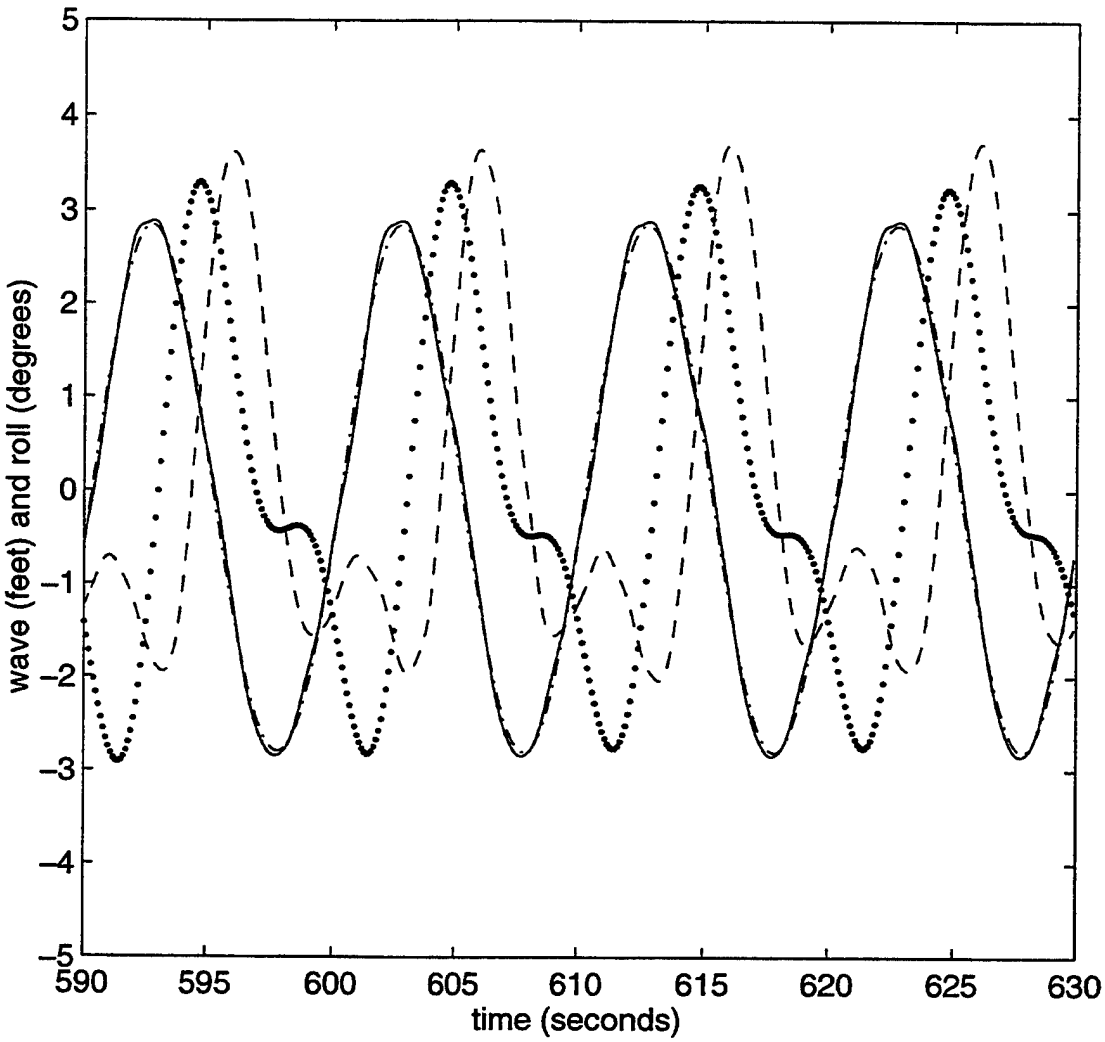

Figure 3.21 Comparison of Measured and Filtered Wave, Measured and Predicted Roll, Regular Wave, H= 5.7 Ft, T= 10 Sec (SB30, eqn 2.8)
- measured wave, -. predicted wave, -- measured roll, .. predicted roll.

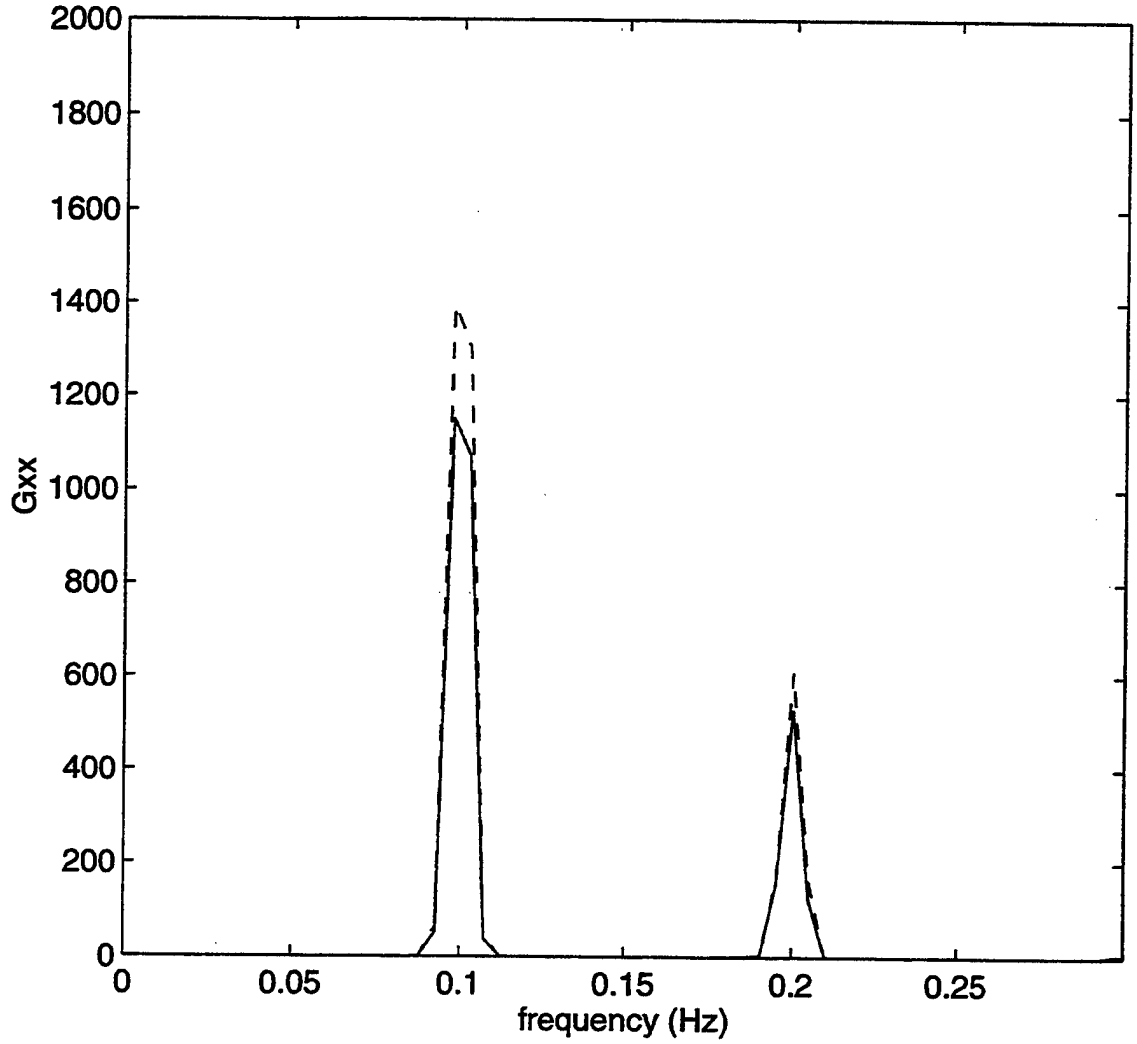

Figure 3.22 Comparison of Spectral Densities (Deg^2/Hz), Measured and Predicted Roll, H= 5.7 Ft, T= 10 Sec (SB30, eqn 2.8), - measured, -- predicted

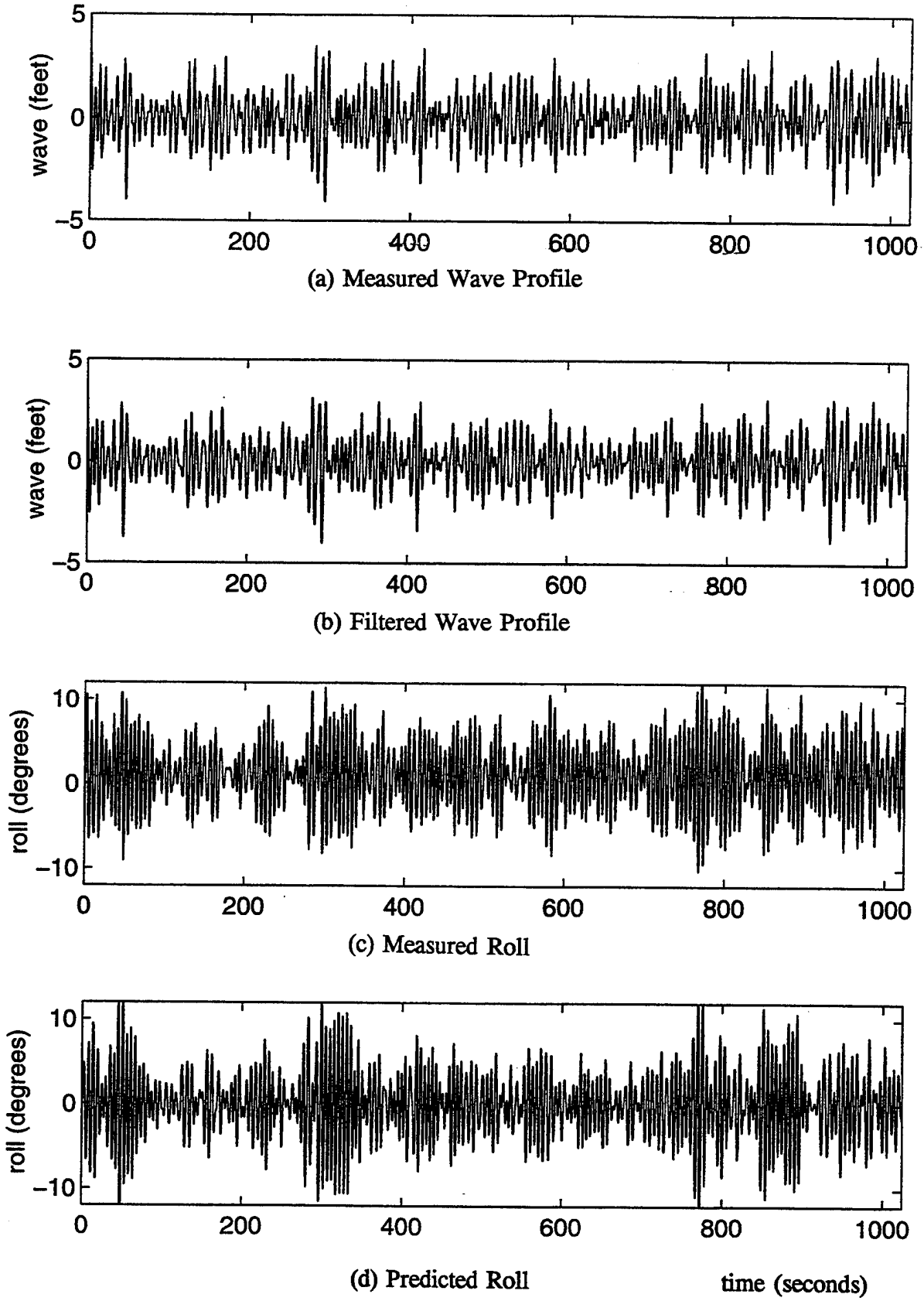

Figure 3.23 Comparison of Measured and Predicted Wave and Roll, Bretschneider Spectrum, Hs= 6 Ft, Tp= 8 Sec (SB25, eqn 2.8)

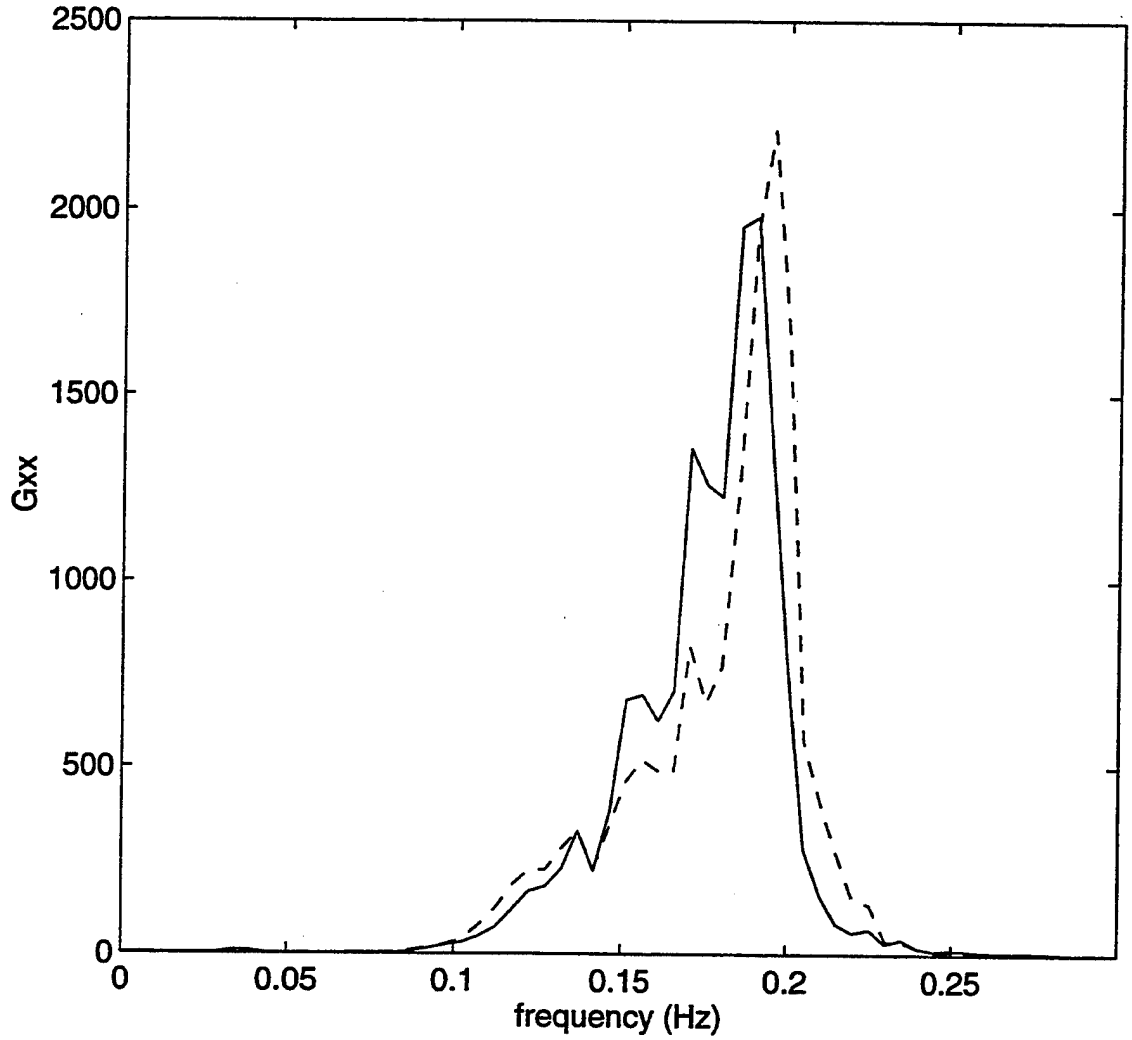

Figure 3.24 Comparison of Spectral Densities (Deg^2/Hz), Measured and Predicted Roll, Bretschneider Spectrum, Hs= 6 Ft, Tp= 8 Sec (SB25, eqn 2.8)
- measured, -- predicted

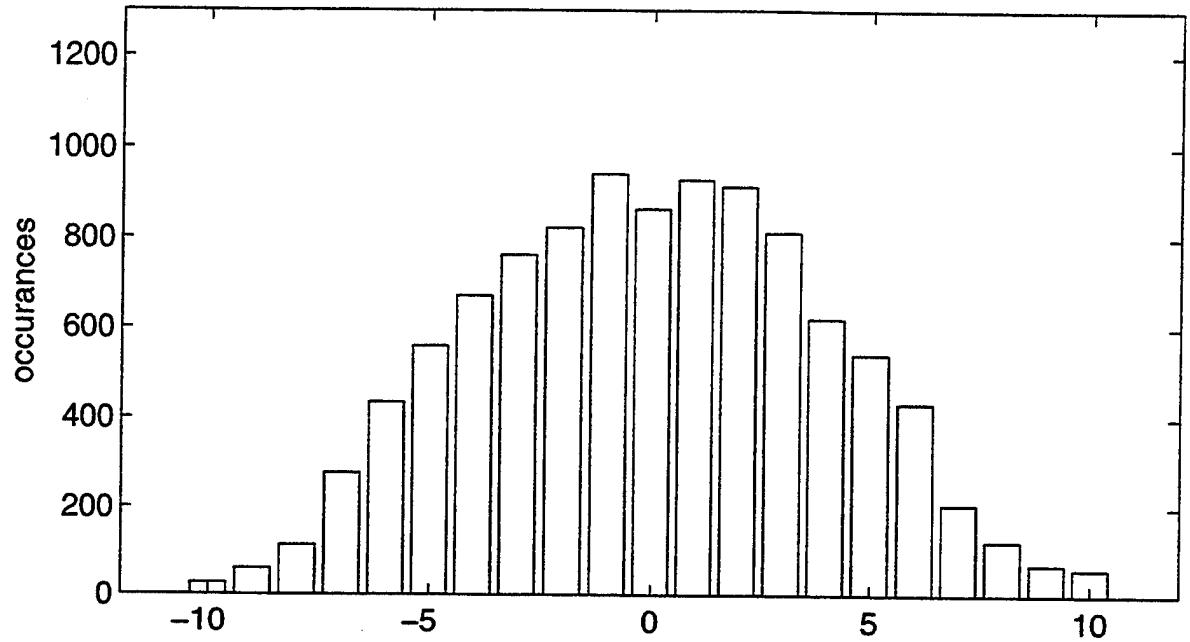

(a) Measured Roll Amplitude (degrees)

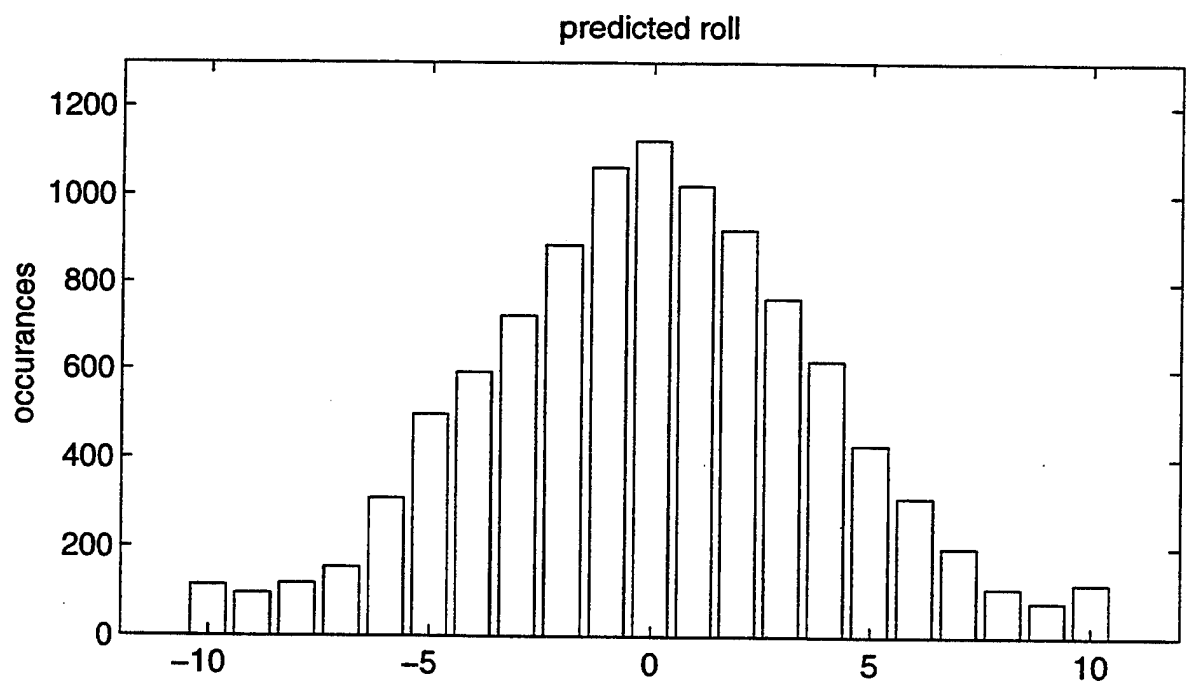

(b) Predicted Roll Amplitude (degrees)

Figure 3.25 Histograms of Measured and Predicted Roll, Bretschneider Spectrum (SB25, eqn 2.8)

3.5.6 White Noise Excitation, Hs= 6 Ft (SB33)

Figures 3.26a - 3.26d display the measured and filtered wave and predicted roll response for a white noise wave excitation with wave periods of 4 to 20 secs and a wave height of 6 ft. The damping parameters used in this model are 0.07 for the linear term and 0.08 for the nonlinear term. The resulting standard deviation for predicted roll response is 5.30 which is very close to the measured response standard deviation of 5.29. A comparison of spectral densities, Figure 3.27, and probability densities, Figures 3.28a and 3.28b, indicate the model provides an accurate prediction of roll response. Again a significant build-up in the extreme values is observed.

3.5 Alternative Forms Considered

Other forms of the damping moment studied are those represented by equations 2.9 and 2.10:

$$I_{44}\ddot{\phi} + I_{A44}(\ddot{\phi} - \partial\ddot{\eta}/\partial y) + C_{44L}\dot{\phi} + C_{44N}(\dot{\phi} - \partial\dot{\eta}/\partial y)\,|\,\dot{\phi} - \partial\dot{\eta}/\partial y\,| + R_{44}(\phi,\eta,\partial\eta/\partial y) = 0 \tag{2.9}$$

$$I_{44}\ddot{\phi} + I_{A44}(\ddot{\phi} - \partial\ddot{\eta}/\partial y) + C_{44N}(\dot{\phi} - \partial\dot{\eta}/\partial y)\,|\,\dot{\phi} - \partial\dot{\eta}/\partial y\,| + R_{44}(\phi,\eta,\partial\eta/\partial y) = 0 \tag{2.10}$$

These forms are capable of simulating the response amplitude, however they are not as accurate in duplicating the measured phase. Figure 3.29a - 3.29d is a comparison of all four forms for test SB26. The two forms which use relative motion in the damping term have the greatest phase error. This indicates the system is inertia dominated and that linear (structural) damping makes a significant contribution to the

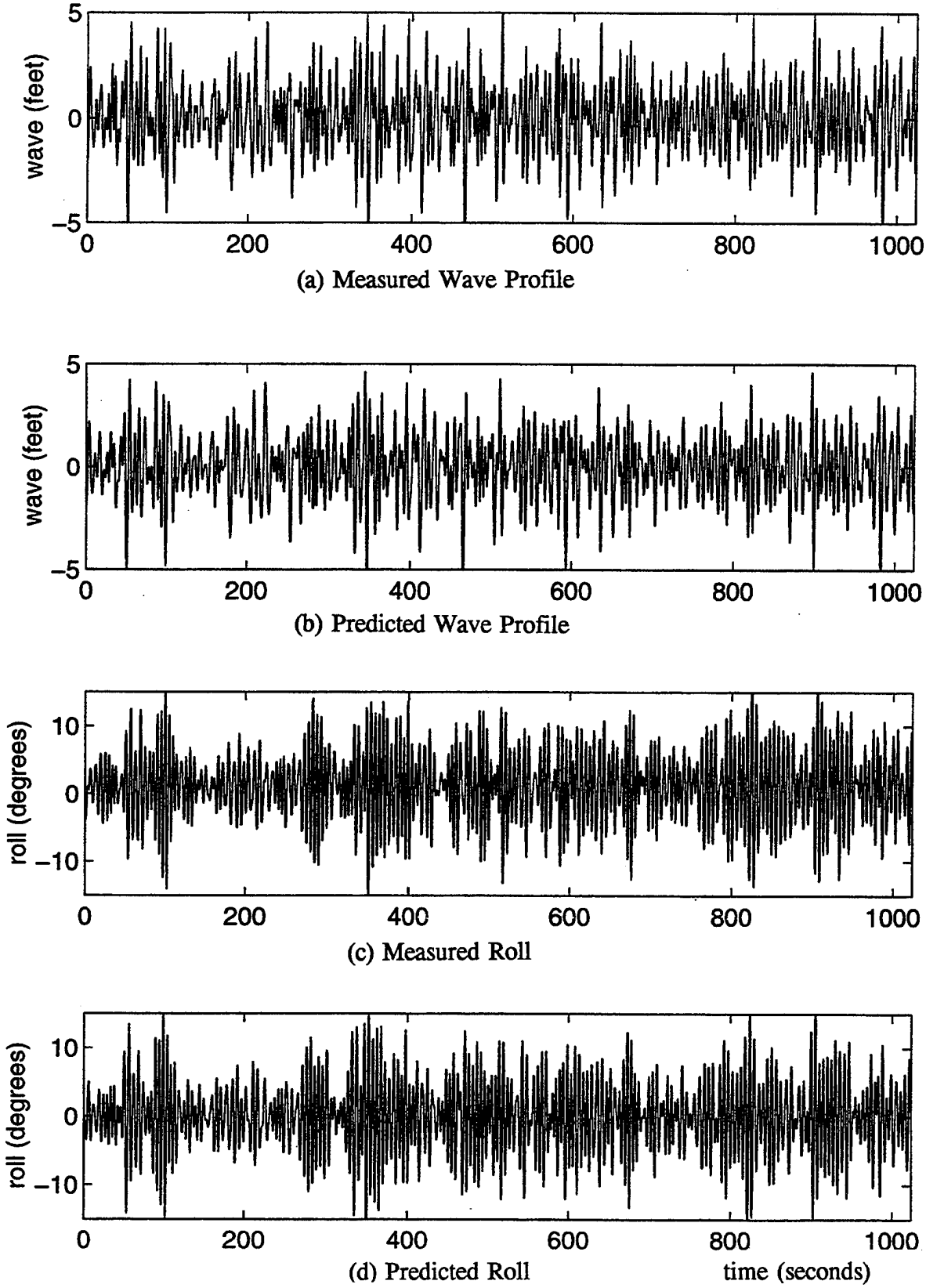

Figure 3.26 Comparison of Measured and Filtered Wave, Measured and Predicted Roll, White Noise Spectrum, Hs= 6 Ft (SB33, eqn 2.8)

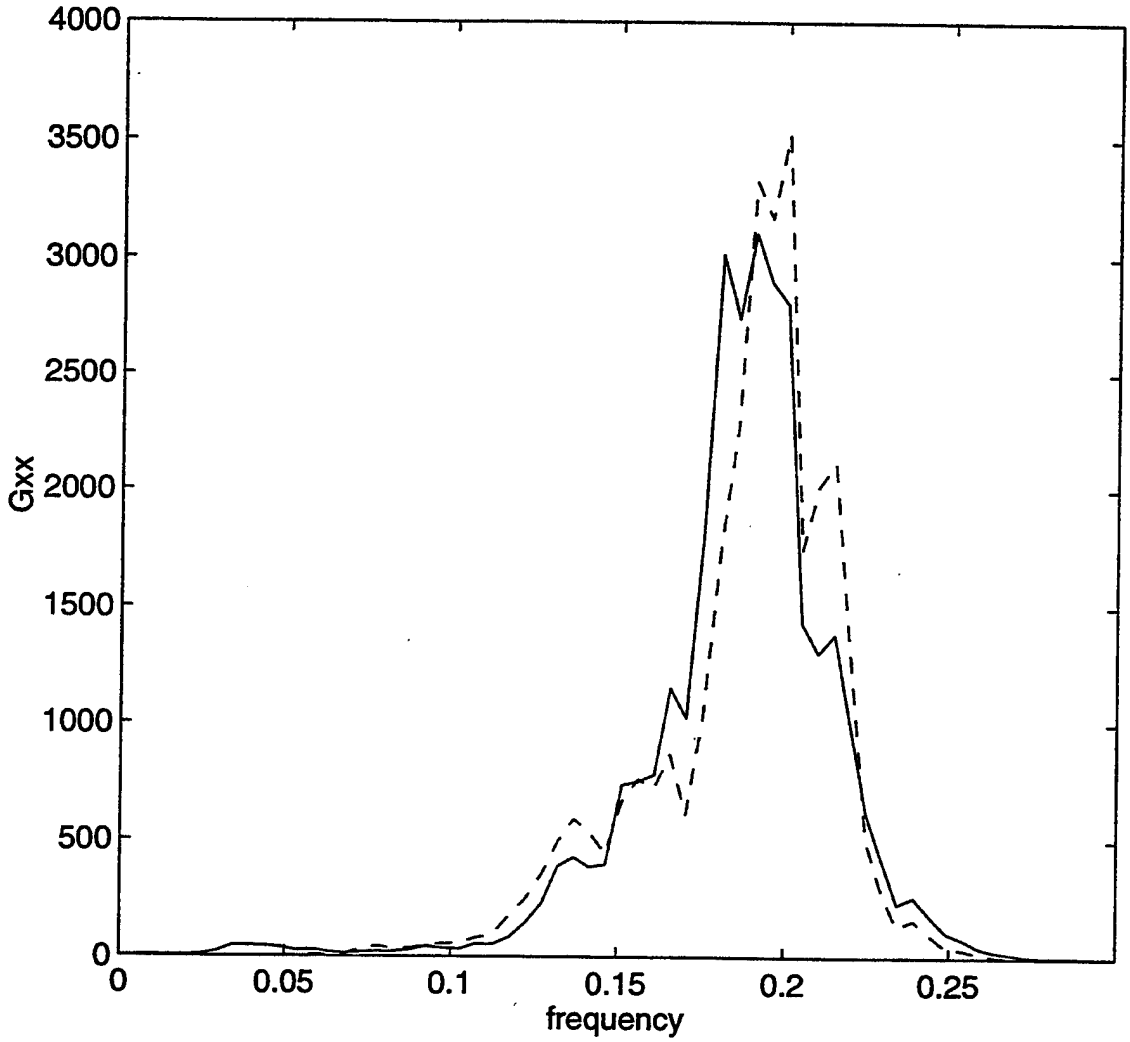

Figure 3.27 Comparison of Spectral Densities (Deg^2/Hz), Measured and Predicted Roll, White Noise Spectrum, Hs= 6 Ft (SB33, eqn 2.8)), - measured, -- predicted

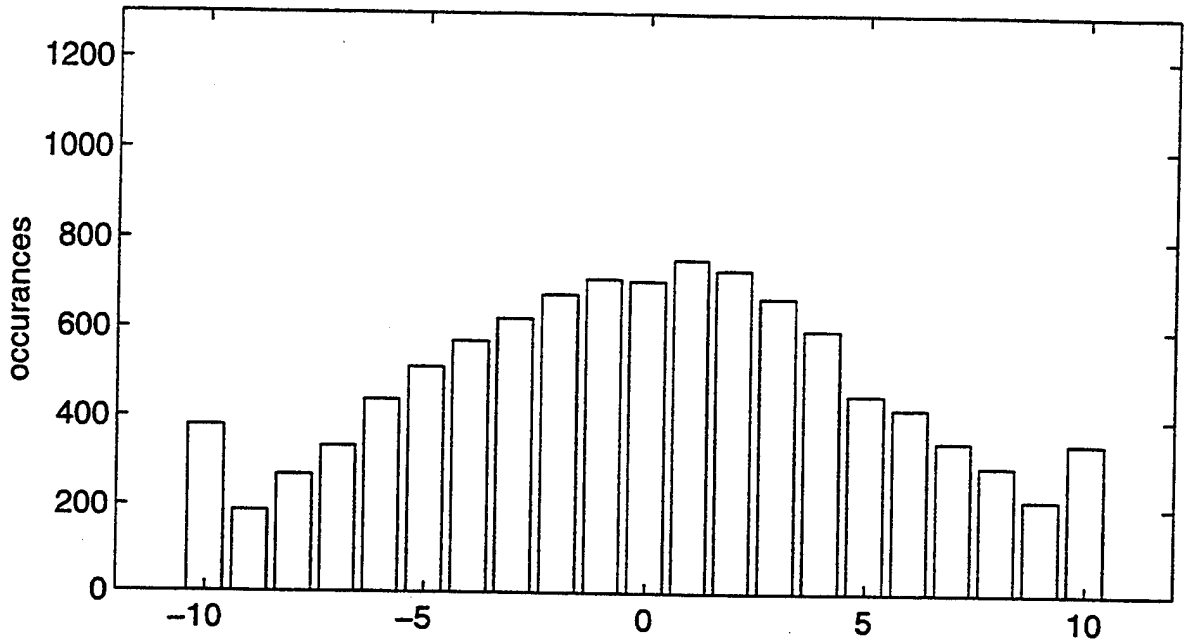

(a) Measured Roll Amplitude (degrees)

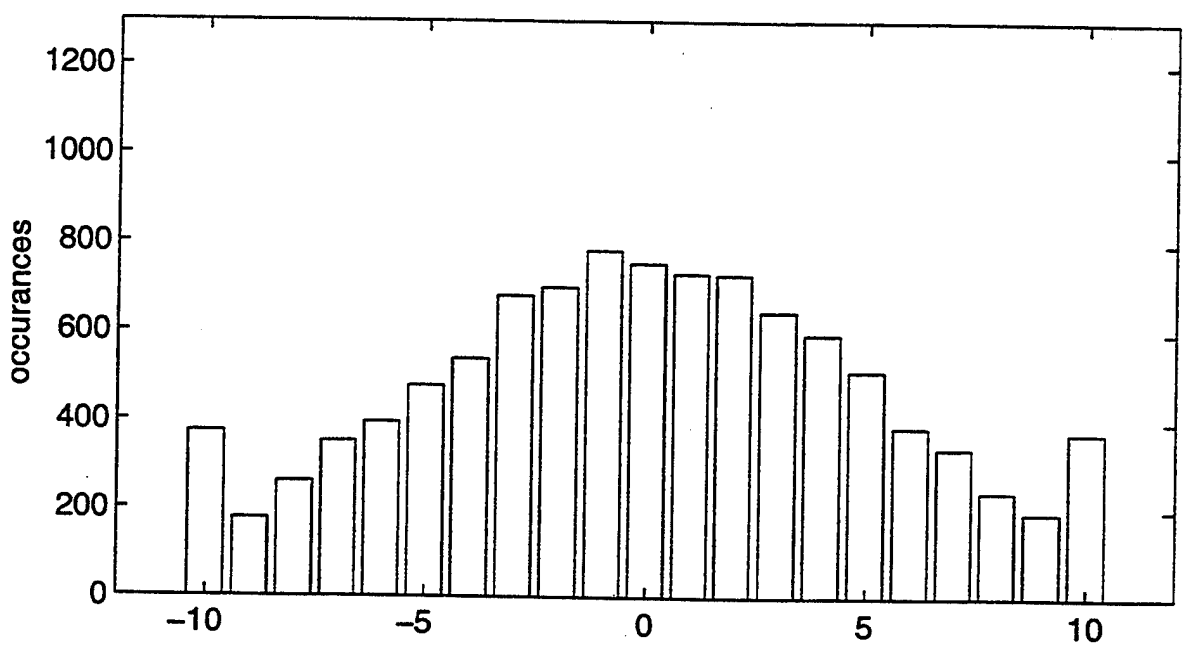

(b) Predicted Roll Amplitude (degrees)

Figure 3.28 Histograms of Measured and Predicted Roll, White Noise Spectrum (SB33, eqn 2.2)

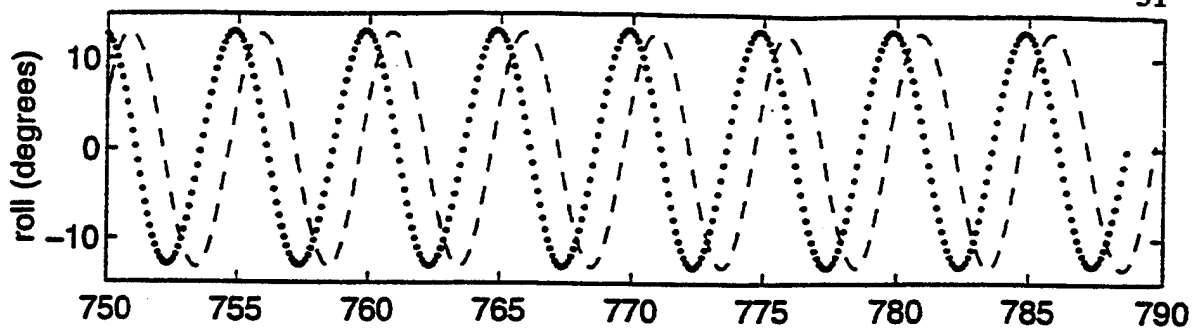

(a) Form 1, Equation 2.2

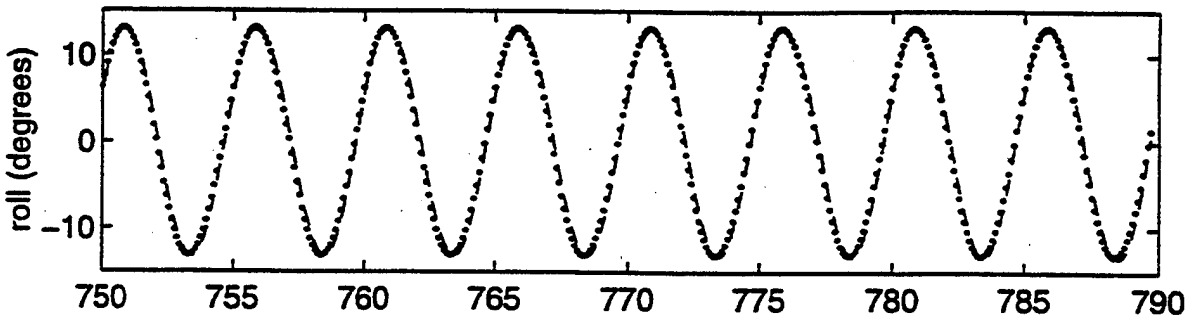

(b) Form 2, Equation 2.8

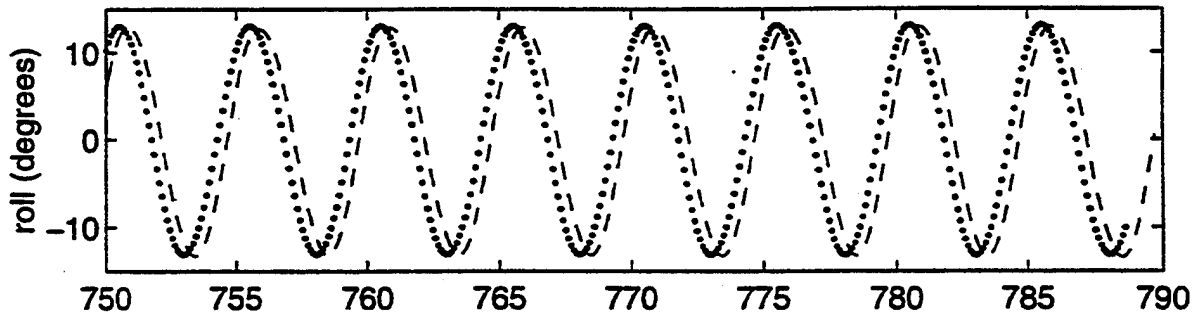

(c) Form 3, Equation 2.9

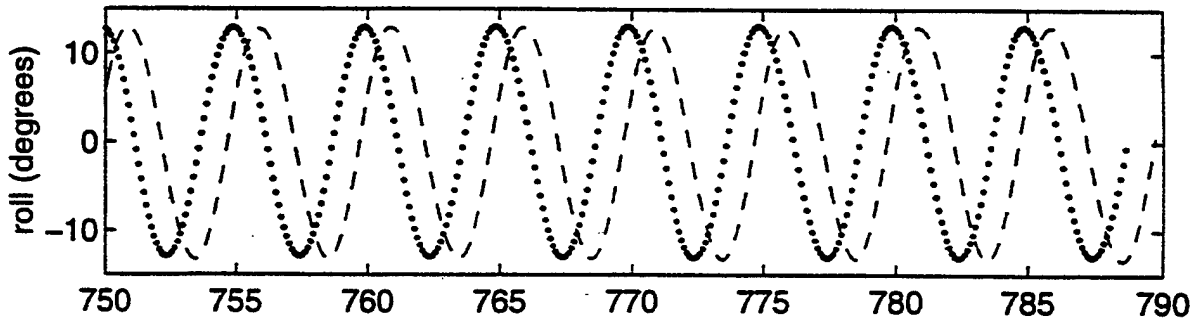

(d) Form 4, Equation 2.10 time (seconds)

Figure 3.29 Comparison of Roll Responses Using Four Different Forms (SB26)
- measured, -- predicted

response. The form which uses linear damping with roll velocity only and relative motion Morison nonlinear damping provides an improvement in the phase error, but is still slightly out of phase. Figure 3.29b represents the model which uses strictly structural damping. It is clear this model provides the best match. This trend is evident for the 6 and 8 sec wave cases as well as shown in Figures 3.30 and 3.31. The 10 sec wave test case displayed the same phase shifted results for all model forms as shown in Figure 3.32.

In the random wave test cases, each model is equally successful at simulating the measured response. Equation 2.10, which uses strictly Morison damping, required a significant increase in the damping parameter for both random wave cases. For example with test SB25, the Bretschneider wave excitation, the damping parameters used for equation 2.2, 2.8, and 2.9 are very close to 0.04 for both the linear and nonlinear damping terms. The damping parameter for equation 2.10, which used only Morison damping, is 0.42. Similar results are obtained with test SB33, the white noise excitation. For equations 2.2, 2.8 and 2.9, the damping parameters are in the range of 0.07 to 0.08, where as the damping parameter for model equation 2.10 is 0.56. Tables 3.3 and 3.4 summarize the resulting damping parameters for equations 2.9 and 2.10.

Form 4 of the SDOF model considered only relative motion Morison damping. It should be noted that all the damping parameters listed in Table 3.4 are extremely high for the regular wave cases. These ratios are unrealistic and indicate that Form 4 is not an acceptable form of the model.

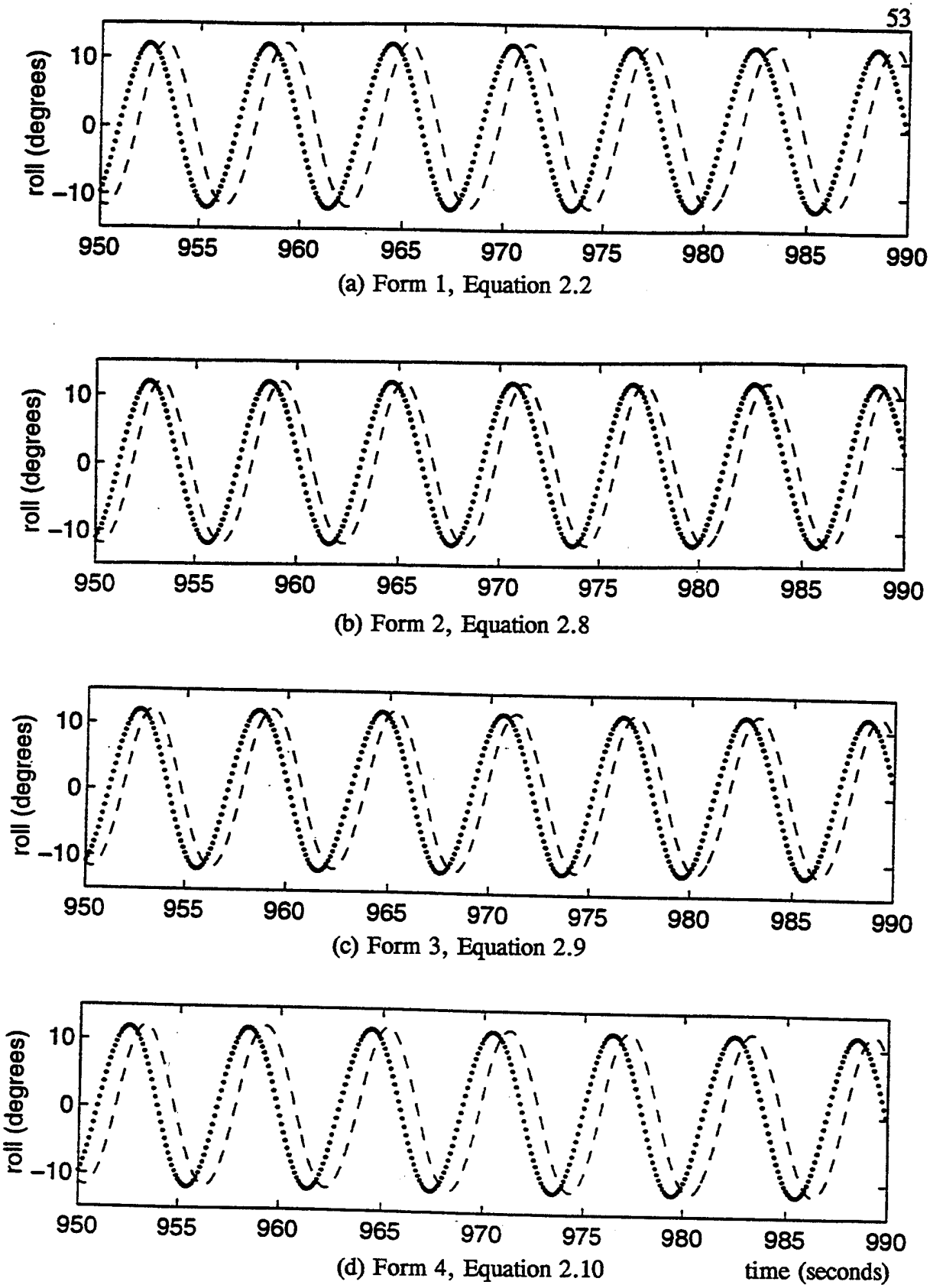

(a) Form 1, Equation 2.2

(b) Form 2, Equation 2.8

(c) Form 3, Equation 2.9

(d) Form 4, Equation 2.10

Figure 3.30 Comparison of Roll Responses Using Four Different Forms (SB27)
- measured, -- predicted

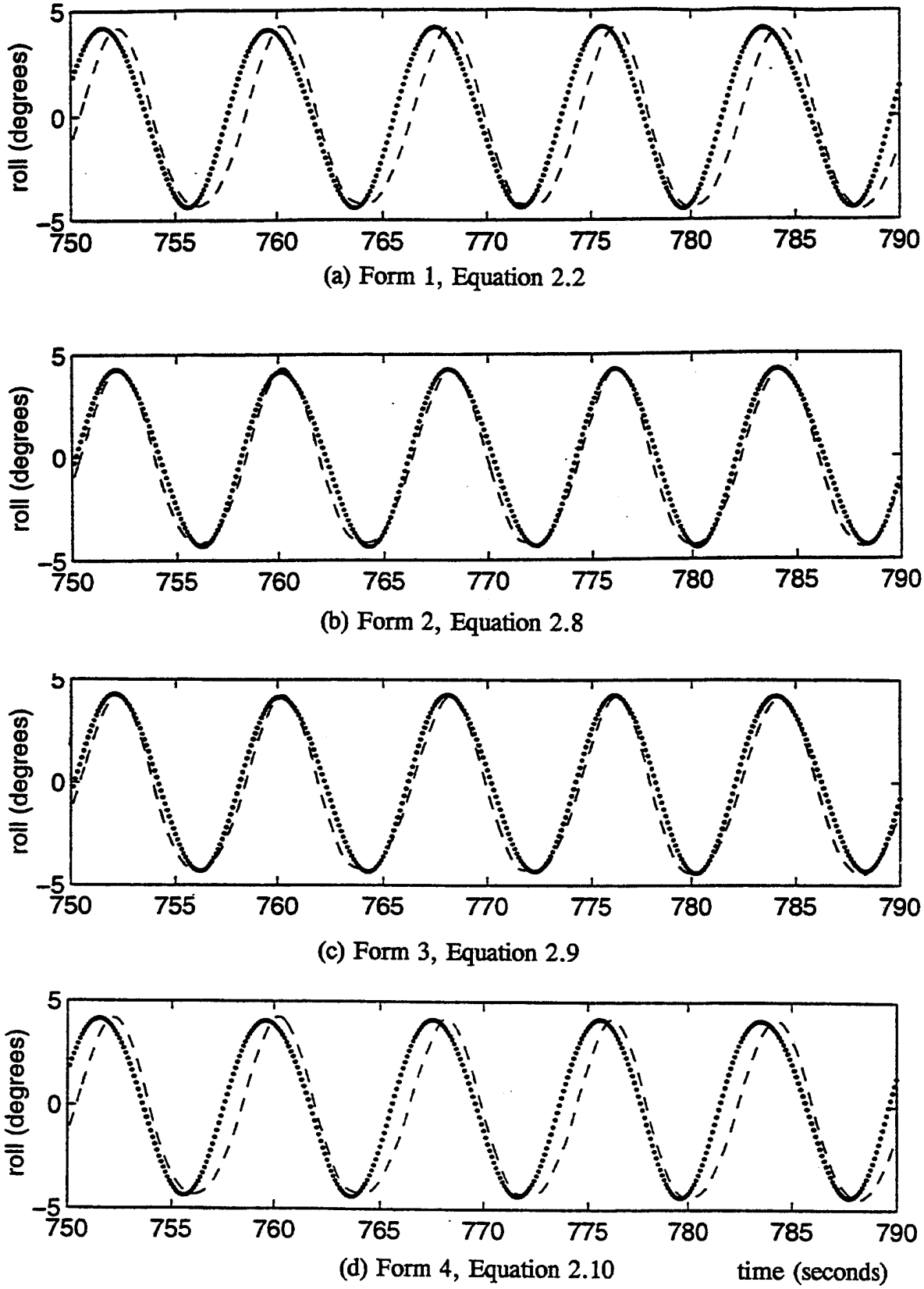

Figure 3.31 Comparison of Roll Responses Using Four Different Forms (SB29)
- measured, -- predicted

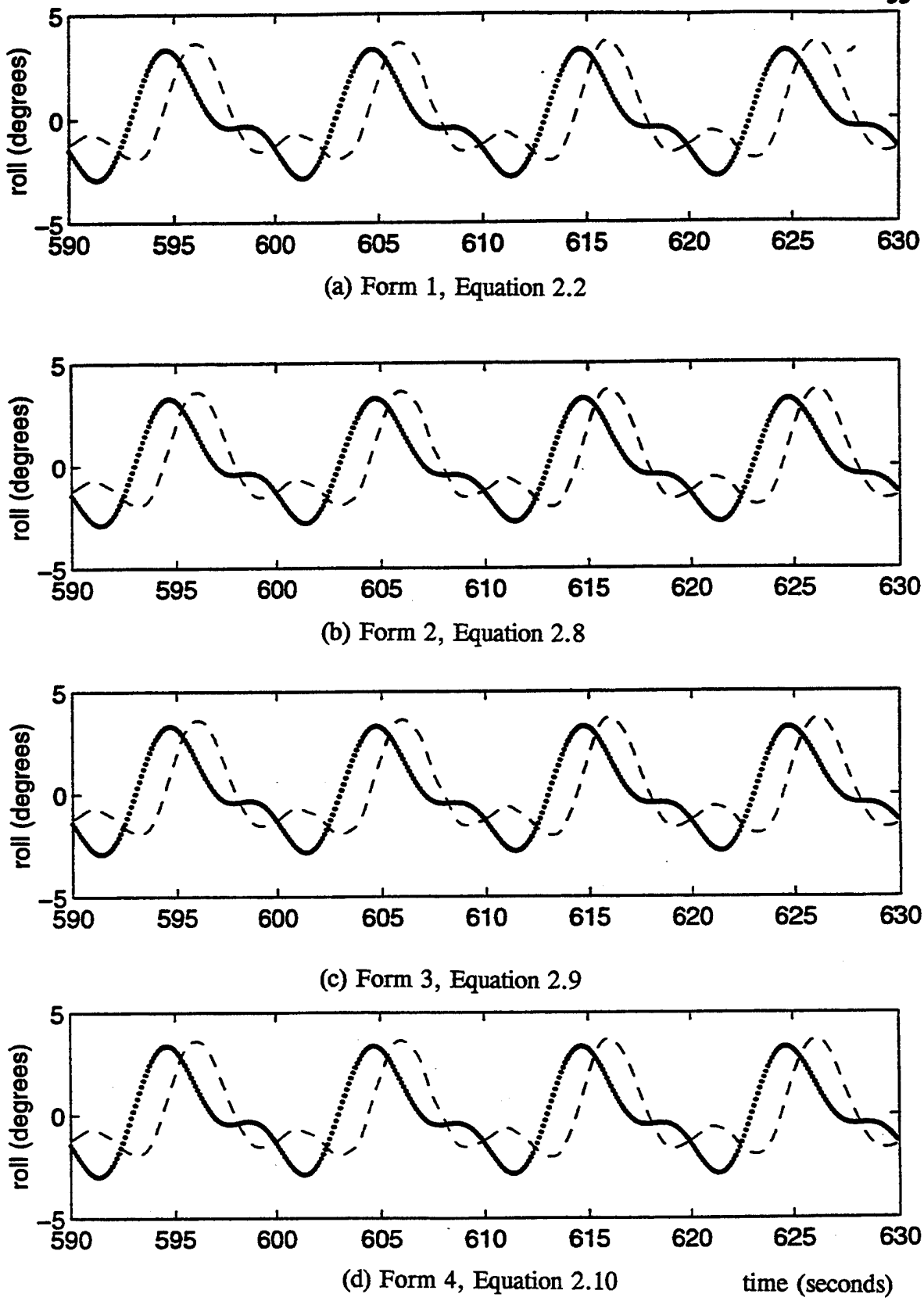

Figure 3.32 Comparison of Roll Responses Using Four Different Forms (SB30)
- measured, -- predicted

Wave Test	Linear Damping Parameter	Nonlinear Damping Parameter
H=6.6 ft, T= 5 sec (SB26)	0.09	0.14
H=6 ft, T=6 sec (SB27)	0.10	0.11
H=7.2 ft, T=8 sec (SB29)	0.34	0.34
H=5.7 ft, T=10 sec (SB30)	0.03	0.07
Bretschneider Spectrum (SB25)	0.04	0.04
White Noise Spectrum (SB33)	0.07	0.08

Table 3.3 Linear and Nonlinear Damping Parameters for Form 3, Equation 2.9

Wave Test	Nonlinear Damping Parameter
H=6.6 ft, T=5 sec (SB26)	1.07
H=6 ft, T=6 sec (SB27)	1.25
H=7.2 ft, T=8 sec (SB29)	88.00
H=5.7 ft, T=10 sec (SB30)	1.25
Bretschneider Spectrum (SB25)	0.42
White Noise Spectrum (SB33)	0.56

Table 3.4 Linear and Nonlinear Damping Parameters for Form 4, Equation 2.10

4.0 Sensitivity Studies

4.1 Variation of Damping Parameters of Form 2, Equation 2.8

A sensitivity study was performed on the model which provided the best results for roll response, equation 2.8, in which damping from the wave excitation was disregarded and only structural damping was considered. For each wave test, the nonlinear damping parameter is held fixed and the linear damping parameter varied by a wide range to determine the effects on simulated response. The linear parameter is then held fixed and the nonlinear damping parameter is varied by a wide range to determine the resulting effects on simulated roll response.

4.1.1 Regular Wave, H= 6 Ft, T= 5 Sec (SB26)

The previously established coefficients for this case were a linear damping parameter of 0.09 and a nonlinear damping parameter of 0.07. Table 4.1. shows a constant decrease in standard deviation as damping parameters increase for both the linear and nonlinear variations.

Linear Damping Parameter	Nonlinear Damping Parameter	Standard Deviation	Linear Damping Parameter	Nonlinear Damping Parameter	Standard Deviation
0.03	0.07	9.89	0.09	0.01	9.54
0.05	0.07	9.77	0.09	0.03	9.48
0.07	0.07	9.59	0.09	0.05	9.42
0.09	0.07	9.33	0.09	0.07	9.33
0.11	0.07	9.00	0.09	0.09	9.28
0.13	0.07	8.60	0.09	0.11	9.20
0.15	0.07	8.15	0.09	0.13	9.12

Table 4.1 Variation in Damping Parameters and Resulting Standard Deviations (SB26)

Figures 4.1a - 4.1e display the amplitude and phase changes which result from varying the linear damping parameter. The trend observed from Figure 4.1 is that with the lower linear damping parameter, the response amplitude is greater than the measured. In addition, the phase of the predicted response lags the measured by approximately 0.25 secs, Figure 4.1a. As the linear damping parameter proceeds through the range, the amplitude decreases and the phase shift transitions from a 0.25 sec lag to leading the measured response by approximately 0.25 secs, Figure 4.1e.

The effects of the variation of the nonlinear damping parameters is not as evident. Figures 4.2a - 4.2e display the change in roll response with variation in the nonlinear damping term. The predicted response phase is almost identical to the measured response. There is not a visual change in the amplitude as the nonlinear parameters proceed through the range. However, a comparison of standard deviations shows a slight decrease as the nonlinear parameter increases, indicating this term does provide a contribution to the response.

4.1.2 Regular Wave, H= 6 Ft, T= 6 Sec (SB27)

The linear and nonlinear damping parameters for this case were established as 0.10 and 0.07 respectively. Table 4.2 indicates a constant decrease in standard deviation as the damping parameters increase. Figure 4.3 represents the resulting changes when the nonlinear damping parameters were held fixed and the linear damping parameters were varied. It is evident that amplitude decreases with an increase in damping parameter. Figure 4.4a - 4.4e represents the results of holding the linear damping parameter fixed and varying the nonlinear damping parameter. The simulated response amplitude decreased through the range of damping

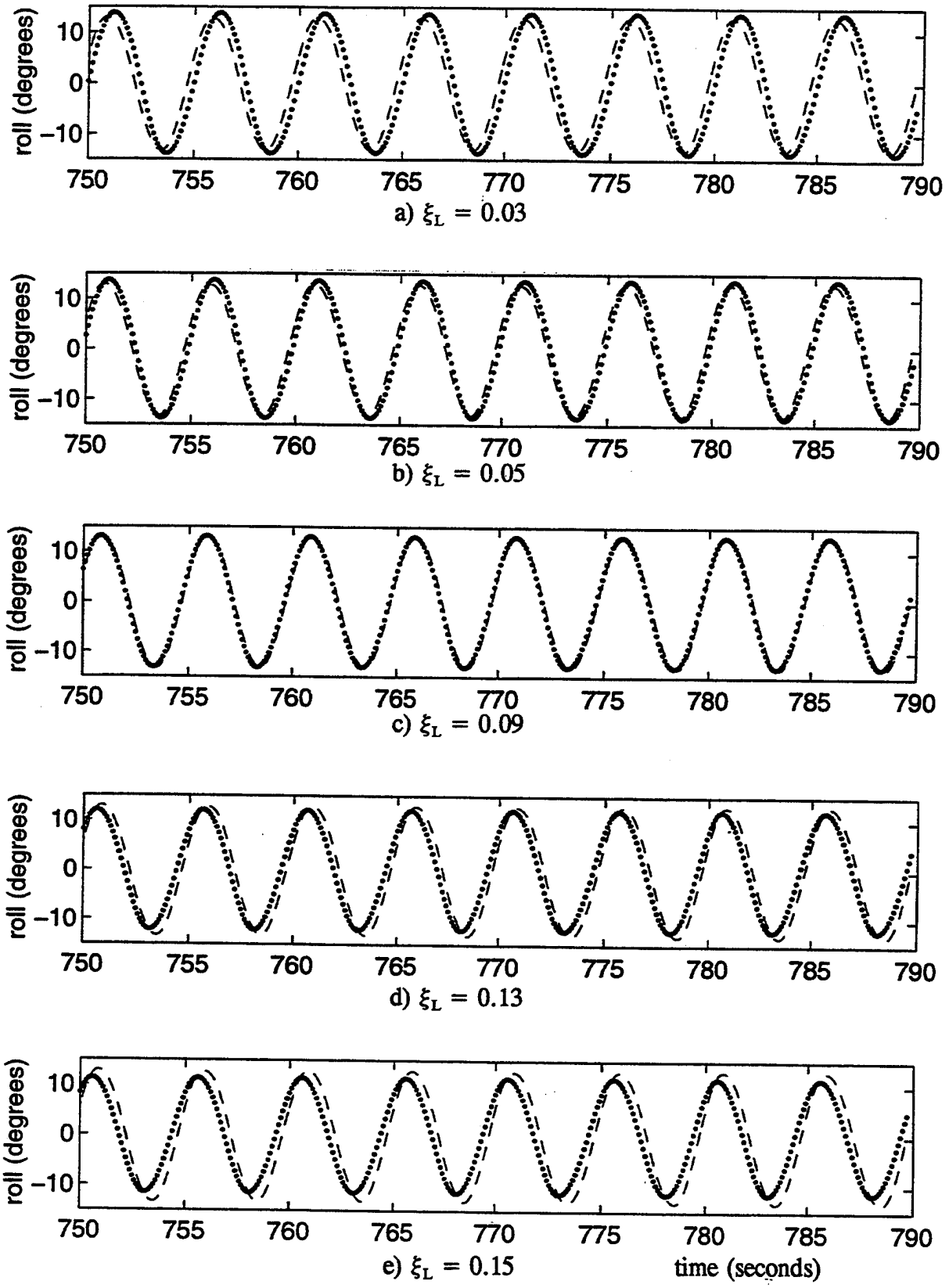

Figure 4.1 Variation of Linear Damping Parameter, Constant Nonlinear Damping Parameter, ξ_N = 0.07, H= 6.6 Ft, T= 5 Sec (SB26, eqn 2.8)
-- measured, .. predicted

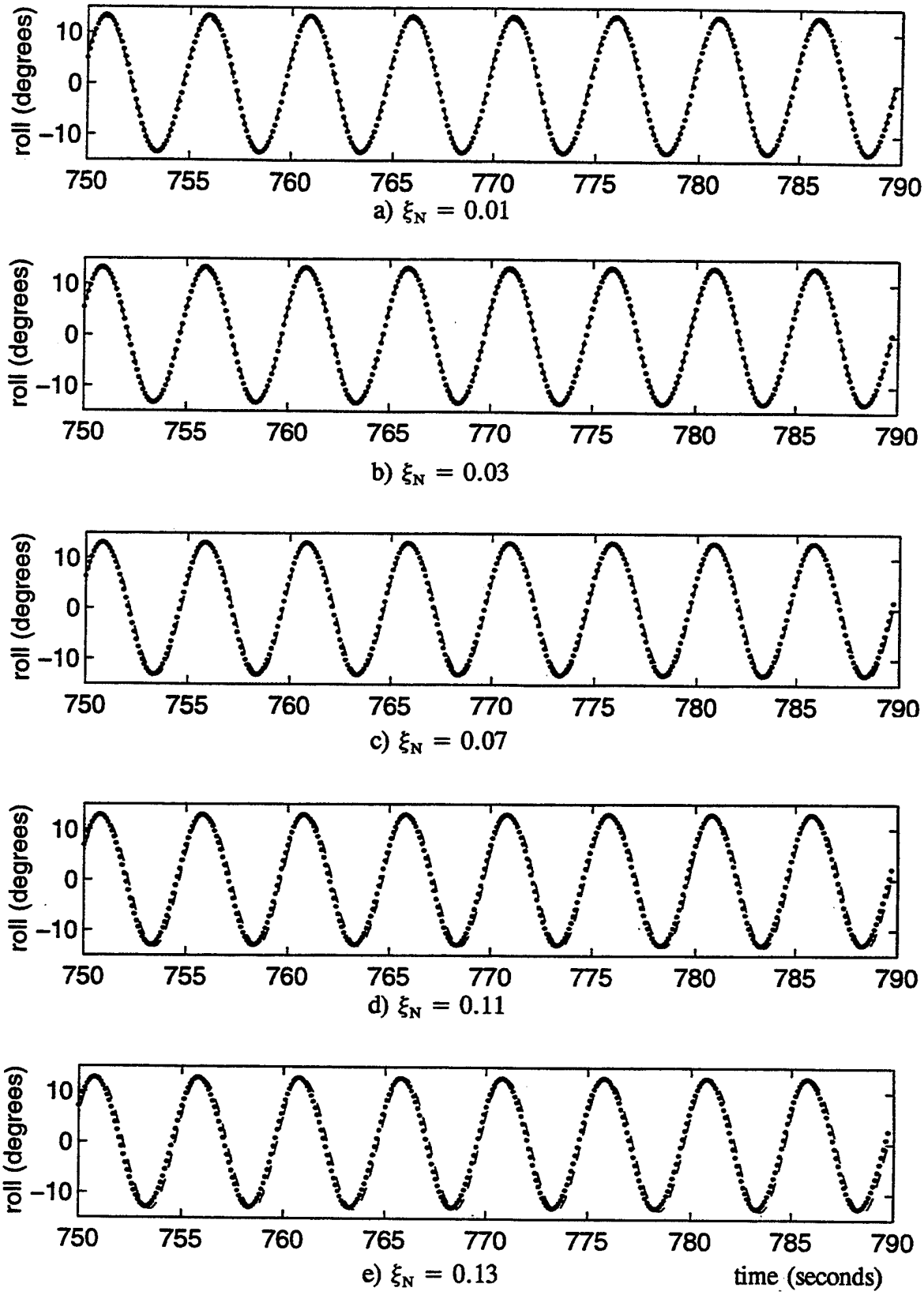

Figure 4.2 Variation of Nonlinear Damping Parameter, Constant Linear Damping Parameter, $\xi_L = 0.09$, H= 6.6 Ft, T= 5 Sec (SB26, eqn 2.8)

parameters. It appears the phase shift remains unchanged throughout the range.

Linear Damping Parameter	Nonlinear Damping Parameter	Standard Deviation	Linear Damping Parameter	Nonlinear Damping Parameter	Standard Deviation
0.04	0.07	9.82	0.10	0.01	8.76
0.06	0.07	9.41	0.10	0.03	8.67
0.08	0.07	8.97	0.10	0.05	8.60
0.10	0.07	8.50	0.10	0.07	8.50
0.12	0.07	7.90	0.10	0.09	8.43
0.14	0.07	7.59	0.10	0.11	8.33
0.16	0.07	7.47	0.10	0.13	8.25

Table 4.2 Variation in Damping Parameters and Resulting Standard Deviations (SB27)

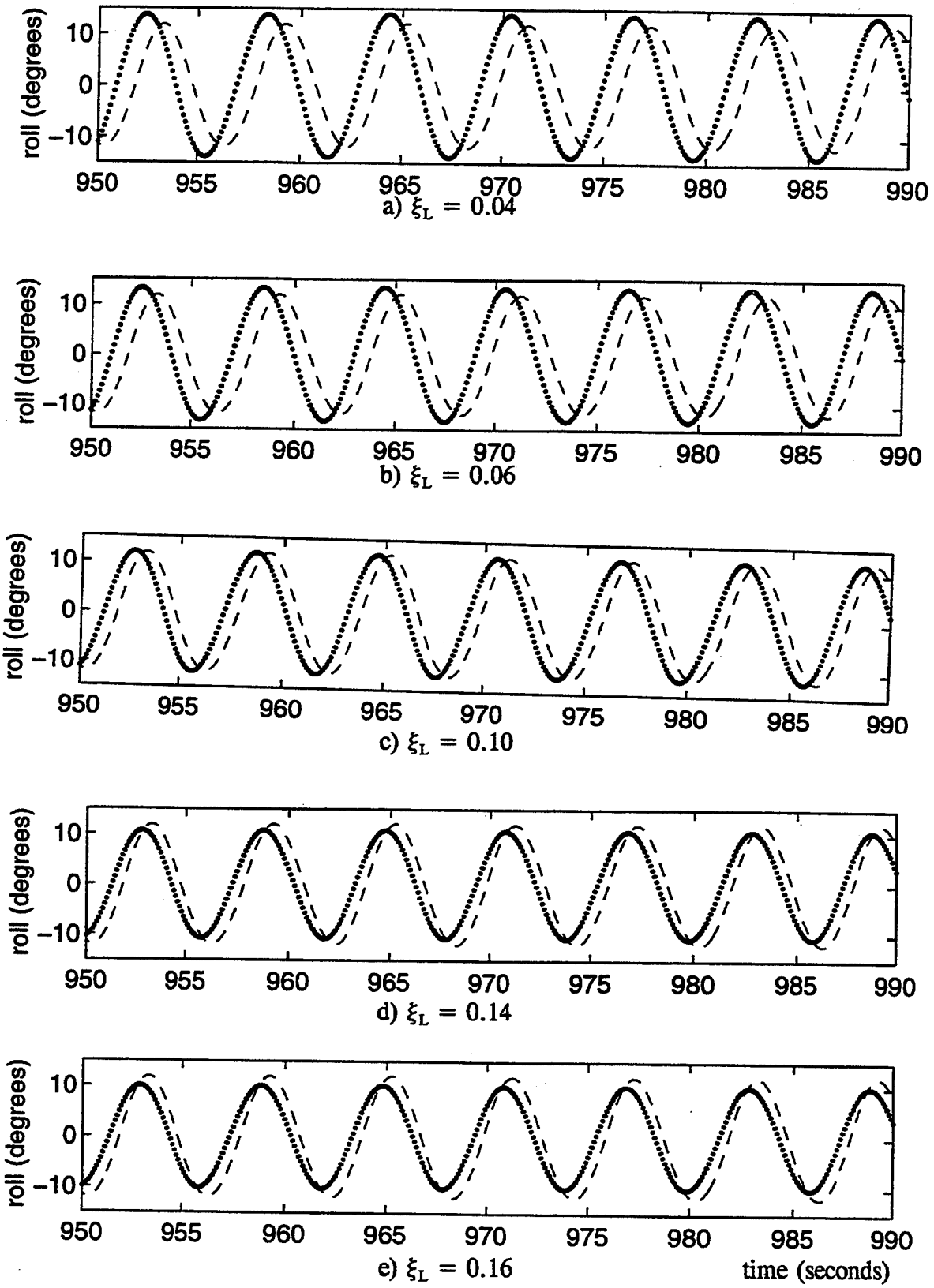

Figure 4.3 Variation of Linear Damping Parameter, Constant Nonlinear Damping Parameter, ξ_N = 0.07, H= 6 Ft, T= 6 Sec (SB27, eqn 2.8)
-- measured, .. predicted

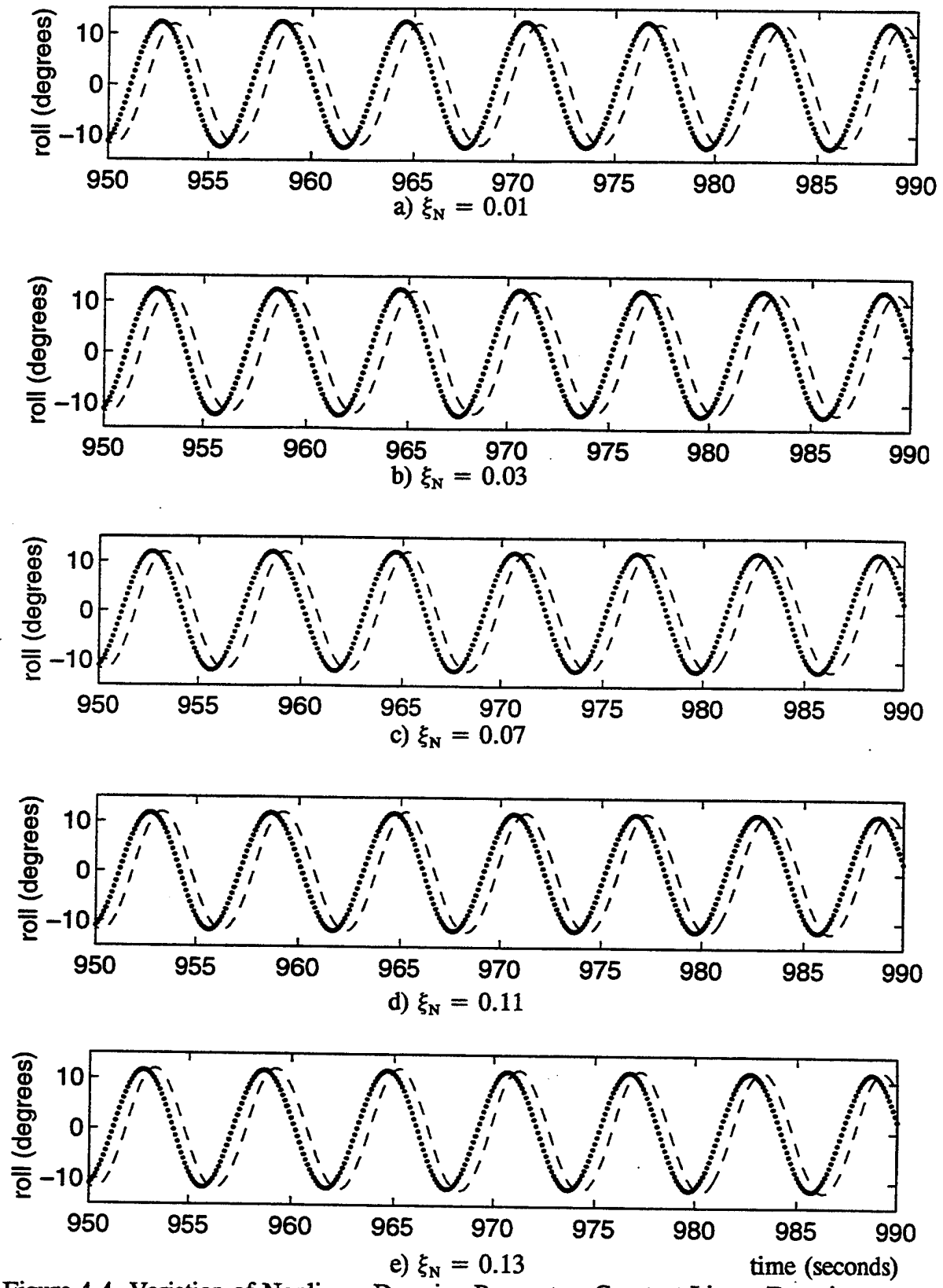

Figure 4.4 Variation of Nonlinear Damping Parameter, Constant Linear Damping Parameter, ξ_L = 0.10, H= 6 Ft, T= 6 Sec (SB27, eqn 2.8)
-- measured, .. predicted

4.1.3 Regular Wave, H= 7.2 Ft, T= 8 Sec (SB29)

The damping parameters established for test case SB29 are 0.33 and 0.40. There is a constant decrease in standard deviation as the damping parameters increase as shown in Table 4.3.

Linear Damping Parameter	Nonlinear Damping Parameter	Standard Deviation	Linear Damping Parameter	Nonlinear Damping Parameter	Standard Deviation
0.20	0.40	3.40	0.33	0.25	3.06
0.25	0.40	3.26	0.33	0.30	3.05
0.30	0.40	3.12	0.33	0.35	3.04
0.33	0.40	3.03	0.33	0.40	3.03
0.40	0.40	2.84	0.33	0.45	3.03
0.45	0.40	2.70	0.33	0.50	3.02
0.50	0.40	2.56	0.33	0.55	3.01

Table 4.3 Variation in Damping Parameters and Resulting Standard Deviations (SB29)

Predicted response amplitude is greater than measured when the nonlinear damping parameter is held fixed and the linear parameter is varied. The phase of the predicted response leads the measured at the lower linear damping parameters. As the linear parameter proceeds through the range, the phase shift changes and eventually the predicted response lags the measured by approximately 0.5 sec. These results are displayed in Figures 4.5a - 4.5e. Holding the linear damping parameters fixed and varying the nonlinear produces no significant change in amplitude or phase difference, as shown in Figures 4.6a - 4.6e.

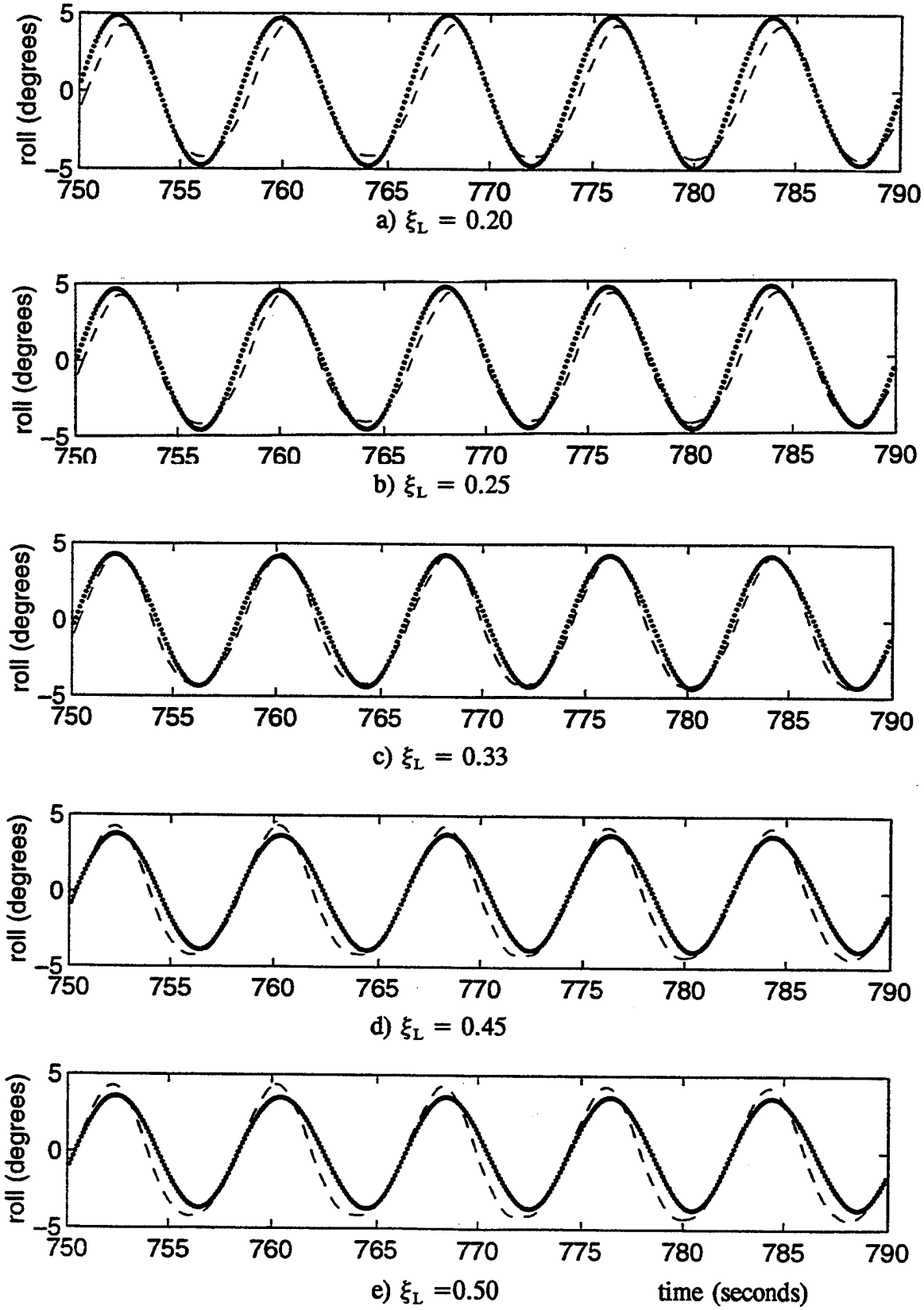

Figure 4.5 Variation of Linear Damping Parameter, Constant Nonlinear Damping Parameter, ξ_N = 0.40, H= 7.2 Ft, T= 8 Sec (SB29, eqn 2.8),
-- measured, .. predicted

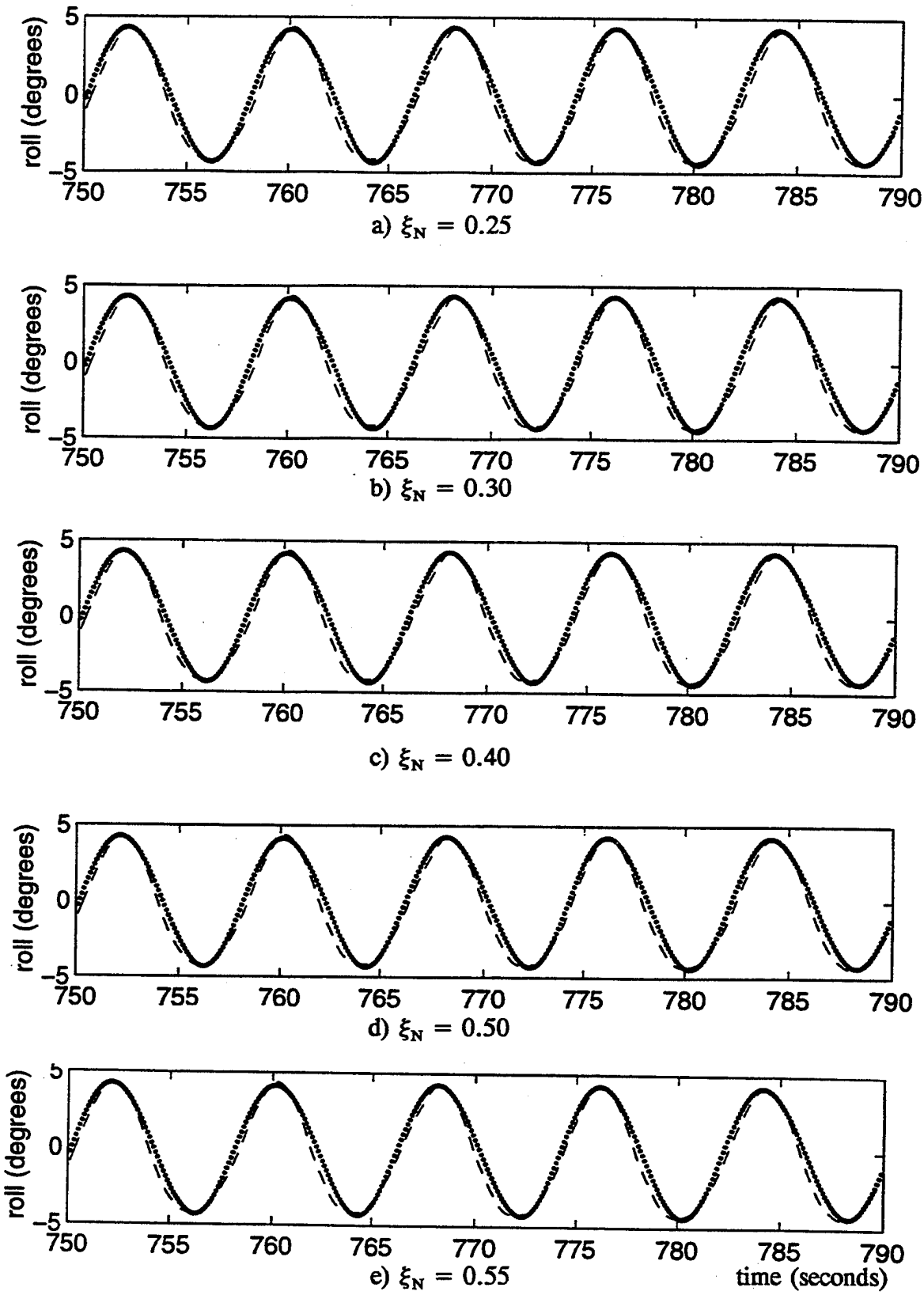

Figure 4.6 Variation of Nonlinear Damping Parameter, Constant Linear Damping Parameter, ξ_L = 0.33, H= 7.2 Ft, T= 8 Sec (SB29, eqn 2.8),
-- measured, .. predicted

4.1.4 Regular Wave, H= 5.7 Ft, T= 10 Sec (SB30)

Test case SB30 is the only test that displays sensitivity to change in damping parameters. Table 4.4 shows the change in standard deviation over the range of damping parameters. The sensitivity is very evident in Figures 4.7a - 4.7e which

Linear Damping Parameter	Nonlinear Damping Parameter	Standard Deviation	Linear Damping Parameter	Nonlinear Damping Parameter	Standard Deviation
0.01	0.07	2.55	0.03	0.01	1.89
0.02	0.07	2.054	0.03	0.03	1.88
0.03	0.07	1.87	0.03	0.05	1.87
0.05	0.07	1.74	0.03	0.07	1.87
0.07	0.07	1.70	0.03	0.09	1.86
0.09	0.07	1.68	0.03	0.11	1.85
0.11	0.07	1.66	0.03	0.13	1.84

Table 4.4 Variation in Damping Parameters and Resulting Standard Deviations (SB30)

show the rapid change in simulated response. The superharmonic virtually disappears once the linear damping parameter reaches 0.05. Figure 4.8 displays the entire 1024 sec time series for this case. It is evident that the damping parameter has a major effect on the occurrence and magnitude of the superharmonic. The standard deviation changes rapidly with the increased damping parameter until the superharmonic is eliminated at 0.05 damping. This is emphasized by the fact that when the linear damping parameter varies from 0.01 to 0.05, the difference in standard deviation is

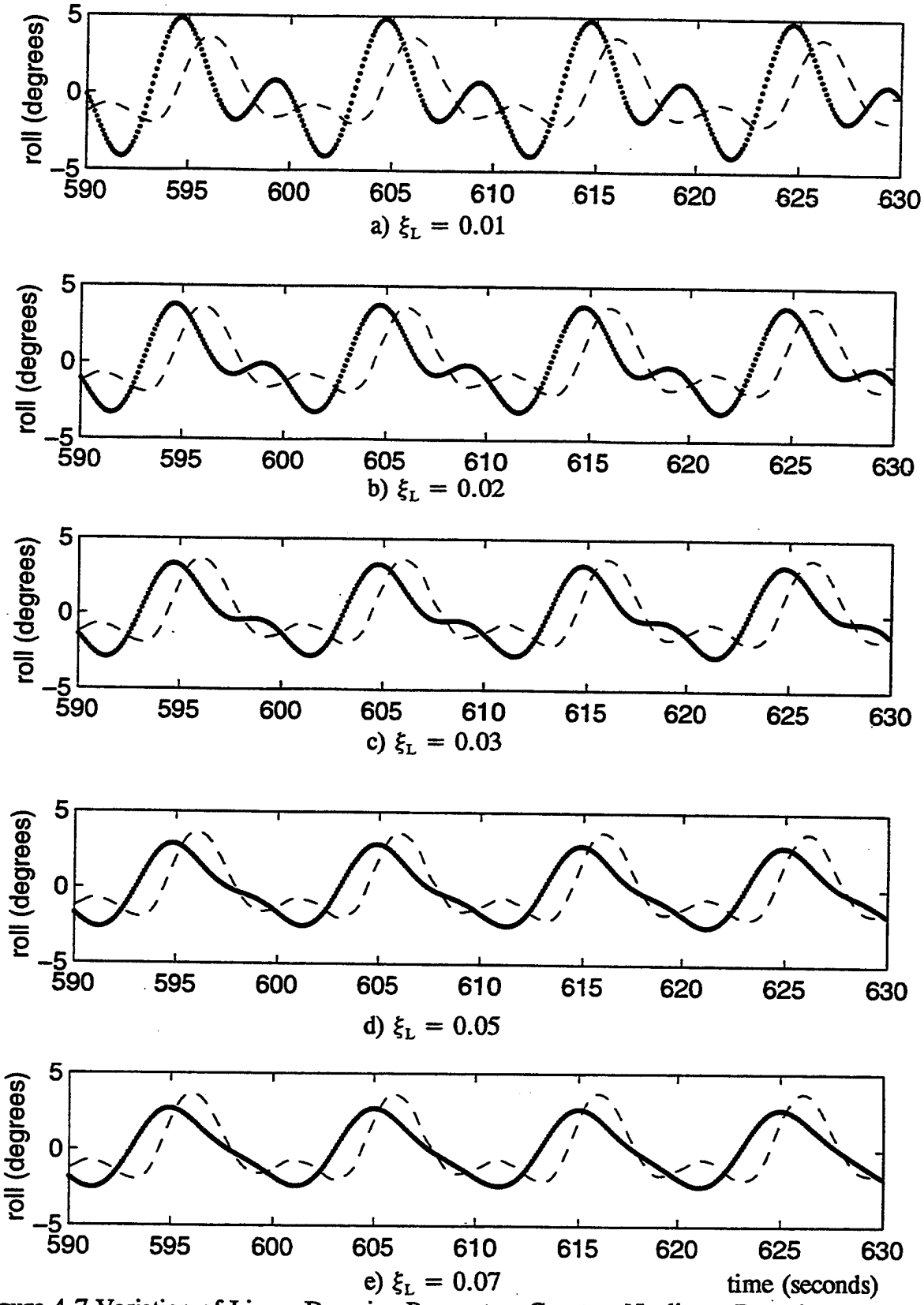

Figure 4.7 Variation of Linear Damping Parameter, Constant Nonlinear Damping Parameter, $\xi_N = 0.07$, H= 5.7 Ft, T= 10 Sec (SB30, eqn 2.8)
-- measured, .. predicted

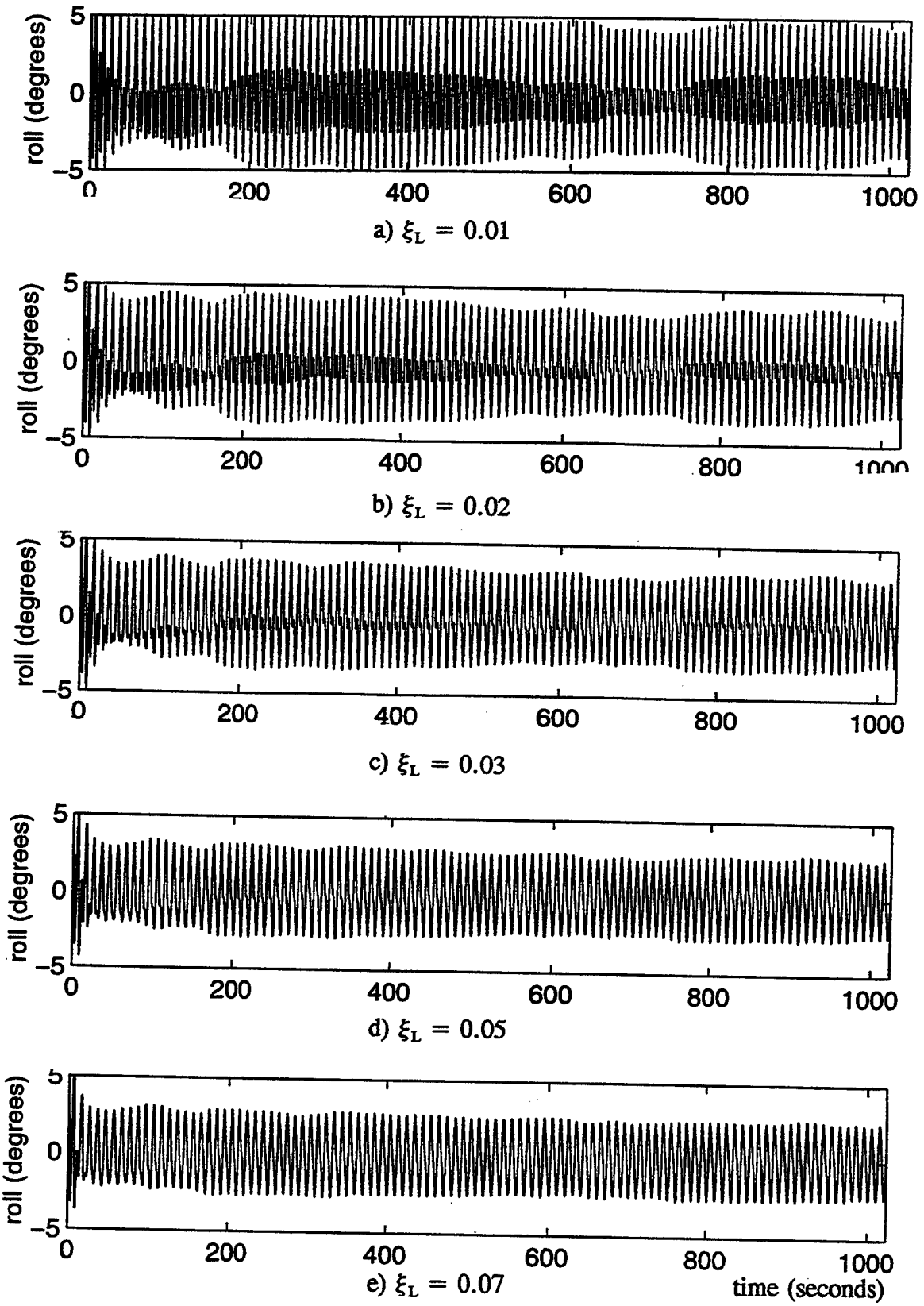

Figure 4.8 Variation of Linear Damping Parameter, Constant Nonlinear Damping Parameter, $\xi_N = 0.07$, H= 5.7 Ft, T= 10 Sec (SB30, eqn 2.8)

0.8025. However, when the damping parameter is varied from 0.05 to 0.11 the change in standard deviation is only 0.08. A variation in the nonlinear damping parameter has very little effect on the response amplitude or superharmonic response as shown in Figure 4.9.

4.1.5 Random Wave Tests

Tables 4.5 and 4.6 show the sensitivity of the model to Bretschneider and white noise wave excitation. Both damping models exhibit a significant change in standard deviation over the range of linear damping parameters. In each case, the standard deviation decreases by over 50% as the linear parameter increases.

Linear Damping Parameter	Nonlinear Damping Parameter	Standard Deviation	Linear Damping Parameter	Nonlinear Damping Parameter	Standard Deviation
0.01	0.04	6.15	0.04	0.01	4.14
0.02	0.04	5.16	0.04	0.02	4.07
0.03	0.04	4.42	0.04	0.03	4.01
0.04	0.04	3.96	0.04	0.04	3.96
0.06	0.04	3.35	0.04	0.06	3.86
0.08	0.04	2.97	0.04	0.08	3.77
0.10	0.04	2.70	0.04	0.10	3.69

Table 4.5 Variation in Damping Parameters and Resulting Standard Deviations (SB25)

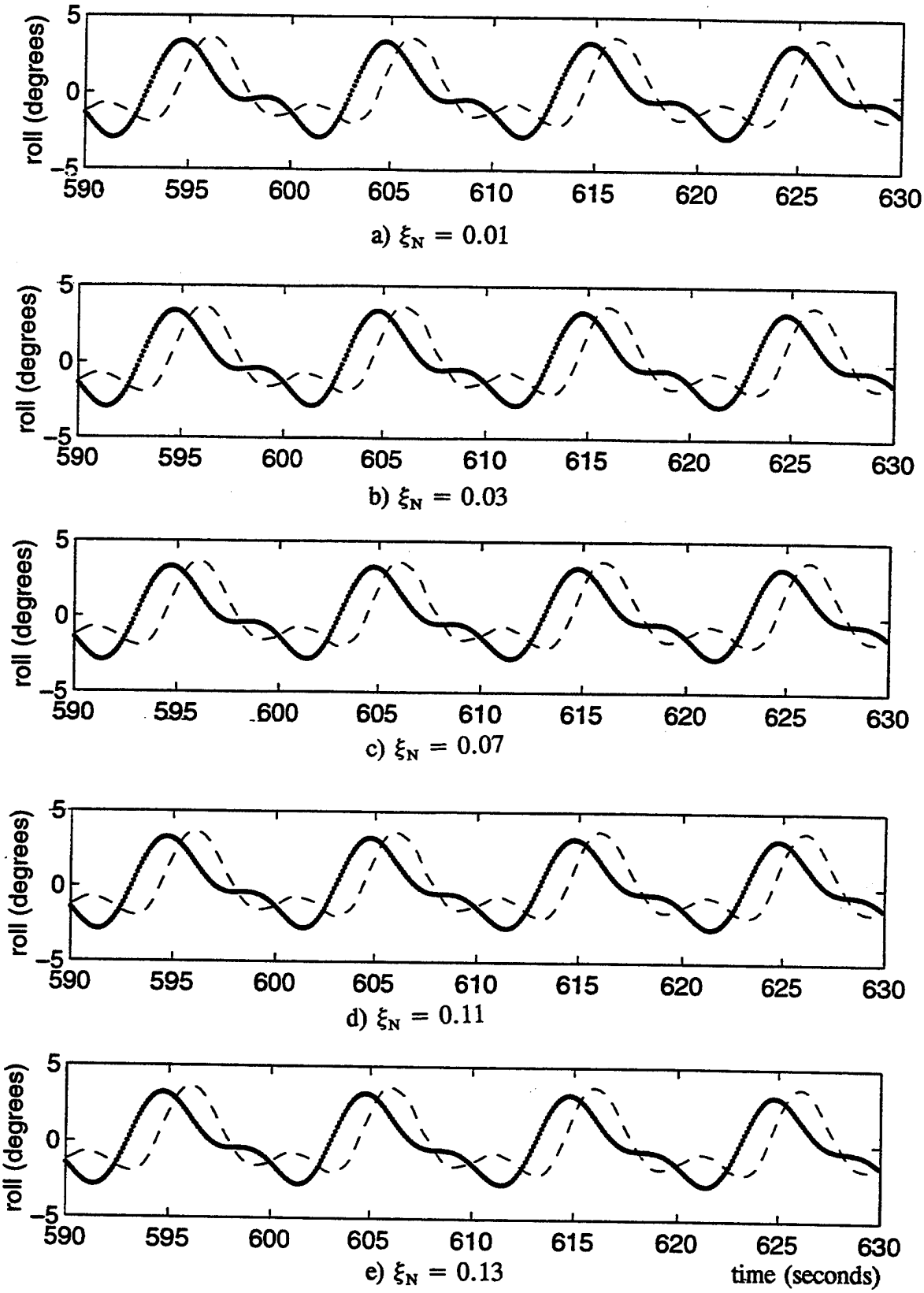

Figure 4.9 Variation of Nonlinear Damping Parameter, Constant Linear Damping Parameter, ξ_L = 0.03, H= 5.7 Ft, T= 10 Sec (SB30, eqn 2.8)
-- measured, .. predicted

Linear Damping Parameter	Nonlinear Damping Parameter	Standard Deviation	Linear Damping Parameter	Nonlinear Damping Parameter	Standard Deviation
0.01	0.08	8.45	0.07	0.02	5.67
0.03	0.08	6.98	0.07	0.04	5.53
0.05	0.08	6.01	0.07	0.06	5.41
0.07	0.08	5.30	0.07	0.08	5.30
0.09	0.08	4.74	0.07	0.10	5.20
0.11	0.08	4.29	0.07	0.12	5.10
0.13	0.08	3.93	0.07	0.14	5.01

Table 4.6 Variation in Damping Parameters and Resulting Standard Deviations (SB33)

4.2 Variation of Nonlinear Restoring Moment

All of the models considered in this analysis have used a 13th-order polynomial restoring moment. A sensitivity test is conducted to determine the effects on the predicted roll response when lower-order polynomials are used to fit the actual restoring moment curve.

4.2.1 Cubic Fit to Restoring Moment Curve

Figure 4.10 shows the actual restoring moment curve and the 3rd-order polynomial used to provide an analytical fit to the curve. This cubic term is then substituted into equation 2.8. The resulting predicted roll response is shown in Figure 4.11. A comparison of the measured and predicted spectral densities for roll response, Figure 4.12, indicates this polynomial is acceptable although it does not

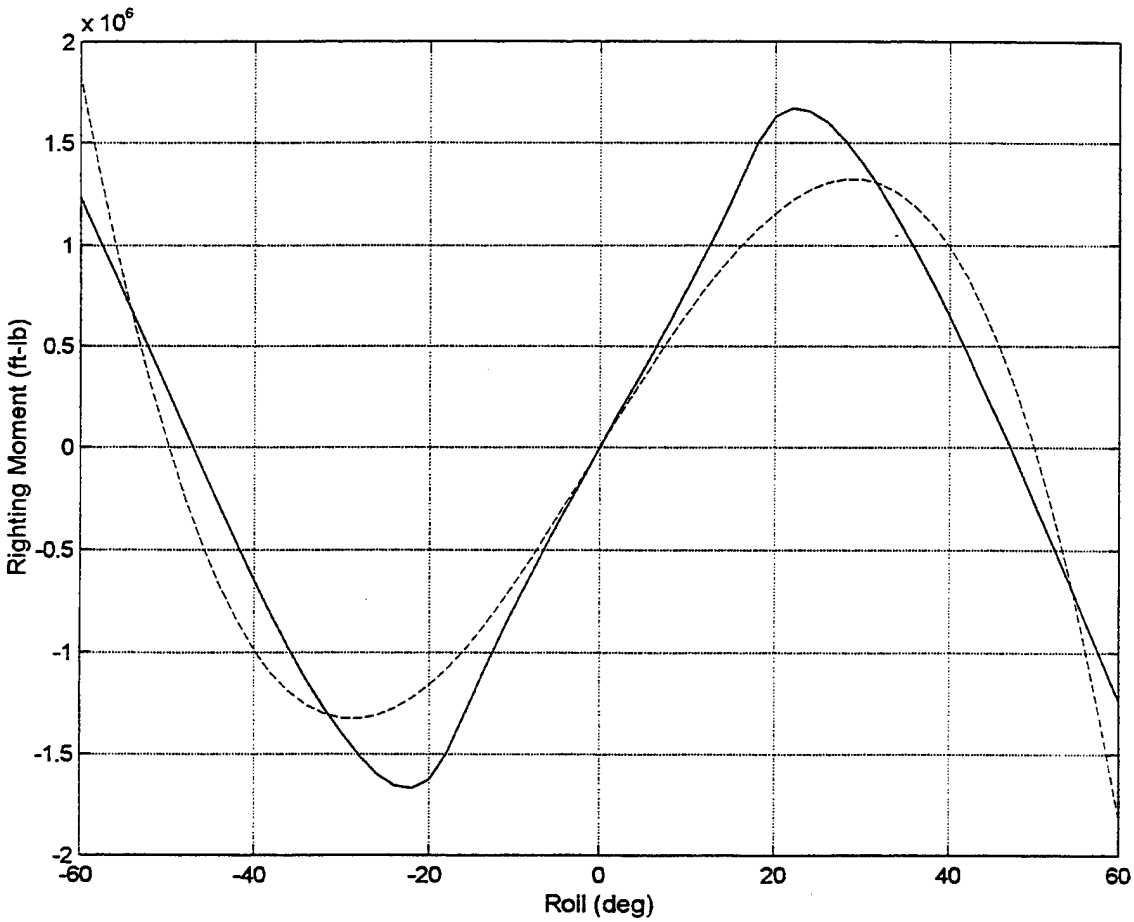

Figure 4.10 Comparison of Numerical (Paulling, 1995) and Analytical (Yim et al. 1995) Restoring Moment Curves, Cubic Fit, - numerical, -- analytical. $B_{13,5}$= 3.9502e6, $B_{11,5}$= -5.1930e6

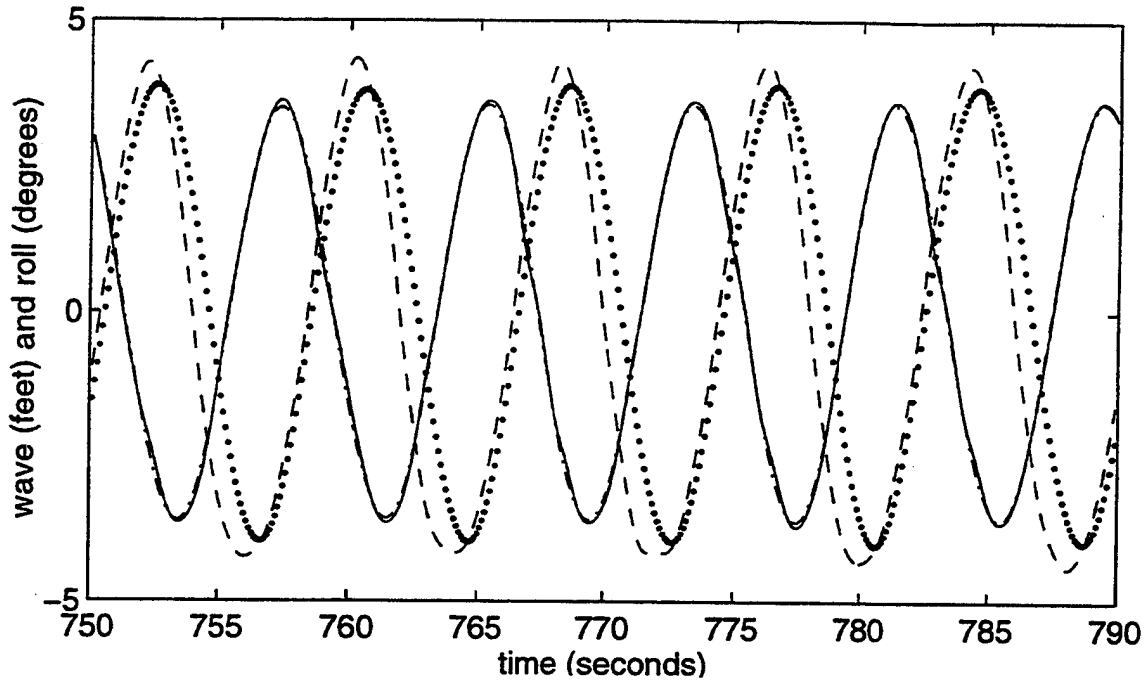

Figure 4.11 Comparison of Measured and Predicted Roll, Cubic Restoring Moment H= 7.2 Ft, T= 8 Sec (SB29), - measured, .. predicted

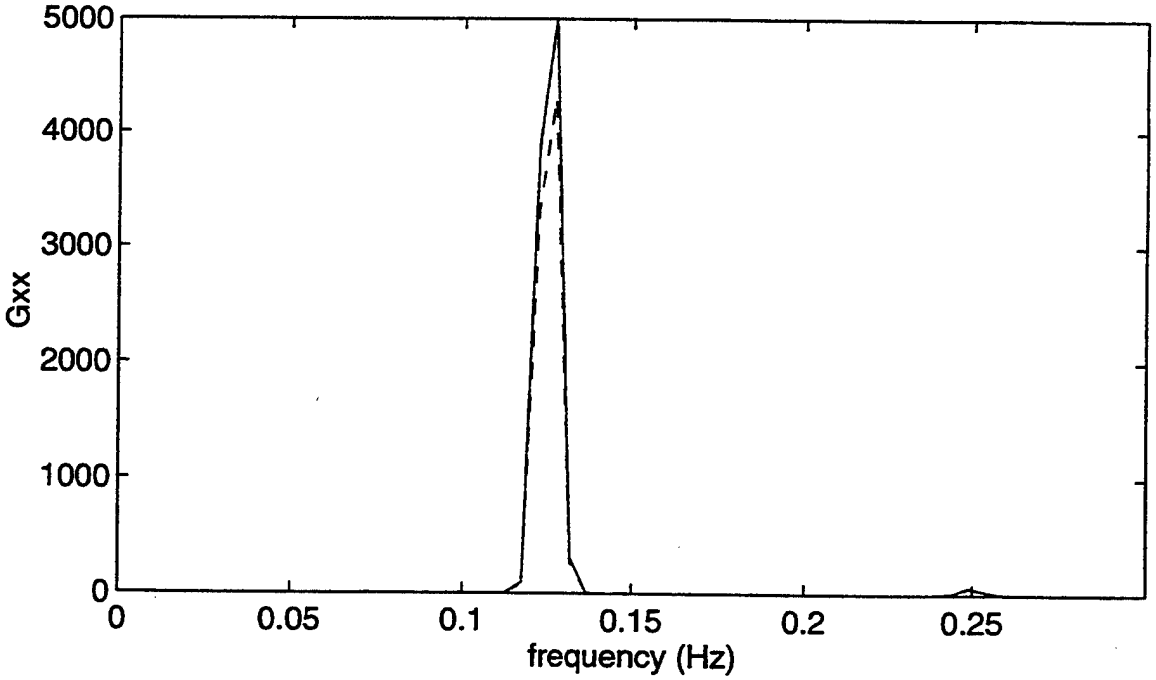

Figure 4.12 Comparison of Spectral Densities (Deg^2/Hz), Measured and Predicted Roll, Cubic Restoring Moment, H= 7.2 Ft, T= 8 Sec (SB29)
- measured, -- predicted

provide and "exact" match of the magnitude of the predict roll response relative to the ones with higher-order terms(see following section).

4.2.2 5th, 9th and 13th-Order Restoring Moment Curves

Figure 4.13 shows the 5th-order polynomial fit to the restoring moment curve. The resulting predicted roll response is shown in Figure 4.14. A comparison of the measured and simulated spectral densities, Figure 4.15, confirms that the 5th-order restoring moment polynomial provides accurate results. Figures 4.16 and 4.17 show the 9th and 13th-order polynomial fits to the restoring moment curve and the resulting roll responses, shown in Figures 4.18 and 4.19.

This sensitivity study indicates that a 3rd or 5th-order polynomial fits the restoring moment curve with sufficient accuracy to provide valid roll response simulation. However, it should be noted that it does not require a significant amount of time or effort to use the 13th-order fit, and this high-order polynomial becomes a requirement to accurately predict roll response at large roll angles.

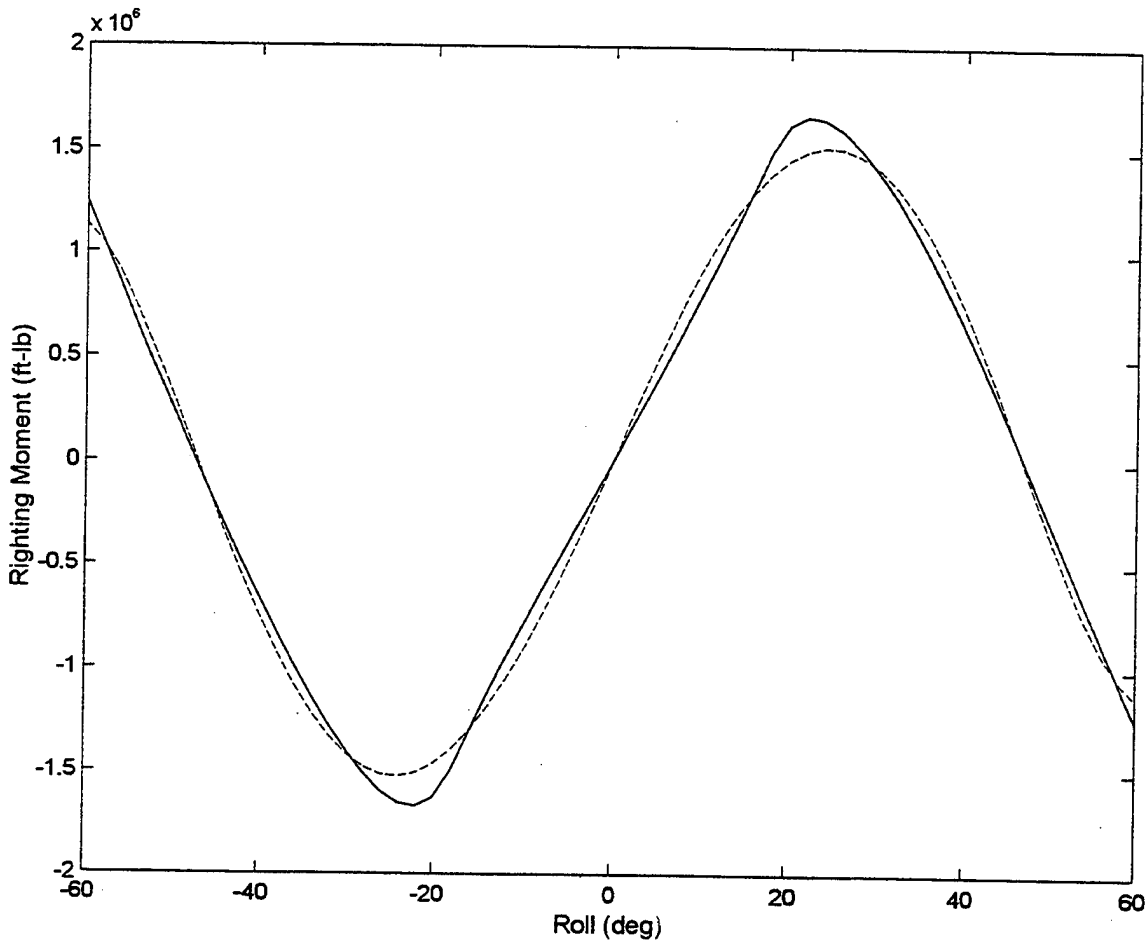

Figure 4.13 Comparison of Numerical (Paulling, 1995) and Analytical (Yim et al. 1995) Restoring Moment Curves, 5th Order Restoring Moment,
- numerical, -- analytical. $B_{13,5}$= 5.5384e6, $B_{11,5}$= -1.1747e7, $B_{9,5}$= 5.2136e6

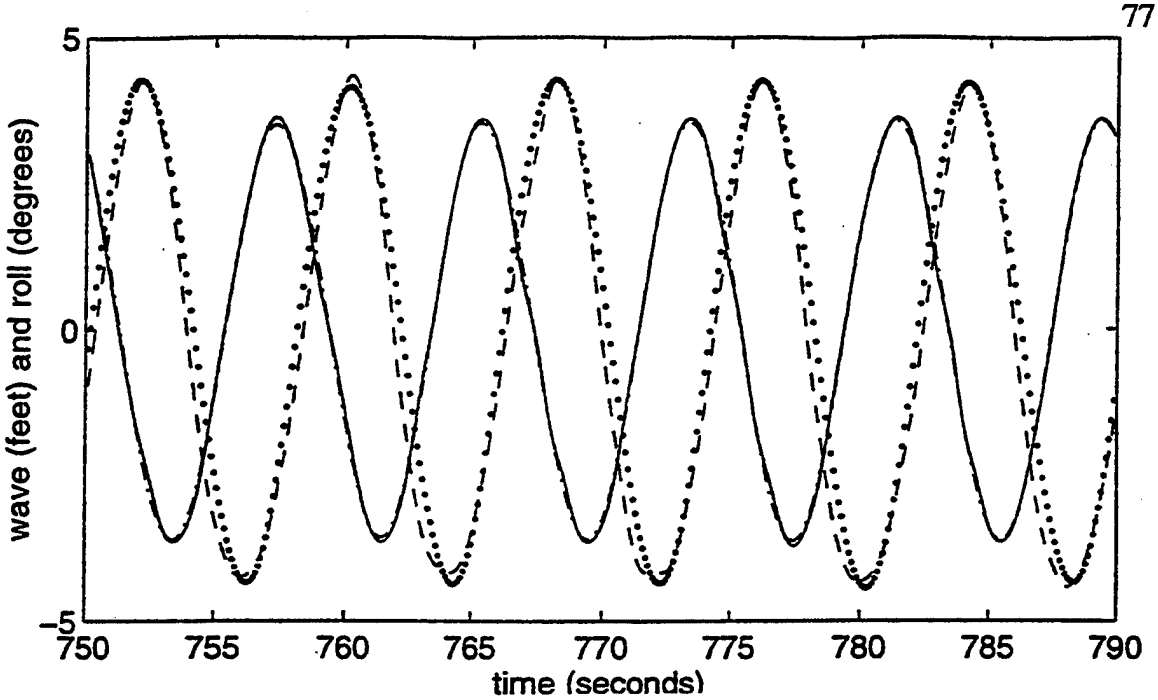

Figure 4.14 Comparison of Measured and Predicted Roll, 5th Order Restoring Moment, H= 7.2 Ft, T= 8 Secs (SB29), -- measured roll, .. predicted roll

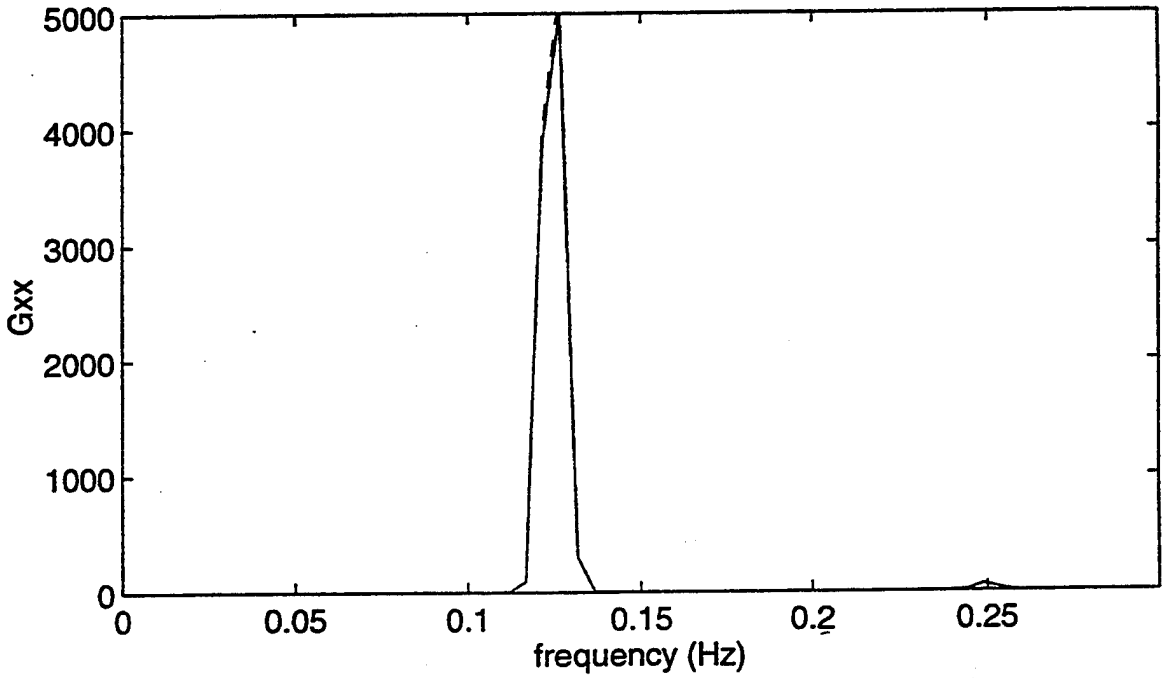

Figure 4.15 Comparison of Spectral Densities (Deg^2/Hz), Measured and Predicted Roll, 5th Order Restoring Moment, H= 7.2 Ft, T= 8 Sec (SB29)
- measured, -- predicted

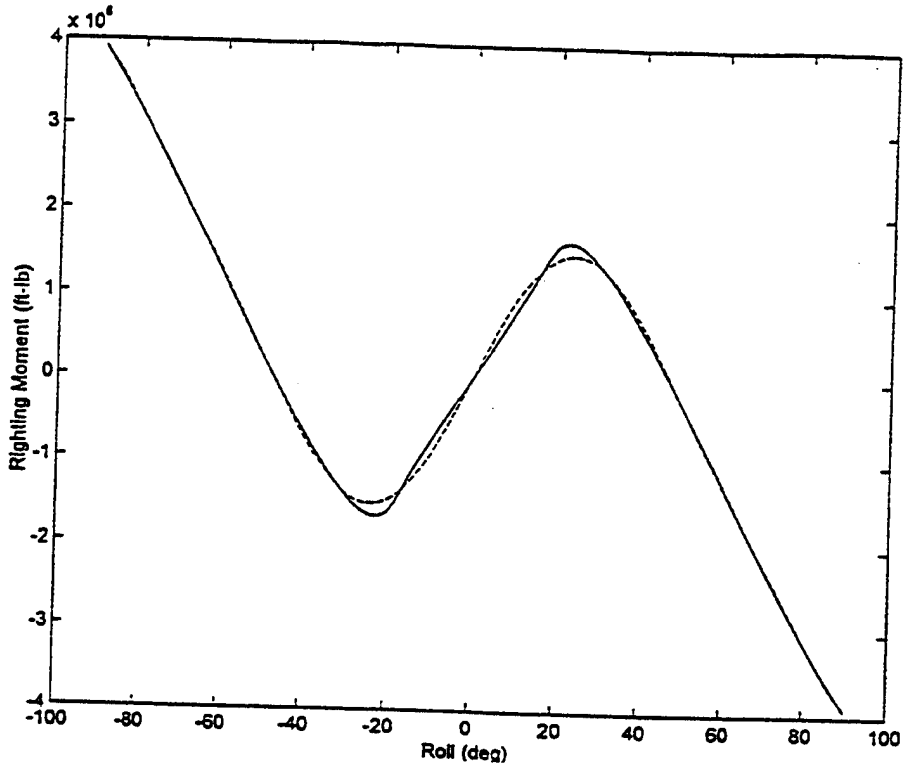

Figure 4.16 9th Order Fit to Restoring Moment Curve. - measured, -- actual
$B_{13,5}$= 5.7927e6, $B_{11,5}$= -1.4128e6, $B_{9,5}$= 1.0693e6, $B_{7,5}$= -3.9235e6,
$B_{5,5}$= 5.5127e6

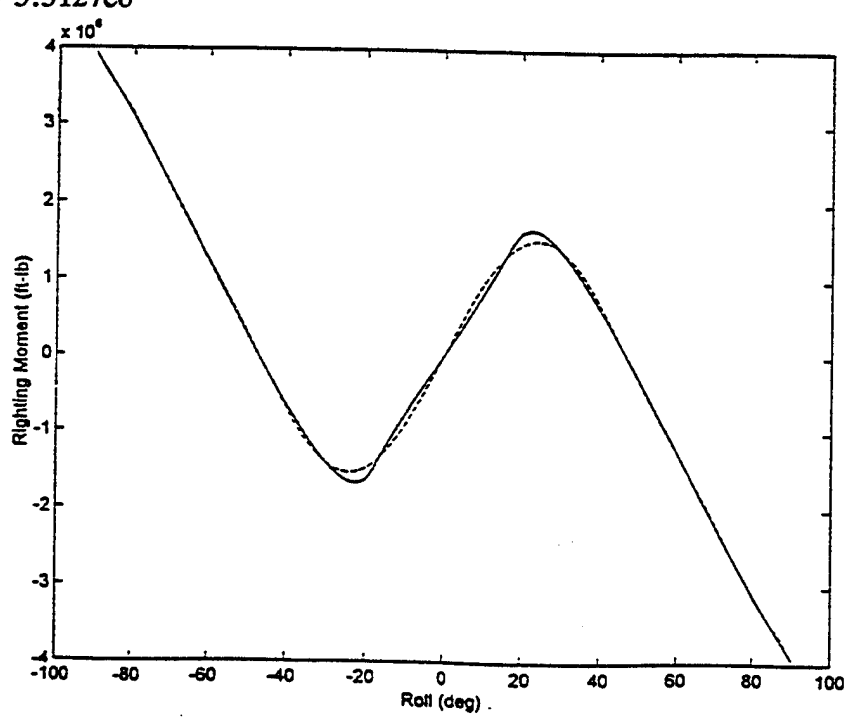

Figure 4.17 13th Order Fit to Restoring Moment Curve. - numerical, -- analytical
$B_{13,5}$= 5.6051e6, $B_{11,5}$= -1.16577, $B_{9,5}$= 1.7258e6, $B_{7,5}$= 9.6915e6,
$B_{5,5}$= -9.3298e6, $B_{3,5}$= 3.3999e6, $B_{1,5}$= -4.4569e5

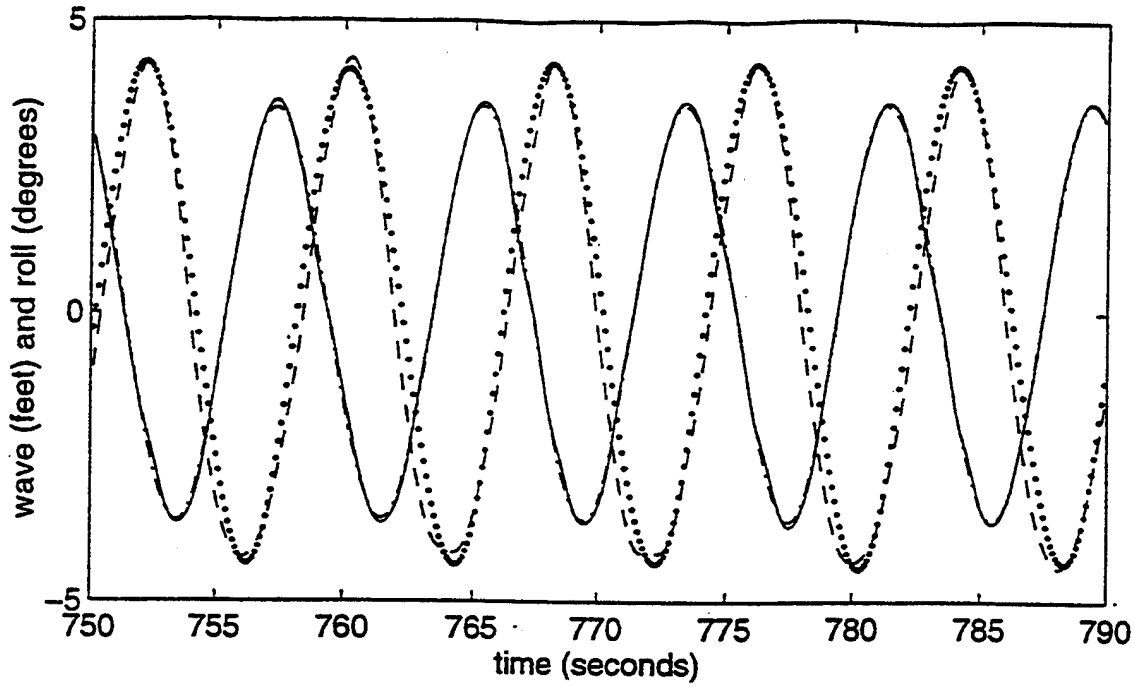

Figure 4.18 Comparison of Measured and Predicted Roll, 9th Order Restoring Moment, H= 7.2 Ft, T= 8 Secs (SB 29), -- measured roll, .. predicted roll

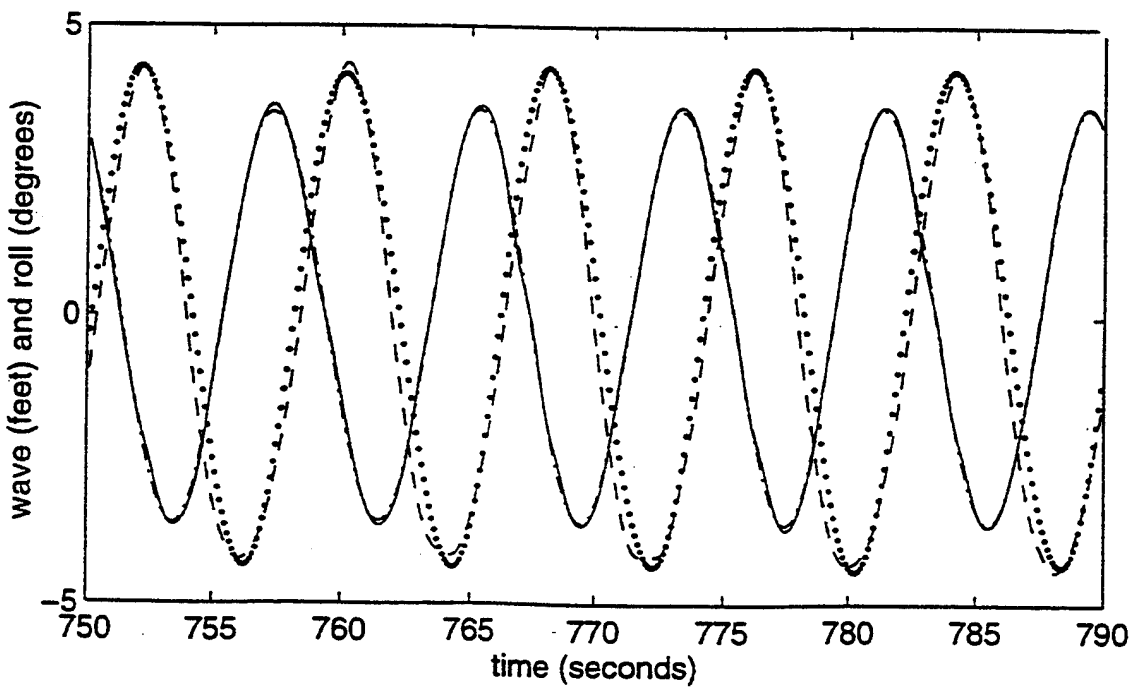

Figure 4.19 Comparison of Measured and Predicted Roll using 13th Order Restoring Moment, H= 7.2 Ft, T= 8 Secs (SB29), -- measured roll, .. predicted roll

5.0 Comparison of Single, 2- and 3- Degree-of-Freedom Models

The final objective of this study is to compare the results of roll response for a 3DOF and a 2DOF model with the SDOF model. A comparison of the 5, 8 and 10 sec regular wave test cases is done as well as the Bretschneider spectrum. Table 5.1 lists a comparison of damping parameters for each of these cases. It is evident from

Wave Test	SDOF Linear Damp-ing Parame ter	SDOF Non linear Damp-ing Parame ter	2DOF Linear Damp-ing Parame ter	2DOF Non linear Damp-ing Parame ter	3DOF Linear Damp-ing Parame ter	3DOF Non linear Damp-ing Parame ter
SB26	0.09	0.07	0.32	0.32	0.40	0.40
SB29	0.33	0.40	0.55	0.55	0.25	0.25
SB30	0.03	0.07	0.02	0.01	0.03	0.03
SB25	0.04	0.04	0.08	0.08	0.05	0.05

Table 5.1 Damping Parameters for SDOF, 2DOF and 3DOF Models

this table that there is a wide range of damping parameters among the different models. There does not appear to be any trend established by the damping parameters for each wave test. In some instances, the parameters are higher in the SDOF model and in others the 2DOF and 3DOF exhibit higher parameters.

Figures 5.1a - 5.1c, which show response to 5 sec wave excitation, indicate that all three models simulate the amplitude of roll response very well. The 3DOF and SDOF model match the phase identically, however, the 2DOF model leads the measured response slightly.

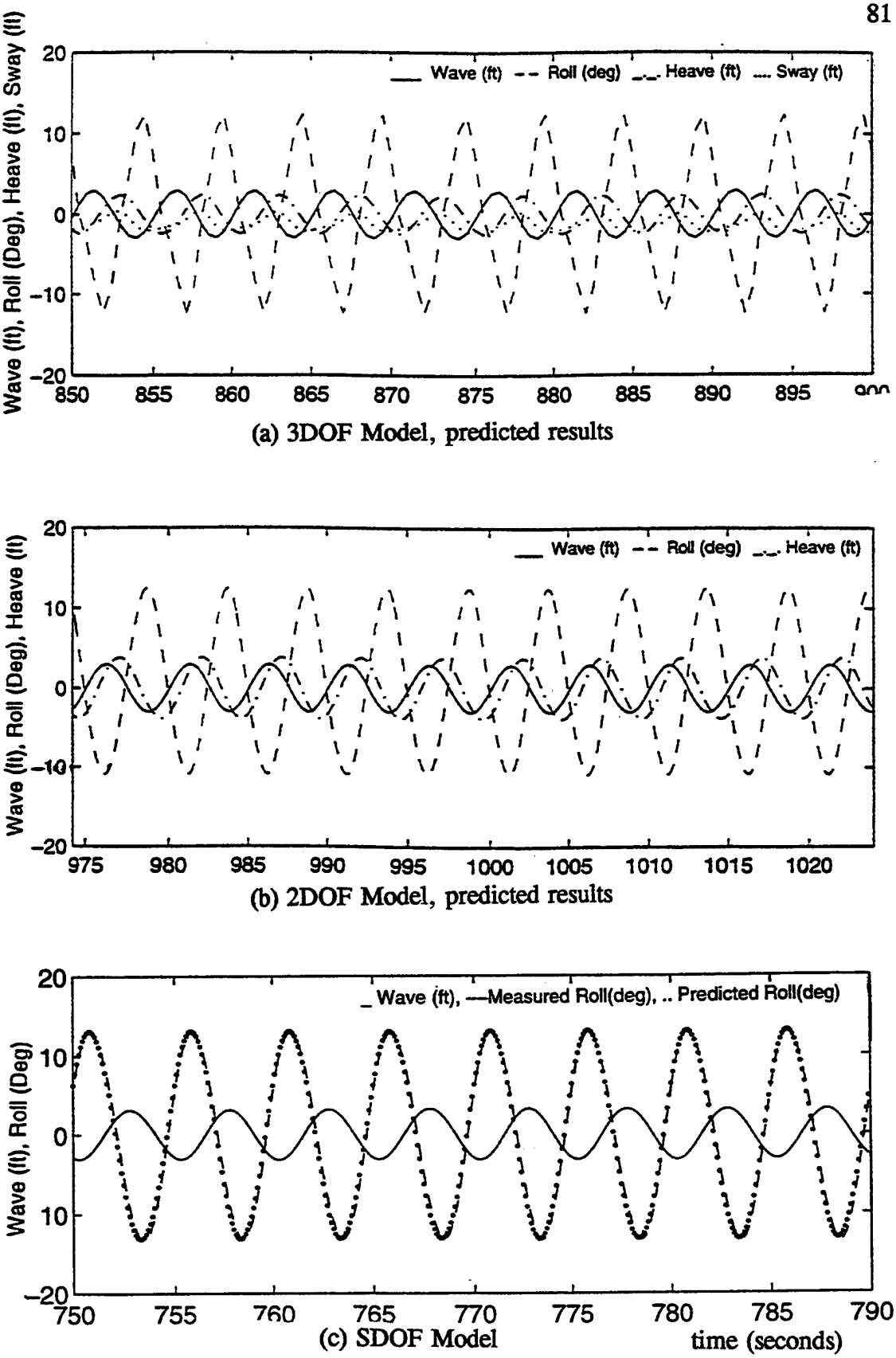

Figure 5.1 Comparison of 3DOF, 2DOF and SDOF Models, H= 6.6 Ft, T= 5 Sec (SB26)

All three models accurately predict the roll response for the 8 sec wave excitation case, Figures 5.2a - 5.2c. The amplitude as well as phase are nearly identical in each case. It is interesting to note that each of the models required unusually high damping parameters for this particular wave case.

Figures 5.3a and 5.3b compare SDOF and 3DOF responses for the 10 sec wave test case. This is the only case observed where the higher-degree-of-freedom model exhibits better prediction capabilities than the SDOF one. It should be noted that the 3DOF and 2DOF models used analytical input and the SDOF used measured input. The SDOF model predicts the subharmonic activity seen in Figure 5.4b. Figure 5.4 compares the entire time series of the 2DOF and SDOF models. Again, the multi-degree-of-freedom model predicts superharmonic response much more accurately. However, results are not available to show prediction capabilities using measured input for all three models.

The final comparison is for the Bretschneider Spectrum test case. This is the only test case in which all models exhibit damping parameters which are close in magnitude. Figures 5.5a - 5.5c indicate the SDOF and 3DOF models provide an accurate prediction in this wave case. The 2DOF model, Figure 5.5b, is observed to be less capable of producing the same results.

A more thorough study is recommended to determine the adequacy of each model and to perhaps determine some correlations between the models. These preliminary results, however, indicate the SDOF model may be equally as accurate and in some cases more accurate than the multi-degrees-of-freedom models. Use of the single degree of freedom model can be an excellent tool for future research.

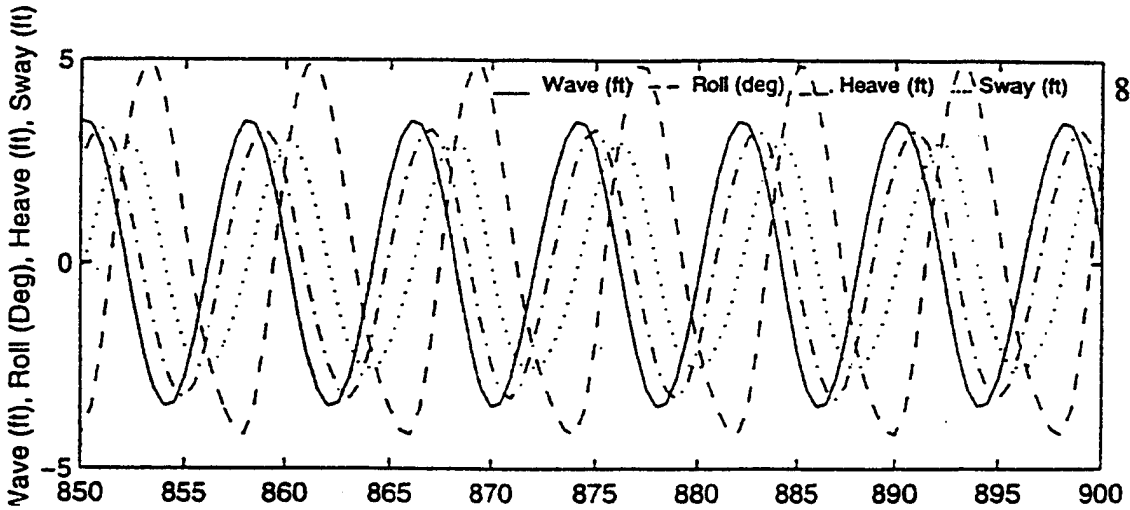

(a) 3DOF Model, predicted results

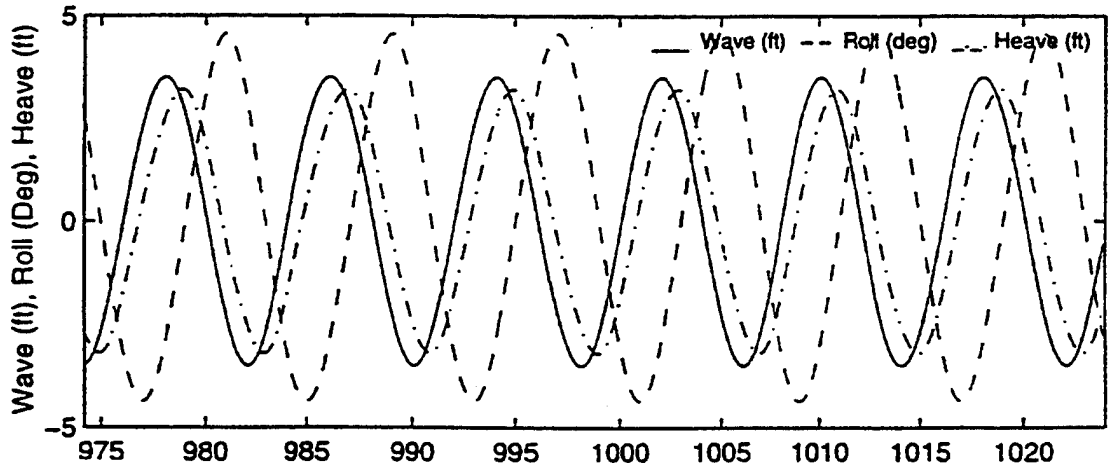

(b) 2DOF Model, predicted results

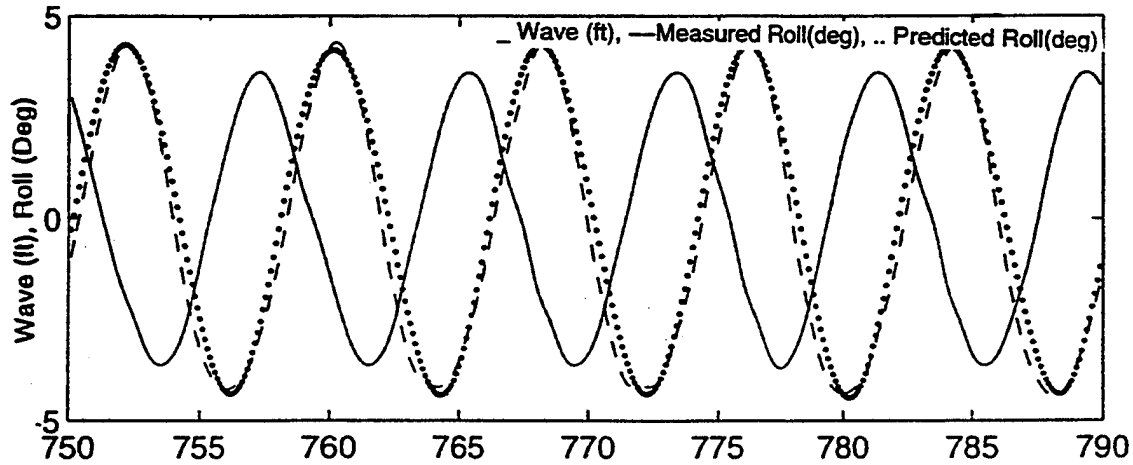

(c) SDOF Model time (seconds)

Figure 5.2 Comparison of 3DOF, 2DOF and SDOF Models, H= 7.2 Ft, T= 8 Sec (SB29)

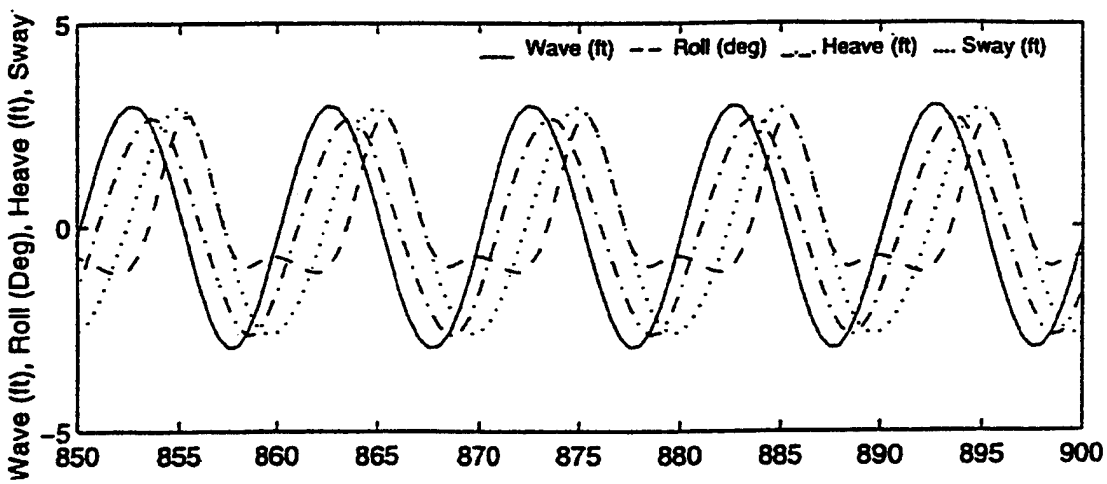

(a) 3DOF Model, predicted results

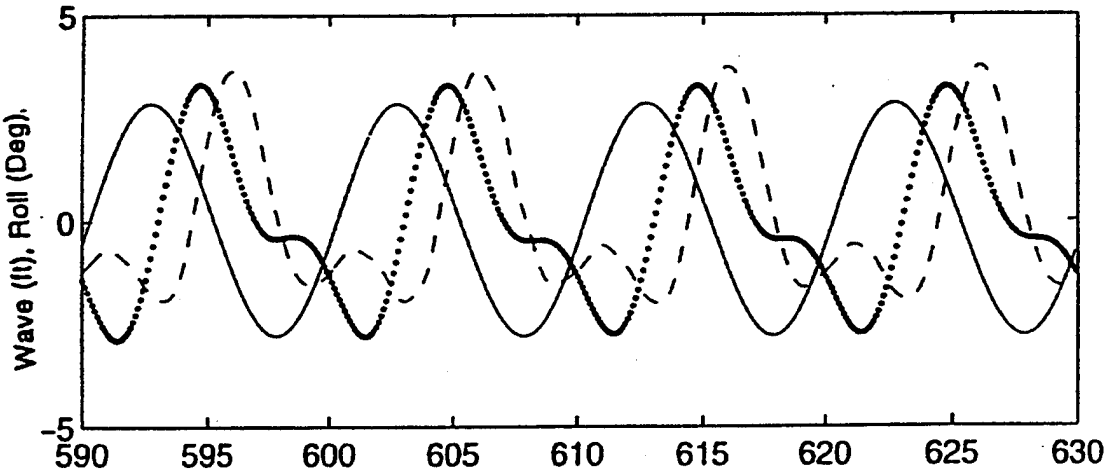

(b) SDOF Model

Figure 5.3 Comparison of 3DOF and SDOF Models, H= 5.7 Ft, T= 10 Sec (SB30)

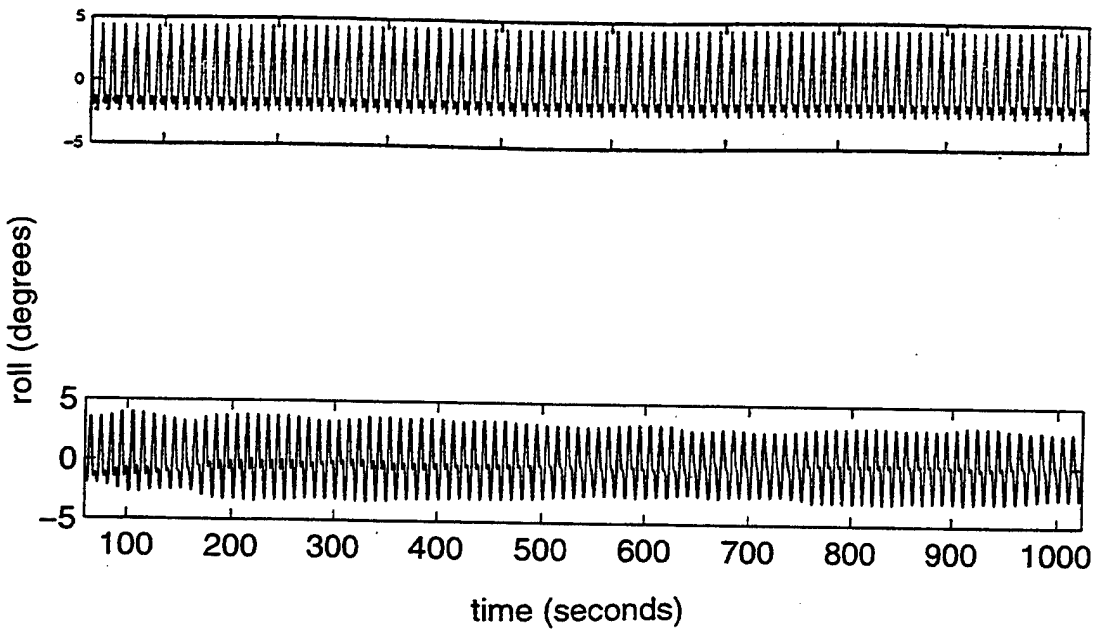

(b) SDOF Model

Figure 5.4 Comparison of 2DOF and SDOF Freedom Models, H= 5.7 Ft, T= 10 Sec (SB30)

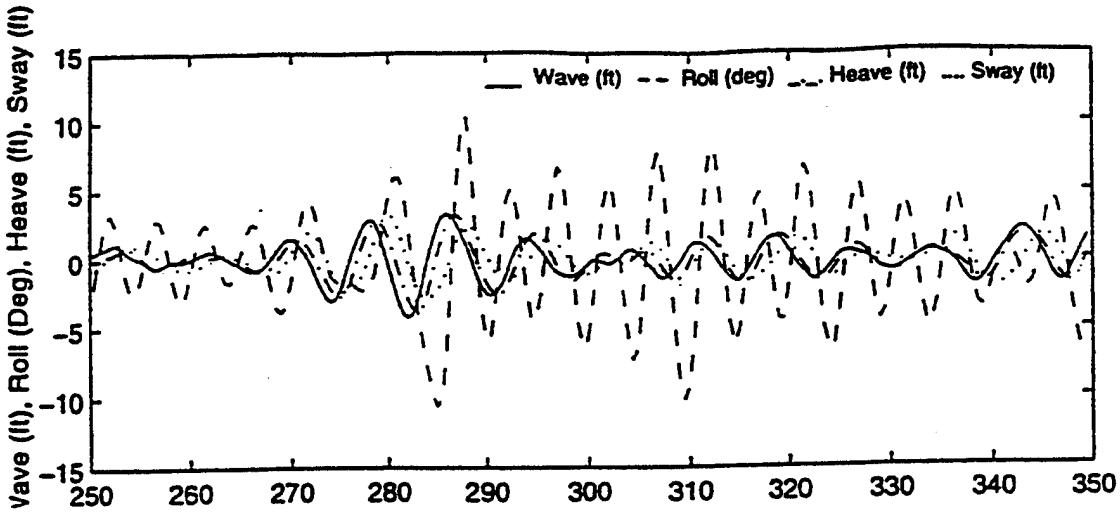

(a) 3DOF Model, predicted results

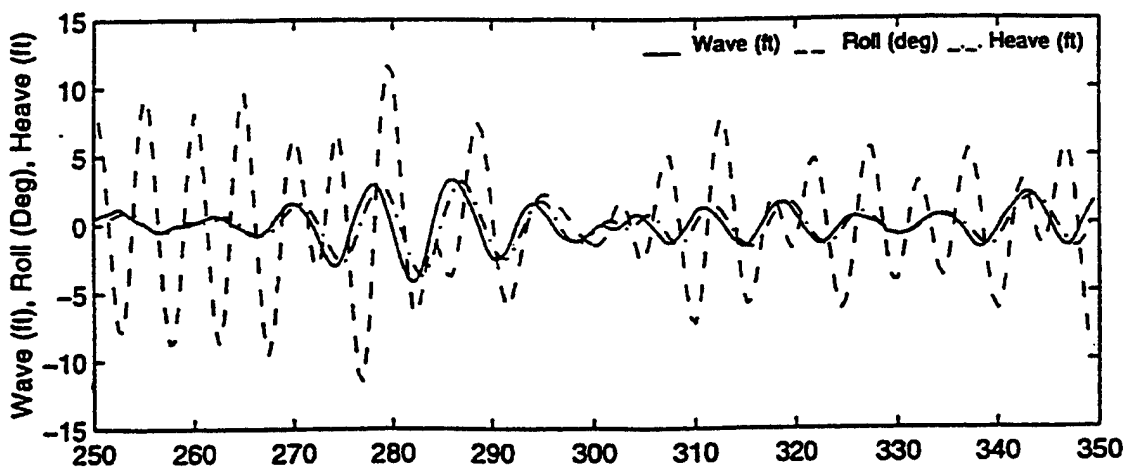

(b) 2DOF Model, predicted results

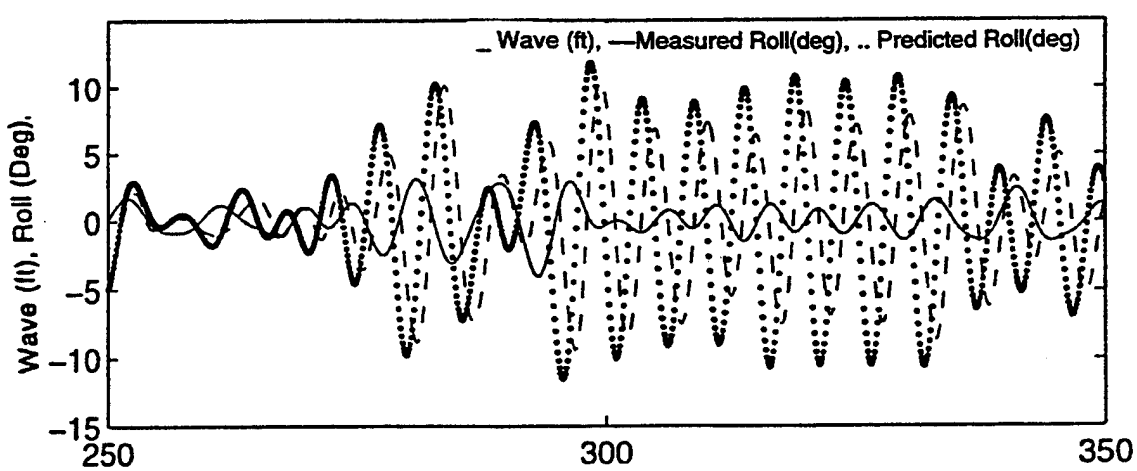

(c) SDOF Model time (seconds)

Figure 5.5 Comparison of 3DOF, 2DOF and SDOF Models, Bretschneider Spectrum (SB25)

6.0 Concluding Remarks

In this report, four different forms, each identical except for a variation in the damping term were studied. From these equations, an SDOF model to predict barge roll motion was identified. The form which provided the most accurate predicted responses proved very capable of simulating barge response in both the regular and random wave environment with the exception of test SB30. A sensitivity study was conducted to determined the effects of varying damping parameters. In addition, the restoring moment term was examined to determine the effects of using 3rd, 5th, 9th, and 13th-order terms. Finally, a comparison was made between the SDOF, 2DOF and 3DOF models to identify the strengths and weaknesses of each model among the different wave test cases.

6.1 Conclusions

1) The model which provided the most accurate response simulation was equation 2.8. This form assumes the relative motion effects can be neglected. As a result, only the barge roll velocity is considered in the damping terms.

2) The SDOF model was capable of predicting barge response for all regular and random wave test cases except SB30, in which the 10 sec wave excitation was a multiple of the barge's natural roll frequency. As a result, the response motion contained a superharmonic which was difficult to simulate.

3) A constant damping parameter cannot be used to predict all responses throughout the wave excitation spectrum. The damping parameters for the regular and random wave excitations summarized in Table 6.1, show no obvious pattern of behavior.

Wave Test	Linear Damping Parameter	Nonlinear Damping Parameter
H= 6.6 Ft, T= 5 Sec (SB26)	0.09	0.07
H= 6 Ft, T= 6 Sec (SB27)	0.10	0.07
H= 7.2 Ft, T= 8 Sec (SB29)	0.33	0.40
H= 5.7 Ft, T= 10 Sec (SB30)	0.03	0.07
Bretschneider Spectrum	0.04	0.04
White Noise Spectrum	0.07	0.08

Table 6.1 Summary of Damping Parameters for Form 2, Equation 2.8

4) A sensitivity study of the restoring moment term determined that a 3rd or 5th-order polynomial is sufficient for simulation when the magnitude of the roll response is not large, although the 3rd-order polynomial tends to slightly underpredict response at times. There is no discernable difference in predicted response provided by a 9th or 13th-order restoring moment polynomial. The incremental computational time using these higher-order polynomials is minimal. In addition, when roll response becomes large, the higher-order polynomials become a requirement.

5) When comparing the SDOF model with the multi-degree-of-freedom models, the results are mixed. In the regular wave tests, the SDOF model provides the same results as the 3DOF, except in the 10 second wave test case. The ability of SDOF and 3DOF models to simulate random response is remarkably better than the

2DOF model. These observations combined with the significant time saving makes the SDOF very desirable to use.

6.2 Recommendations for Future Studies

1) Further studies in variation of the damping terms may improve the ability to predict superharmonic response. Varying the effects of relative motion, roll velocity and wave slope velocity could possibly produce better results.

2) A computer program is currently under development to predict the probability of barge capsize. A comparison of the SDOF, 2DOF and 3DOF models can be used in this program to establish further strengths and weaknesses of each model. Although simplistic compared to the 2DOF and 3DOF models, the SDOF model may provide equally adequate results with much less time invested.

3) In determining the damping parameters in this study, the standard deviation of the amplitude was used as the criterion for determination. This assumes the phase shift is unimportant. The focus of an alternate study could be to use a least-square criterion which weighs both amplitude and phase shift in the error calculation.

4) In the random wave cases, a comparison of spectral densities showed a shift in peak frequencies between the measured and predicted spectrum. Variations in input data such as dominant period of wave spectrum could be analyzed to determine if this shift may be eliminated or decreased.

References

Bartel, W, *Modelling, Validation, and Simulation of Multi-Degree of Freedom Nonlinear Stochastic Barge Motions*, 1996

Chakrabarti, S.K., Hydrodynamics of Offshore Structures, 1987.

Falzarano, J., Shaw S. W. and Troesch, A. W., Application of Global Methods for Analyzing Dynamical Systems to Ship Rolling Motion and Capsizing, *International Journal of Bifurcation and Chaos*, 1992, 2, 101-115.

McAllister, M., "Evolution and State of the Art of the Log Barge," *Marine Technology*, SNAME 1995, 32, No.2 , 132-139.

Paulling, J.R., "Capsize Assessment Technology Program, Comparison of Model Tests and Results of Numerical Simulations," *Report Submitted to Naval Facilities Engineering Service Center*, Port Hueneme, CA, Jan 1995.

Soliman M. and Thompson, J.M. T., Transition and Steady State Analysis of Capsize Phenomena, Applied Ocean Research, 1991, **13**, 82-92.

Yim, S.C.S., Bartel, W.A., Huang, E.T., Lin, H., "Nonlinear Roll Motion and Capsizing of Barges in Random Seas, Part I: Modelling and System Identification", *Report Submitted to Naval Facilities Engineering Service Center*, Port Hueneme, CA, 1995, 1-41.